12-2010

VENA CAVA AS AN ALTERNATIVE TO PERICARDIUM IN BIOPROSTHETIC PERCUTANEOUS HEART VALVES

Amy Munnelly
Clemson University, amunn3@gmail.com

VENA CAVA AS AN ALTERNATIVE TO PERICARDIUM IN BIOPROSTHETIC PERCUTANEOUS HEART VALVES

A Thesis
Presented to
the Graduate School of
Clemson University

In Partial Fulfillment
of the Requirements for the Degree
Master of Science
Bioengineering

---

by
Amy Munnelly
December 2010

Accepted by:
Dr. Naren Vyavahare, Committee Chair
Dr. Bruce Gao
Dr. Anand Ramamurthi

ABSTRACT

Valve disease is a specialized form of cardiovascular disease that specifically affects the heart valves. Heart valves serve the vital function of maintaining unidirectional blood flow through the chambers of the heart during the cardiac cycle; however, as valve disease progresses, this function can become severely compromised [1]. Currently, the only cure for valve disease is to replace the defective valve with an engineered substitute. Each year, over 300,000 heart valve replacement surgeries are performed worldwide [2], and this number is expected to continue growing as life expectancies increase [3].

In the United States, the most common form of valve disease is aortic stenosis [4], which can become severe enough to necessitate valve replacement surgery. Although the demand for replacement valves is growing, current clinically available valve substitutes have still not been perfected. Mechanical valves present problems with thrombosis and necessitate lifetime anticoagulation therapy, whereas bioprosthetic valves have limited durability [1, 5]. Furthermore, valve replacement surgery is very invasive, and high risk patient populations are often denied surgery. Over 50% of elderly populations with aortic stenosis are not offered surgery because the mortality risk is too great [6, 7].

Due to the limitations of traditional heart valve replacement surgery, a new, less invasive option, percutaneous aortic valve replacement (PAVR), has been developed [8, 9]. PAVR involves transcatheter delivery of a crimped, stented valve to the aortic annulus. The valve is deployed by a balloon catheter or self-expansion. While not yet commercially available, two percutaneous heart valves (PVRs) are currently in clinical trials [9]. These models are composed of glutaraldehyde-fixed pericardial tissue.

A major limitation of PVRs is the diameter to which the stent can be crimped. The device profile precludes use in small or tortuous vascular systems, limiting the candidate patient pool for PAVR [10]. An alternative material for PHVs may be porcine vena cava, as this tissue may provide enhanced flexibility and resilience. This study evaluates the feasibility of utilizing vena cava as a bioprosthetic tissue in PHVs by comparing its structural, mechanical, and *in vivo* properties to those of bovine pericardium. While the extracellular matrix fibers of pericardium are randomly oriented, the vena cava contains highly aligned collagen and elastin fibers that impart strength to the vessel in the circumferential direction and elasticity in the longitudinal. Mechanically, the vena cava is significantly less stiff than the pericardium, even after crosslinking with glutaraldehyde (GLUT) or combined neomycin and glutaraldehyde (NG) protocols. Furthermore, the vena cava's mechanical compliance is preserved after compression under forces similar to those exerted by a stent, whereas pericardium is significantly stiffened by this process. However, the high elastin content of the vena cava may be responsible for enhanced calcification as compared to the pericardium, and an effective anticalcification strategy is necessary if the vena cava is to be clinically useful. Taken together, these results suggest that the vena cava may enhance leaflet flexibility, tissue resilience, and tissue integrity in PHVs, ultimately reducing the device profile while improving the durability of these valves.

DEDICATION

To personal growth, perseverance, and achievement.

To all those who have supported me throughout my graduate studies.

To my parents and sister for constant encouragement and love.

ACKNOWLEDGMENTS

I wish to thank my advisor, Dr. Naren Vyavahare, for supporting this research effort. Additionally, I would like to extend my appreciation to my committee members, Dr. Bruce Gao and Dr. Anand Ramamurthi. I have gained a vast amount of knowledge from this experience, and I am eager to put my skills to use in industry and develop my career as a biomedical engineer.

Thank you to Mrs. Linda Jenkins, for advice and assistance with histology. Thanks to Jeremy Mercuri for advice relating to laboratory techniques and troubleshooting experiments. Thank you to Joshua Leong for supplying me with animal tissue and for general laboratory support.

Thanks to Lee Cochrane and Daniel Tripi for assistance with mechanical testing and rat surgery, to Chih-Chou Yang for help with the stereomicroscope, and to Brianna Liberio for general lab assistance.

Finally, I would like to extend my appreciation to Clemson University and the Department of Bioengineering for this opportunity.

TABLE OF CONTENTS

Page

LIST OF TABLES

LIST OF FIGURES

List of Figures (Continued)

Figure Page

List of Figures (Continued)

Figure Page

CHAPTER ONE

INTRODUCTION

1.1. Heart Valve Anatomy and Physiology

In order to create a viable replacement valve, a thorough understanding of heart valve function and structure is required. Any successful prosthesis will have to withstand the dynamic operating environment and adequately reproduce natural valve function.

1.1.1 Valve Function

The cardiovascular system is composed of the systemic and pulmonary circulation. The pulmonary system is responsible for oxygenating the blood, while the systemic circulation carries this oxygenated blood to the body's organs. The heart, which is the muscular pump that provides the force necessary for blood flow, has four chambers which collect and distribute the blood. Additionally, four valves within the heart open and close to allow for unidirectional blood flow through the circulatory system. The tricuspid and mitral valve are between the atria and ventricles. The pulmonary valve controls blood flow from the right ventricle to the pulmonary artery, while the aortic valve controls blood flow from the left ventricle to the aorta [1]. The mechanical action of the valves is controlled by pressure gradients within the heart chambers. All of the valves open and close once per cardiac cycle, totaling more than 3 billion cycles in a lifetime [1]. A schematic of the cardiac anatomy is given in Figure 1.1.

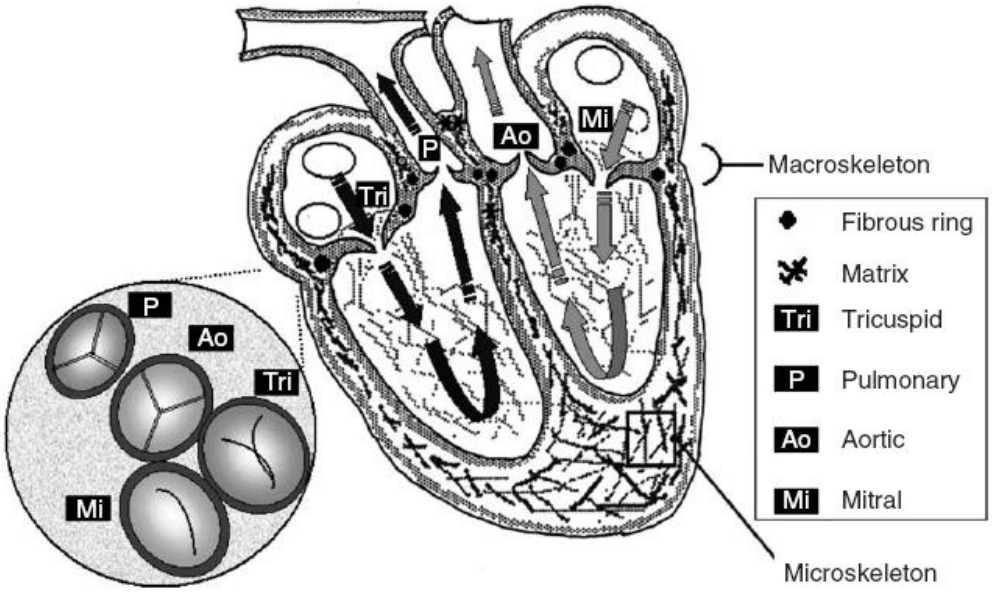

Figure 1.1: Anatomy of the heart valves [1]

1.1.2 Tissue Structure and Function Correlation

The aortic valve is the most frequently diseased and transplanted valve, likely because the great pressure and forces required to pump blood from the left ventricle throughout the entire body [5]. The aortic valve is also the most widely studied, and the valve of greatest interest to our lab; thus, further discussion will focus specifically on this valve.

Replacement valves intend to mimic the natural function of the heart valve, and bioprosthetic valves further aim to replicate the native valve structure as well. The structure and function of the aortic valve are highly correlated. The aortic valve opens during ventricular systole to allow blood to pump into the aorta. As blood fills the aorta, the aortic pressure rises. Once a critical backpressure is reached, the aortic valve closes and remains completely closed during ventricular diastole [5]. The valve is composed of three cusps or leaflets, which coapt

(contact) during valve closure to prevent leakage. The unique architecture of the cusp tissue prevents the leaflets from collapsing and allows them to withstand cyclical deformations and stretching [5].

The heart valve cusps are composed of three tissue layers: the fibrosa, ventricularis, and spongiosa. The fibrosa, located on the aortic face of the cusp, is composed of circumferentially-aligned, crimped collagen fibers. The collagen fibers impart strength to this load-bearing layer [11]. The ventricularis is located on the blood inflow surface, which faces the ventricle. This layer is predominantly composed of radially-aligned elastic fibers that allow for flexibility and elastic recoil of the cusps [1, 12]. Between these two layers is the spongiosa, a highly hydrophilic layer composed of loose connective tissue with abundant glycosaminoglycans (GAGs) [13]. The gel-like matrix of the spongiosa acts as a lubricant and shock-absorber to reduce shearing between the other two layers [1]. They also aid in diffusion of oxygen and nutrients through the valve tissue, which is largely avascular [14].

This complex, multi-layer architecture renders the leaflets highly anisotropic, but promotes smooth valve opening and closing [5]. The crimped fibers make the valve much more compliant in the radial direction than the circumferential. As the valve closes, the crimps expand radially to allow for elongation and coaptation without great stress on the tissue. The extended collagen fibers impart stiffness to prevent cuspal sagging or collapse [5]. The elastin fibers recoil during valve opening to decrease the dimensions of the cusp and maximize blood flow through the orifice [15]. The shear stresses generated by these movements are dissipated by the spongiosa [5]. A diagram of the valve architecture during ventricular systole and diastole is shown in Figure 1.2.

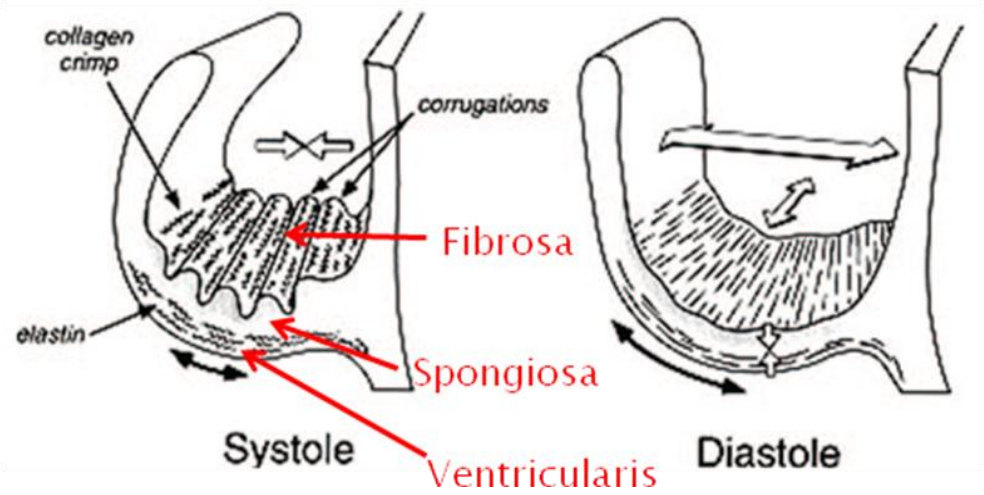

Figure 1.2: Structure of the aortic valve during ventricular systole and diastole [5]

1.2 Heart Valve Biomechanics

1.2.1 Hemodynamics

Aortic valve disease preferentially affects the fibrosa, which is on the aortic side of the leaflets; it is thought that complex fluid flow and shear stress profiles cause this phenomenon [16]. Computational fluid flow models have been used to study the dynamics of blood flow on both the aortic and ventricular sides of the cusps. While the valve is in the open position, flow on the ventricular side is smooth, straight, and accelerating due to the pressure from ejection. Flow through a healthy valve reaches a peak velocity of approximately 1.2 m/s [16]. However, on the aortic side a rapid increase in cross-sectional area due to the aortic sinuses causes a large change in the pressure gradient that results in more disorganized flow. While the valve is closing, the flow on the ventricular side remains relatively straight, while the flow on the aortic side becomes increasingly chaotic [16]. The flow fields of a fully open and a closing aortic valve are shown in Figure 1.3.

As the valve is closing, the pressure gradient between the ventricle and aorta causes flow reversal across the leaflets. Once the valve is fully closed, vortices occur behind the leaflets to facilitate more quick and efficient cusp movement to the fully coapted position [17].

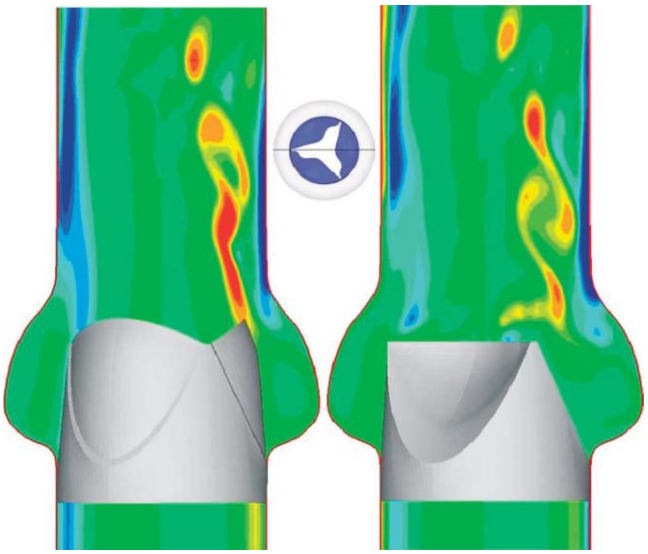

Figure 1.3: Fluid flow in a fully open valve (left) and closing valve (right). [16].

1.2.2 Mechanical Testing

In vitro testing is a valuable tool for assessing the biomechanical properties of heart valve tissue. Four types of mechanical tests are commonly used: uniaxial, biaxial, flexure, and fatigue. Each method gives different types of information about the valve properties, and they are often used in combination to fully characterize the tissue response to loading.

Uniaxial testing was widely used in the past to quickly record basic information about the tissue mechanics. During this test, thin strips of tissue are stretched until failure. Physical properties such as elastic modulus and ultimate tensile stress are obtained. Additionally, cycling the load rather than loading until failure can be performed to produce hysteresis curves.

However, uniaxial testing does not simulate physiological conditions, as the valve experiences forces in all directions *in vivo*. Thus, uniaxial tests are inadequate to fully describe the tensile response of the tissue [2, 18].

In order to overcome the limitations of uniaxial testing, biaxial tests were introduced. Equibiaxial testing simultaneously exerts equal force in the radial and circumferential directions. Multi-protocol loading schemes were also adopted [19] to characterize the tissue when varying loads are applied in each direction. Biaxial testing allows one to calculate stiffness and extensibility values for leaflets that have been loaded in ways that better mimic physiological stress patterns. Areal strain is a measure also commonly used by Sacks et al. to characterize the change in cusp area due to the applied biaxial tension [2].

Flexure is defined as the bending or curvature of the valve leaflets. During flexure, each layer of the cusp is loaded differently; for example, the fibrosa may be in tension while the ventricularis is in compression. Flexure is generally examined with a three-point bending apparatus [20] and the cusps are marked with graphite markers to visualize the deformations. Each test specimen is bent with its natural curvature and against its natural curvature, and the stiffness and strain responses are observed [18].

Finally, fatigue testing is used to measure the valve's response to simulated cardiac cycles. The valves are mounted in silicone tubes in a chamber that pumps fluid through the system in a periodic fashion that replicates pulsatile blood flow. Accelerated fatigue tests are performed at a rate of approximately 1 million cycles per day, allowing researchers to simulate years of valve function in a matter of months. After the valves are fatigued, they undergo other assays to characterize how the tissue responded to the cyclic stresses. For example, biaxial

testing may be repeated to determine how fatigue alters tissue stiffness [18]. It has been suggested, however, that the accelerated "heart rate" used in fatigue testing alters the loading pattern on the valves, since the leaflets are not closed for as long as they would be physiologically and thus do not experience peak stresses for the same duration [18]. While this may be true, *in vitro* fatigue testing provides invaluable information about valve durability and tissue response to simulated functional conditions, and eliminates the need for large-scale animal studies to investigate valve dynamics or to screen valve prostheses. Fatigue testing can generally be considered a reliable method for assessing a valve's mechanical performance under physiologic flow conditions.

1.2.3 Heart Valve Loading Response

Over the cardiac cycle, the aortic valve experiences several types of forces. Three basic modes of loading have been characterized: tension, flexure, and shear [2]. Flexure, which is defined as bending or curving of the cusps, occurs during opening and closing of the valve. Shear occurs when blood flows through the valve orifice. The valve is in tension when it closes and must resist the backflow of blood from the aorta. The valve leaflets are fully loaded and unloaded during each cycle, which is in contrast to other tissues, such as blood vessels, which are preloaded, but do not experience significant loading cycles. Additionally, the cusps stretch significantly in response to small pressure changes during valve closure. Peak strains as high as 1000% have been observed. Once the valve is closed, deformation ceases, but the leaflets must withstand peak stresses of 50-100 N/m [2].

1.2.3.1 Tension

The unique cuspal architecture facilitates movement and enables the valve to endure the imposed stresses. The valve experiences the highest loads when it is closed and must bear the stress of blood backflow. The collagen in the cusp plays a large role in withstanding the imposed tensile forces. The alignment of collagen fibers is highly correlated to the directional extensibility and strength of the leaflets. Collagen is very strong under tension, but cannot withstand high torsional or compressive loads. The direction orthogonal to collagen alignment will be more compliant, whereas the direction parallel to the collagen fibers will be able to resist more tensile stress [21]. The circumferential alignment of the fibrosa collagen leads to higher compliance in the radial direction than in the circumferential [22]. Higher peak stretch has been observed in the radial direction (1.7) than the circumferential (1.02) [18].

As the valve is strained, the crimped collagen fibers straighten and rotate toward the axis under tension [2, 23]. Fully aligned collagen helps to prevent cuspal prolapse, while also transferring load to the aortic wall [21]. The tight, angular distribution of collagen fibers leads to a highly anisotropic leaflet with a high degree of coupling between the radial and circumferential directions. As the valve closes, the radial axis is loaded in tension, which causes the collagen fibers to rotate and leads to contraction in the circumferential direction. As the ratio of radial load to circumferential load increases, negative strains in the circumferential direction may be observed. Ultimately, the radial loading is opposed by the circumferentially-aligned collagen fibers of the fibrosa, and high radial strains result [2]. Work has been done to separate the contributions of the fibrosa and ventricularis in load-bearing. The two layers were carefully peeled apart, and then each was subjected to mechanical testing. It was observed that the

ventricularis dominates the radial response while the fibrosa dominates the circumferential response [16]. At full leaflet deformation, the ventricularis experiences twice the stress level as the fibrosa [2]. Furthermore, it was also observed that the spongiosa contains fibers that can couple the two outer layers [16].

1.2.3.2 Flexure

Flexure is the natural leaflet bending that occurs during opening and closing of the valve. During flexure, the three distinct tissue layers experience different forces and strains [2]. As mentioned earlier, flexure testing allows one to discern the individual contributions of each tissue layer to the applied stress. When the cusp is flexed in the direction of natural curvature, the ventricularis is in tension and dominates the stiffness response, whereas the fibrosa is in compression so the collagen fibers contribute little. When the cusp is bent against its natural curvature, the situation is reversed and the ventricularis is in compression while the fibrosa is in tension; thus the collagen fibers contribute highly to the observed stiffness in this case [2].

The cuspal commissures, the region where the leaflets come into contact with each other and with the aortic wall (Fig. 1.4), experience very high flexure during valve opening. When the valve is fully opened, the flexure angle is 65° in this area [24, 25]. The collagen fibers in the commissure region are more aligned than in the belly region and also align more rapidly under pressure [20]. However, the stiffness at the commissures is about 1/3 that of the belly stiffness. The stiffness at the commissures decreases with increasing opening angle to reduce the opening force. The stiffer belly region may facilitate smoother cusp movements and prevent wrinkling of the tissue [24].

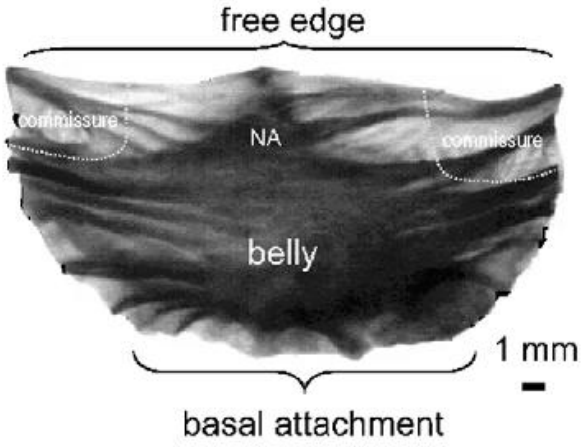

Figure 1.4: Cuspal commissures [24]

Flexural stiffness is thought to play a large role in valve durability. Large curvature of the tissue may be a failure mode of bioprosthetic valves. After 50 million fatigue test cycles, equivalent to 1.5 years of valve function, a significant loss of flexural rigidity is observed [18]. Geometrical changes in the cusps may occur during valve opening and closing, possibly resulting in kinks or buckles in the tissue, especially at areas of high curvature. Buckling is due to local collapse of the tissue, which presents histologically as notches (Fig. 1.5). Vesely et al showed that the higher the curvature of the cusp during fatigue cycling, the greater the depth of the buckles in bioprosthetic valves [12]. Thus, the ability of the cusps to flex smoothly is just as vital to proper function as the ability to bear load.

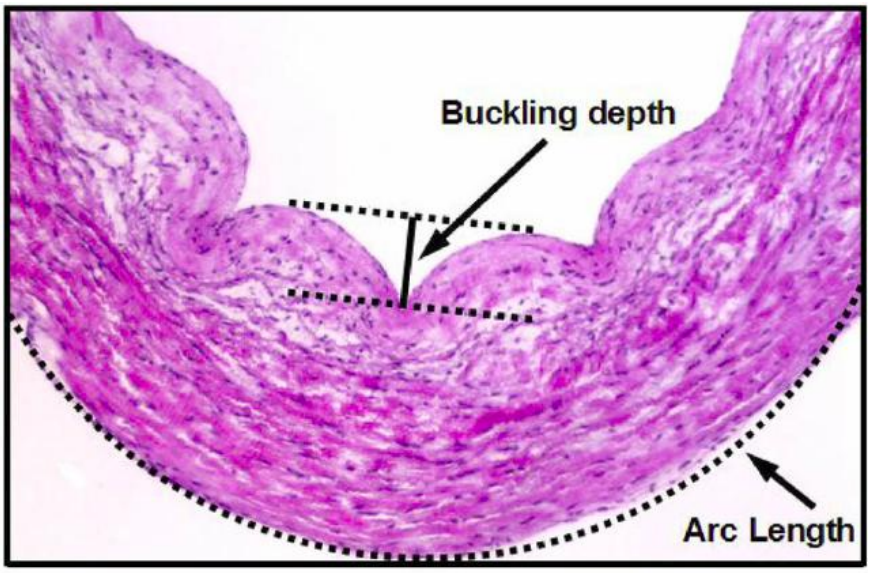

Figure 1.5: Example of tissue buckling [27]

1.2.3.3 Shear

Heart valve cusps experience complex shear forces that are generally not as well understood as the tensile and flexure stresses. During normal valve function, shear helps to reduce compression, tension, and tissue buckling [26, 28]. Shear strain is an internal slippage mechanism. The more shear the tissue experiences, the greater the decrease in bending stiffness during flexure, allowing the valve to open more smoothly with less internal stresses and less tissue buckling [29]. While the tensile properties of the cusp are dominated by the strongest layer, the shear response is dominated by the weakest layer, the spongiosa [29]. The spongiosa layer of the tissue is thought to work as a lubricant to facilitate slipping between the fibrosa and ventricularis [30]. Loss of the GAGs in the spongiosa can lead to increase stiffness due to internal bonding between the ventricularis and fibrosa. Contrarily, loss of spongiosa can also lead to delamination of the tissue layers [31, 32].

The shear properties of the cusp can be observed using uniaxial or biaxial testing. Shear stress versus shear strain curves can be plotted to calculate the hysteresis, which is a measure of viscous loss in the tissue [29]. Other viscoelastic properties, such as creep and stress relaxation, have also been studied in native valve cusps. Results show that cusps undergo high stress relaxation but little creep during three hour tests. Stress relaxation is thought to be due to the internal slipping between layers, which is modulated by GAGs and proteoglycans. The lack of creep behavior suggests that sliding can only occur under constant strain, not constant load. Thus the valve is able to withstand loading without time-dependent effects [2]. The functionality of the viscoelastic responses is still not completely understood, but it appears that shear between the tissue layers may help dissipate stress in the cusps.

1.3 Heart Valve Disease

Heart valve disease generally presents in one of two ways: improper closure of the valves which can lead to backflow (regurgitation) or incomplete opening of the valve (stenosis) [1]. The causes of valve disease are conditions that lead to alterations in the structure of the valve tissue, which subsequently cause malfunction. For example, valve disease is often associated with congenital defects, infections such as endocarditis, rheumatic fever, or atherosclerosis [33]. Thickening of the valve tissue can occur due to carcinoid heart disease or use of certain drugs, such as the diet supplement Phen-Fen [21]. Endocarditis and rheumatic fever can destroy the valve tissue and lead to regurgitation, whereas atherosclerosis leads to plaque formation and calcification that can cause stenosis or tears in the tissue [33].

Figure 1.6: Example of a diseased heart valve [34]

Valve disease is irreversible and may be fatal if left untreated. Pharmacological agents cannot prevent valve disease or help to repair damaged valves, as valve tissue is unable to spontaneously regenerate [1, 35]. Thus, heart valve replacement surgery is the only current clinically available treatment. This procedure is traditionally performed by open-chest surgery, but there has recently been a push to develop a substitute valve that can be delivered percutaneously, reducing the trauma to the patient [9]. In either case, the diseased valve is replaced by a mechanical or bioprosthetic substitute, which is intended to restore proper valve function.

1.4 Mechanical Valves

1.4.1 History and Design Evolution

Mechanical valves have been used in valve replacement for over 50 years. In 1952, Charles Hugnafel implanted the ball-and-cage valve into the descending aorta [36]. Shortly after, major advances in surgery, such as the advent of the heart-lung machine, allowed for open

chest surgery, with the first valve replacement surgery performed in Sheffield, England in 1955 [36]. These events sparked an era of major innovation in heart valve prostheses. During the 1960's and 1970's, the mechanical valve prosthesis evolved dramatically, from the early ball-and-cage valve to a tilting disc model to the bileaflet design. Improvements in materials accompanied the design changes to produce safer and more effective valves.

The ball-and-cage valve was first used in the descending aorta to treat valvular insufficiency, but did not replace the native valve. In 1960, Albert Starr and Miles Edwards improved the ball-and-cage valve so that it can be implanted in humans (Fig. 1.7) [37, 38]. The first models were made with stainless steel, but soon a cobalt-chromium alloy and later titanium became the material of choice for the cage. The ball was made from silicone. While this model was used for a number of years, improvements in the understanding of fluid dynamics and valve mechanics revealed that the design had poor hemodynamic properties. In a native valve, central flow is unimpeded, thus there is no loss of pumping energy and blood flow is efficient. However, in the ball-and-cage model, central flow is entirely impeded, leading to unnatural flow patterns, turbulence, and vortices [36]. Additionally, thrombus formation and tissue overgrowth also occurred in some patients, leading to valve failure [39].

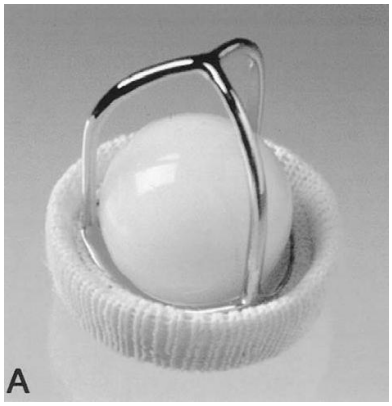

Figure 1.7: Starr-Edwards ball-and-cage valve [37]

To address the shortcomings of the ball-and-cage valve, the tilting disc model was developed in the 1970's (Fig. 1.8). The tilting disc valve is composed of a housing ring which is covered with a fabric sewing ring to facilitate implantation. A single strut and central pivot axis allow the disc to rotate in response to pressure gradients to open and close the valve orifice. The opening angle of the tilting disc is of extreme importance, as higher angles reduce transvalvular pressure gradients and lead to superior hemodynamics [36]. This model was an improvement over the ball-and-cage valve, as the tilting disc allows for partial central flow. A number of companies developed tilting disc models, and many acquisitions and buyouts ensued. In the late 1970's Pfizer took over Shiley and redesigned the Bjork-Shiley tilting disc valve. However, the redesigned valves suffered huge mechanical failures due to fracture at the outflow strut [36, 40, 41]. The valves were removed from many recipients. The cause of the failures was clarified in 1984. Apparently, over-rotation of the disc caused transient impact and bending stresses that were in excess of the valve's fatigue limit [36]. Following this disaster, strut and pivot designs were improved to reduce erosion and load impact. Today tilting disc valves are still

commercially available and manufactured by both European and American companies, including AorTech, Medical CV, Medtronic, and Sorin Biomedic [37].

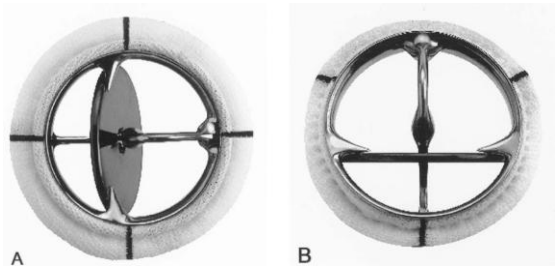

Figure 1.8: Medtronic Hall tilting disc valve [37]

While the tilting disc valve offered superior hemodynamics to the ball-and-cage valve, a major breakthrough came in 1977 when St. Jude Medical introduced the bileaflet valve (Fig. 1.9). The bileaflet valve improved central flow through the valve and also increased the valve's effective orifice area to 2.4-3.2 cm^2, as compared to 1.5 to 2.1 cm^2 in the tilting disc [36]. If the leaflets are aligned parallel to the blood stream, central flow is almost entirely unobstructed, offering hemodynamics similar to the natural valve. During the 1980's St. Jude's bileaflet valve became the most commonly implanted mechanical valve prosthesis. The bileaflet model has a number of advantages over the tilting disc, including improved flow, lower transvalvular pressure gradients, reduced turbulence, increased orifice area, and lower risk of thromboembolism [42]. The introduction of this model in 1977 marked the end of major innovations in mechanical valve prosthesis; only incremental improvements have been introduced since then.

Figure 1.9: Edwards Lifesciences bileaflet valve [37]

Along with major design modifications came improvements in material choice, as well. The early ball-and-cage valves were composed first of stainless steel, then cobalt-chromium alloy, and then titanium. It was soon observed that pyrolytic carbon used in atomic reactors was stronger and had reduced cracking. When tested in biological environments, it also showed reduced incidence of thrombosis [36]. Since the 1970's, all mechanical valves have used pyrolytic carbon either as a surface coating or to construct entire housings and leaflets. Titanium is still used for valve housing in some models. Many bileaflet models include leaflets of pyrolytic carbon coated onto a graphite substrate that is doped with tungsten to allow for radiographic imaging. Originally, silicone was added to the carbon to increase wear resistance and strength, but pure carbon was found to produce a 50% stronger material and provide a smoother surface finish [36]. In addition to the housing and leaflet material, the sewing ring fabric is also a design consideration. Since the ball-and-cage model, sewing rings have been made from Dacron, PTFE, or PET. These materials facilitate implantation and also allow for tissue ingrowth and incorporation of the prosthesis into the annulus, which helps to prevent leakage [37]. Recently a thin coating of pyrolytic carbon has been added to the sewing ring for

surface smoothness and controlled tissue growth. Sewing ring porosity, weave, and flexibility have also been modified to increase ease of implantation [37].

1.4.2 Current designs

Many of the aforementioned mechanical valve prostheses have been discontinued as design flaws are revealed or improved models are introduced to the market. However, a number of bileaflet models and a few tilting disc valves are FDA approved and commercially available in the US.

Although the bileaflet model has become the most commonly implanted mechanical valve prosthesis, the Medtronic-Hall tilting disc valve is still occasionally used. This valve features titanium housing and a pyrolytic carbon disc. The sewing ring is made from knitted PTFE or knitted PET in the EZ-Fit version. The Medtronic-Hall valve encourages more central flow than other tilting disc valves because it has a high orifice to annulus ratio. The cage material is free of welds and bends, which reduces the risk of thrombosis, and the central disc can rotate, allowing for even wear across the surface [37]. In fact, one study revealed that the Medtronic-Hall tilting disc valve reduced turbulence and increased hemodynamic performance as compared to some bileaflet valves [43], making this model competitive with the latest bileaflet technologies.

Since its introduction in 1977, the bileaflet valve has gained the favor of surgeons and is the most widely implanted mechanical valve. FDA-approved bileaflet valves are manufactured by four companies: St. Jude Medical, CarboMedics by Sorin CarboMedica Inc., Medical Carbon Research Institute (MCRI), and ATS Medical [42]. All of the valves made by these companies

utilize the same basic design, but minor differences in materials or features differentiate each model. Most design modifications focus on maximizing the orifice area for a given annular size, in order to minimize outflow gradients and produce efficient, unimpeded flow.

St. Jude offers the Hemodynamic Plus (HP) line and the newer Regent model. Both are composed of two pyrolytic carbon semi-circular discs in a pyrolytic carbon housing and Dacron sewing ring. The Regent model has a modified, low-profile sewing ring that allows a larger valve to be implanted into a small annulus. Additionally, the Regent valve may be implanted into the supra-annular rather than intra-annular position, another feature which allows for large valves to be implanted into smaller annuli. Thus, the Regent increases the effective orifice area and may provide better hemodynamics for a given annulus size [42].

The CarboMedics valve was introduced in 1986. It is made from pyrolytic carbon and has no pivot guards or struts, which helps to reduce blood flow impedance. A titanium ring around the valve housing allows for rotation to the optimal position after implantation [37]. The sewing ring is pliable and cork-shaped, which may decrease the risk of perivalvular leaks. Additionally, the CarboMedics Top Hat model was the first mechanical valve prosthesis designed specifically for supra-annular implantation [37]. Because the supra-annular space is less restricted, the surgeon may size up the implant one size larger than that which would be implanted intra-annularly. However, the CarboMedics valves have a smaller opening angle and slightly taller vertical profile than other valves, which may increase transvalvular pressure gradients and impede aortic closure [42].

The ATS bileaflet valve is similar to the St. Jude models. Its main design modification is that the pivot area that holds the hinges is not a cavity, but rather reverses outward into the blood

stream to allow better washing of the hinges and decreased stagnation, which may reduce the risk of thrombosis [44]. ATS also boasts that the valve has a lower-profile than others and reduced noise upon closing [45].

Finally, MCRI manufactures the On-X bileaflet valves. These have the largest opening angle (90°) of any valve on the market. They are made from pure pyrolytic carbon, with no silicone additives, which increases surface smoothness and decreases thrombogenicity. The valve is implanted supra-annularly, with a flared housing extending into the annulus. The flared design may minimize tissue in-growth near the leaflets while also improving hemodynamics by increasing laminar flow and decreasing hemolysis [46, 47]. Furthermore, a small amount of regurgitant blood flow is built into the design to improve washing of the hinge surfaces, thus reducing the risk of thrombosis [42].

All of these mechanical valves have proved durable in clinical studies for up to 25 years [42, 48]. The bileaflet valve will likely remain the mechanical valve standard, with minor design modifications aimed at reducing thrombosis and maximizing the effective orifice area.

1.4.3 Complications and failure modes

While mechanical valve prostheses have excellent long-term durability and hemodynamic properties, they also have several drawbacks. The most serious and prevalent complications associated with mechanical valves is the risk of thromboembolism. Foreign bodies, such as implants, in blood-contacting positions activate the blood-coagulation cascade, which can lead to clot formation (thrombosis) and possibly embolism if the thrombus becomes immobilized. Blood trauma and platelet activation may result from high shear stresses or

turbulent flow. The blood coagulation cascade ensues, leading to the production of thrombin and eventually a fibrin clot. Because the prosthetic surface is not endothelialized, clots are predisposed to form at the surface. Thrombosis generally initiates in areas of stagnation, such as around hinges and pivots [36]. To reduce thrombus in these areas, valves are designed to allow backwash of blood over the surface to help clear the surface of adherent platelets and clot materials [36, 49, 50]. With ball-and-cage valves, the incidence of thromboembolism was 4.5% per patient year [36, 51]. That statistic has been lowered to 0.6%-2.5% with the tilting disc and 1.1-3.7% in bileaflet valves [52, 53, 54]. While design modifications and material selection may help to mitigate thrombosis, the risk remains. Thus all patients receiving mechanical valves require life-long anti-coagulation therapy [36].

The American Heart Association recommends mechanical valve prostheses for patients under the age of 65 who can tolerate anticoagulants [42]. Indeed, mechanical valves are routinely implanted into pediatric patients and young adults because of their high durability. In the past there was a concern that a second replacement would be needed as the young patient grew, but new, supra-annular designs with large orifice areas may eliminate that limitation. However, the need for lifetime anti-coagulants remains the greatest weakness of mechanical valves. Proper anti-coagulation therapy with Coumadin (Warfarin) minimizes the risk of thrombosis, but bleeding complications such as hemorrhage may result [36]. The incidence rate of intracranial hemorrhage is 0.8%-3.7% per year in prosthetic valve patients [55]. At a ten-year follow-up, 15% of St. Jude Medical valve recipients had been hospitalized for hemorrhaging [56]. Furthermore, certain patients cannot tolerate anticoagulant therapy or should not be put on it because of comorbidities, possibility of pregnancy, or insufficient access to anticoagulants

[42]. Because anti-coagulation therapy presents such a major limitation to mechanical valve use, companies are attempting to design their valves to minimize thrombosis and decrease the dosage of anticoagulants required. Clinical trials are currently underway in patients receiving low or no anti-coagulation therapy, but results will not be available until 2013 [42].

In patients who follow proper anti-coagulation therapy, the most common cause of valve failure is pannus overgrowth, which causes obstructive failure in 31-53% of cases [57, 58]. Excessive tissue growth into the sewing ring can narrow the orifice or cause leaflet immobilization [36]. The cause of tissue overgrowth is not completely understood, but the inflammatory response is thought to play a large role. A chronic foreign body response to the sewing ring causes macrophages and giant cells to remain at the valve site. These cells release cytokines and growth factors that can signal a hyperplastic tissue response [59]. New valve designs have attempted to prevent overgrowth from interfering with the leaflets by making the housing cylinder longer or tapered to act as an in-growth barrier. Furthermore, coating the sewing ring with a thin layer of pyrolytic carbon may also help to attenuate excessive growth [36].

Major failure modes of mechanical heart valves are related to the aforementioned complications. Catastrophic mechanical failures such as leaflet immobilization, strut fracture, and valve immobilization have largely been eliminated by design modifications. CarboMedics valves boast a 95% freedom from valve-related mortality over 10 years, while St. Jude Medical reports a 93% freedom from mortality [60]. The need for secondary replacement of the valves is less than 2% over the 25 year period [48]. The durability of the mechanical valve has not been matched by any biological tissue valve prosthesis, making the mechanical valve preferred for

younger patients. New technology will aim to reduce the risk of thrombosis and the reliance on anticoagulants to improve the safety of these prostheses.

1.5 Tissue Valves

1.5.1 Types

Tissue-based heart valves, which are composed of fresh or preserved human or animal tissue, have been used since the early 1960's [5]. Over the years, tissue valves have become increasingly popular and are currently used in over 50% of valve replacements [61]. There are three categories of tissue heart valves: allograft, autograft, and xenograft.

1.5.1.1 Allografts

Allografts are defined as tissue that has been transplanted between members of the same species [5]. Heart valve allografts are obtained from cadavers and cryopreserved without undergoing any crosslinking. The tissue is protected during storage by freezing it in dimethyl sulfoxide to prevent ice crystal formation. The valves are stored at extremely low temperatures, usually -196°C in the vapor of liquid nitrogen [5]. Cryopreservation of the fresh tissue has several advantages, such as enabling a long shelf life and the possibility of a valve banking system. To commercialize such a product, however, the quality of the preservation process must be carefully monitored, as factors like freeze/thaw cycles and the interval between death and harvest can impact the valve's viability.

The allograft valve can be implanted in a number of ways, including into the aortic root without a stent as an isolated valve or with a full root replacement. Allografts that have been implanted into the aortic and pulmonary positions do not cause an immune response and exhibit excellent hemodynamics and a low risk of thrombosis, even without anticoagulation therapy [62, 63, 64]. However, allograft valves, like all tissue valve replacements, are subject to material deterioration, and their durability is limited by progressive degeneration. The main failure mode of allograft valves implanted into the aortic position is tissue incompetence, generally presenting as cusp rupture or perforations [5]. Although the allograft valve has not been crosslinked by any cytotoxic chemicals, valvular cells are not viable after the valve has been transplanted. It is hypothesized that cells are lost due to ischemia during harvest, the cyropreservation technique, and ischemia during surgery. These events may signal the cells to undergo apoptosis and cause massive loss of viable valvular cells [65]. Because of this cell loss, the implanted valve cannot grow, remodel, or produce active metabolic functions [66]. Fatigue failure ensues because the valve cannot repair the injuries that occur due to normal repetitive functioning. One year after implantation, the allografts exhibited flattened and thinned cusps, with no evidence of collagen crimping or corrugations. The three-layer tissue structure is not well defined and there are no obvious endothelial or interstitial cells [5]. The cusps generally do not calcify, but aortic wall calcification may be severe. Longer-term implants show similar trends, with no viable cells and calcification occurring around cellular debris. While the collagen fibers are preserved, they are distorted and lose crimp, much like crosslinked bioprosthetic valves. The allograft heart valve shows slightly better durability than the bioprosthetic valve (50-90% survival at 10-15 years for the allograft as compared to 40-60% for the bioprosthesis) [5]. However, allograft valve success

is greatly limited by the ability to preserve the extracellular matrix and prevent degenerative tissue damage.

1.5.1.2 Autografts

Autograft heart valves are prepared from the patient's own tissue. The most common type of autograft heart valve replacement is the Ross procedure, which was first performed in 1968 [5]. The surgery entails replacing the patient's aortic valve or entire aortic root with his own pulmonary valve [67]. The pulmonary valve is hemodynamically superior to any other replacement valve that may be put in the aortic position. This procedure is often performed in young patients, as it is possible that the pulmonary valve will remain viable and grow with the somatic growth of the child [68]. The transplanted pulmonary valve is generally replaced by an allograft pulmonary valve. The allograft performs better in the pulmonary position than in the aortic position because pressures and stresses are less in the pulmonary circulation than in the systemic. The cusps of the aortic autograft have been shown to retain their normal ECM architecture, and viable cells have been observed up to six years after implantation [5]. However, the aortic wall may suffer inflammation, scarring, or necrosis after the procedure. Furthermore, the pulmonary artery will experience greater pressures in the aortic position than in the pulmonary position and is not perfectly adapted to function there. Progressive remodeling of the pulmonary wall occurs, leading to progressive dilation of the valve lumen [67, 68]. However, the autograft option is still in use for young patients, since it may help to avoid secondary replacements as the patient grows.

A second type of autograft valve is made from the patient's pericardium. During surgery, a piece of the pericardium is excised and fixed briefly in glutaraldehyde to stiffen it and facilitate

handling. The tissue is then cut with a special die and mounted on a two-piece stent that snaps together to hold the leaflets [69]. However, it was found that significant scarring occurred when the pericardial tissue was subjected to high hemodynamic forces in its new environment [70]. The brief glutaraldehyde immersion mitigated this problem, but added additional concerns about leaflet stiffness and potential calcification. Results of early clinical trials were variable, with some valves lasting for years and others failing quickly due to leaflet tearing and prolapse [70]. Because of design issues and uncertain results, this procedure never gained wide popularity and has largely been abandoned.

1.5.1.3 Xenograft

Xenograft tissue is transplanted from one species into a patient of a different species. Xenograft heart valves are commonly referred to as bioprostheses and are comprised of animal tissue that has been preserved in some way, usually by chemical crosslinking [5]. While a number of crosslinking methods have been used experimentally, including β-propriolactone, glycerine, β-irradiation, polyepoxides, and photooxidation [1, 5, 71, 72,], fixation with glutaraldehyde is the method used in all commercial valves. Two types of heart valve bioprostheses are available: intact porcine aortic valves or valves crafted from bovine pericardium (Fig. 1.10)

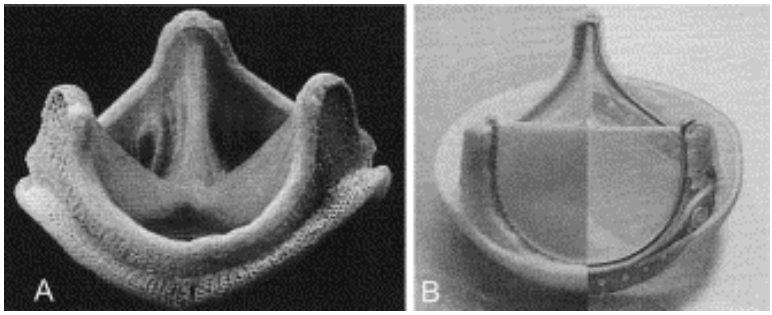

Figure 1.10: A porcine aortic valve (A) and a bovine pericardial valve (B) [70]

The cardiovascular system of pigs is similar to that of humans; thus the porcine aortic valve can be successfully transplanted between species. The glutaraldehyde-fixed valve is generally mounted in a stent or a sewing ring before implantation. Glutaraldehyde diminishes the immunogenicity of the foreign tissue, nearly eliminating the risk of immune rejection [5]. Glutaraldehyde also preserves structural elements such as collagen. The porcine heart valve contains the same three-layer, oriented tissue structure as the human valve. However, fixation in glutaraldehyde causes many alterations in tissue chemistry and mechanics, and over time the cusp architecture is damaged by fatigue. Valve durability is limited, and 50% fail within 12-15 years [73, 74].

Bovine pericardial valves differ from porcine bioprostheses in a number of key ways. Bovine valves are comprised of glutaraldehyde-treated parietal pericardium which has been cut into cusps and attached to a frame. While porcine valves are constrained to the normal tricuspid shape, the design of bovine valves is much more flexible, and unicuspid and bicuspid valves are possible [75, 76]. However, pericardial valve fabrication may also affect durability. The porcine aortic valve is naturally intact, but the pericardial valve is trimmed and attached to a stent. The attachment points may be weak areas that have a higher risk of tearing. Also, the trimmed surfaces at the inflow and free edge of the cusp usually exhibit collagen splaying during function. Loss of integrity at the edge may facilitate an influx of host cells and fluid, which could have implications in inflammation and calcification [5]. Despite these complications, the bovine pericardial valve remains an attractive option, especially for new technologies like percutaneous

valves, because it offers greater design flexibility than the porcine aortic prosthesis. Pericardial valves also offer better hemodynamics than the porcine aortic xenograft valve. While the porcine valve naturally coapts due to radial extensibility caused by collagen alignment, the pericardial collagen is unoriented, so the cusps do not naturally coapt. Thus, a coaptation mechanism is built in: the three leaflets are fabricated as three sections of a cylinder and are aligned parallel to the blood flow. During closure, the three edges of the cylinders are pressed together and during opening, the cylinders reverse curvature and snap open to reveal a wide, circular orifice [70]. This coaptation mechanism imparts excellent hemodynamics, but can also be a weakness of pericardial valves. If one leaflet experiences greater stresses and stretches more than the others, it may prolapse slightly so that the three leaflets do not align and seal together properly. Single leaflet prolapse is a major cause of early cusp rupture in bovine pericardial valves [70]. However, as both porcine and bovine valves have advantages and disadvantages, both models are commercially available and used clinically today.

1.5.2 Current bioprosthetic designs

Several types of bioprosthetic heart valves are FDA-approved and commercially available. Porcine, bovine, and autograft valves are all currently implanted. The models differ by fixation procedures, anti-calcification treatments, and use of stents. Figure 1.11 classifies today's clinically available valve prostheses.

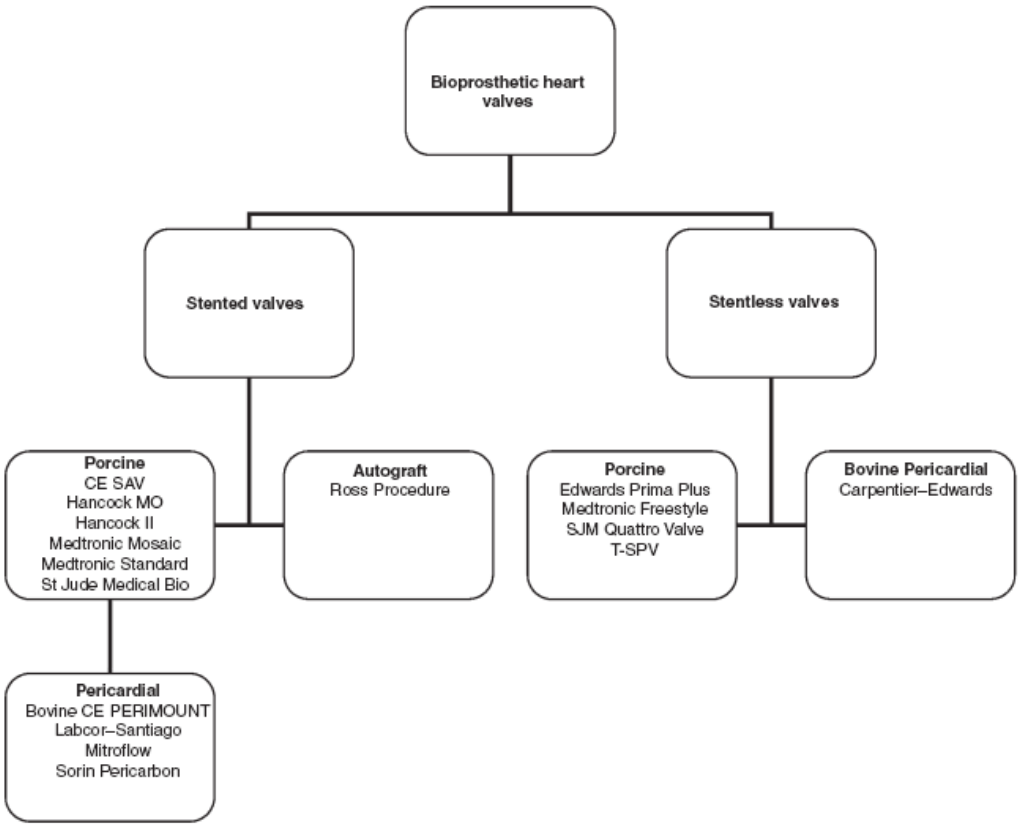

Figure 1.11: Classification of bioprosthetic valves [77]

Bioprosthetic valves are broadly separated into two categories: stented and unstented. Most first and second generation bioprosthetic valve models are mounted on a stent, which is made from plastic or a metal, such as a cobalt-nickel alloy [77]. The stent is additionally covered in a Dacron skirt, which prevents stent thrombogenicity and facilitates implantation by sewing. The stent also renders the valve easier to handle and minimizes the surgical duration. However, the stent and the sewing fabric both take up space in the annulus, leading to a smaller orifice area that may lead to residual stenosis [77]. Additionally, the stent may restrict aortic wall expansion and contraction, leading to abnormal hemodynamics [70]. Thus, stentless valves

were adopted in many third generation bioprostheses. Edwards Lifesciences manufactures the Carpentier-Edwards stentless bovine pericardial valve. Several stentless porcine valves are also marketed, such as Edwards Prima Plus, Medtronic Freestyle, and St. Jude Medical's Quattro and Toronto valves [77]. Stentless porcine valves are fabricated by excising the entire aortic root and aorta, and trimming it to the desired profile. A Dacron cloth may still be included around the base. Because the stent has been eliminated, there is more room in the annulus for a larger valve to be implanted, thereby increasing the effective orifice area of the valve. The movement of the prosthetic valve in the annulus is less constrained and improved hemodynamics have been noted. However, significantly more aortic wall is exposed to blood flow than in the stented valves, and aortic wall calcification has been a major limitation of the stentless model. Rapid calcification after implantation causes the root to stiffen, eliminating the advantage of greater flexibility [70]. The benefits of stentless valves are highly debated and clinical outcomes are widely variable [78]. Thus, stentless valves have not replaced stented valves, and the choice of implant is based on the surgeon's preference.

Prosthetic valves also differ in fixation mechanism. While all valves are crosslinked with glutaraldehyde, the concentration and duration of the treatment varies slightly between companies [5]. Additionally, the back pressure applied to the valves during fixation can also be a factor in valve performance. First generation valves were fixed under a pressure of 80 mmHg, which is equivalent to systolic blood pressure [70]. However, it was later discovered that high-pressure fixation produces cusps that are very stiff and subject to significant tissue buckling during functioning [16, 18, 26]. Fixation pressures as low as 4 mmHg can produce these detrimental effects. Consequently, in the 1980's, low-pressure fixation was used in second-

generation valves, producing more flexible valves with improved mechanical properties [70]. Zero-pressure fixation has also been used, for example in Medtronic's Intact valve [79]. These valves only coapt when back pressure is applied. Furthermore, when the aortic root is depressurized, its elastic fibers recoil and the orifice collapses by about 35%. This leads to excessive leaflet area in the annulus, which may be obstructive during valve opening [11]. A solution to this problem has been to fix the leaflets at zero pressure while pressurizing the valve root at approximately 40 mmHg [70]. This technique is employed by Medtronic in its Freestyle and Mosaic valves [80].

Finally, bioprosthetic valve manufacturers use anti-calcification technology to differentiate their products. Calcification of the cusps and aortic wall is a critical factor in tissue deterioration and valve failure [77]. Medical device companies aim to improve the durability of their valves by reducing the risk of calcification. Medtronic treats its valves with 2-alpha-amino-oleic acid (AOA), which binds to the tissue to inhibit calcium influx [81]. However, AOA has been shown to only prevent calcification of the cusps, not the aortic wall. To address both cuspal and aortic calcification, St. Jude Medical uses a two-part treatment on its valves. The valves are first treated with aluminum chloride which prevents aortic wall calcification and then with an ethanol solution, which prevents cuspal calcification [82]. Edwards Lifesciences, on the other hand, uses a proprietary process called XenoLogiX to remove calcification-initiating phospholipids from the tissue. The treatment is a combination of ethanol and polysorbate-80, which is a surfactant [83]. The mechanisms of action of each of these treatments will be discussed below. Each method has been successful at reducing calcification and extending the average lifetime of the prostheses.

In summary, the current market for bioprosthetic heart valves is dominated by three major companies: Medtronic, St. Jude Medical, and Edwards Lifesciences. Each company offers stented and stentless valves. St. Jude and Medtronic deal mainly with porcine aortic valves while Edwards offers both porcine and bovine models. All of today's models employ glutaraldehyde fixation under low back pressure. Thus, the main feature differentiating each company's valves is the anti-calcification technology.

1.5.3 Complications and failure modes

While bioprosthetic heart valves have benefits over mechanical valves, such as being nonthrombogenic and eliminating the need for anti-coagulation therapy, they are not as durable as the mechanical model, and progressive tissue degeneration is the main failure mode [5]. Over half of bioprosthetic valves fail in adults 10-15 years post-implantation [73]. In patients less than 35 years old, and especially in children and teenagers, tissue deterioration and failure occur much more quickly due to a stronger immune response and higher metabolic activity [1]. Bioprosthetic valve failure is generally caused by four major complications, which may act alone or synergistically: endocarditis, calcification, mechanical malfunction, and pannus overgrowth [77].

1.5.3.1 Endocarditis

Infective endocarditis can affect both mechanical and bioprosthetic valve implants. The risk of infection is greatest in the first two years after implantation and is more common in patients who have previously experienced endocarditis [77]. The incidence of infection is approximately 1-6%, and a multitude of microorganisms, including Streptococci, Staphylococcus

epidermidis, Gram-negative bacilli, and fungi, have been reported to cause endocarditis [77, 84]. Infection usually begins in the sewing ring and then spreads to the cusps, potential leading to tears and valvular insufficiency. Endocarditis is diagnosed based on the presence of microorganisms, vegetations, fibrosis, necrosis, and calcification. In addition to valvular incompetence, the infection can cause congestive heart failure and embolism, and has a 60% mortality rate if valve replacement surgery is not performed [85]. However, infective endocarditis is an acute condition that affects a limited subset of patients and is not considered a major cause of long-term tissue degeneration and valve failure.

1.5.3.2 Calcification

Calcification is one of the main causes of valve failure (Fig. 1.12). Approximately 75% of porcine valve degenerative failures present as regurgitation due to tears in calcified cusps. Pure stenosis due to calcification causes failure in 10-15% of valves. Tears and perforations unrelated to calcification cause calcification in only 10% of valves [86]. Thus, calcification is a major factor in valve performance and durability.

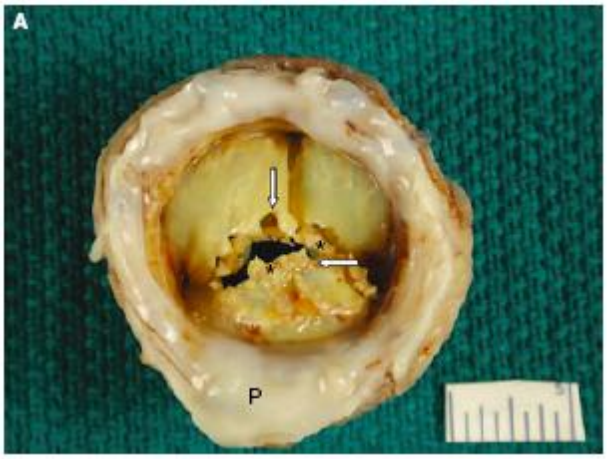

Figure 1.12: Calcified heart valve prosthesis [77]

It is generally accepted that four main factors—glutaraldehyde, cellular injury, matrix composition, and mechanical stress—are responsible for pathologic calcification of bioprosthetic heart valves [87]. Glutaraldehyde-induced devitilization of the tissue leads to loss of cellular calcium regulation, which has a significant impact on calcification potential [88]. In healthy cells, the intracellular calcium concentration is approximately 1000 times below that of the extracellular calcium concentration. The gradient is maintained by energy-requiring processes such as calcium ion pumps [88]. Glutaraldehyde is cytotoxic and devitalizes the valvular cells. Following glutaraldehyde fixation, all energy-requiring processes, including calcium regulation, are eliminated. Studies show that glutaraldehyde permeabilizes the cell membrane, causing intracellular calcium levels to increase in a dose-dependent manner immediately after glutaraldehyde exposure [87]. Since the cell's natural calcium pumps are not functional, the cell cannot extrude the extra calcium, and intracellular calcium concentrations increase dramatically.

Phosphorous concentrations are normally greater inside the cell than outside, but glutaraldehyde fixation also causes an influx of phosphorous. When intracellular concentrations of calcium and phosphorous reach sufficiently high levels, nucleation of hydroxyapatite crystals occurs [87]. Phospholipid-rich bodies, such as the plasma membrane and organelles, are nucleation sites for calcification [88]. The calcium deposits at each nucleation site grow larger and eventually can converge into nodules that stiffen and weaken the tissue [86].

In addition to devitalized cells and cellular debris, extracellular matrix proteins, such as collagen and elastin, have also been implicated in calcification [86]. However, glutaraldehyde is likely also responsible for matrix calcification, since non-glutaraldehyde-treated tissue and Type

I collagen sponges do not calcify *in vivo* [89]. When glutaraldehyde devitalizes the tissue, it removes cellular components, exposing matrix sites for mineral nucleation [89]. Loss of matrix material from the fixed tissue over time may also contribute to mineralization. For example, glycosaminoglycans (GAGs) are not stabilized by glutaraldehyde. GAG degradation may expose calcifiable sites in the extracellular matrix, leading to further nucleation [90]. Furthermore, calcification and mechanical stress may work synergistically to cause tissue deterioration. Calcification is generally enhanced in areas of high mechanical stress [86, 87]. Cyclic deformations may allow a greater influx of calcium ions, as well as calcium deposit migration and aggregation in deformed areas [87].

The extent of calcification is highly variable among patients, although calcific deposits can often be seen histologically within three years of implantation [77]. Pathologic calcification can produce disastrous consequences, such as severe tissue stiffening, stenosis, and cuspal tears. Due to the prevalence of calcification-related valve degeneration, most commercially available bioprosthetic valves undergo anti-mineralization treatments. Medtronic valves are treated with two-alpha-amino oleic acid (AOA), a detergent that binds to residual aldehyde groups to become incorporated into the tissue. AOA works by altering calcium influx kinetics, significantly inhibiting the penetration of calcium ions into the tissue. Furthermore, AOA disrupts the interactions between calcium and phosphorous, thereby suppressing crystallization [91]. However, the aortic wall is resistant to AOA penetration, and its calcification potential is not significantly decreased by AOA. Thus, AOA is effective only in inhibiting cuspal calcification [86]. Similarly, the method of ethanol pretreatment, used by both St. Jude Medical and Edwards Lifesciences, is only effective on the cusps. Ethanol extracts phospholipids and cellular debris

from the valve tissue, thus reducing the number of available mineralization nucleation sites [92]. Edwards Lifesciences combines the ethanol with polysorbate-80, a surfactant that also targets phospholipids. Edwards XenoLogiX treatment of ethanol and polysorbate-80 is reported to remove 95% of phospholipids from the valve tissue [83]. While this greatly reduces the cell-related calcification that is prevalent in the cusp tissue, aortic wall calcification may still be problematic. Thus, St. Jude Medical additionally treats its valves with aluminum chloride. Metal ions such as iron and aluminum can complex with phosphate ions and prevent binding of calcium, thus inhibiting calcium phosphate crystallization [5]. Aluminum chloride also binds to elastin to cause a structural change which renders the molecule resistant to crystal deposition. Since the aortic wall has a high elastin content, aluminum chloride treatment is especially effective at limiting calcification at the wall [1,5]. Currently, St. Jude Medical is the only company whose anti-calcification treatments target both the aortic wall and cusp tissue. While each of the aforementioned treatments are clinically effective in reducing pathologic calcification, none can completely eliminate mineralization; thus, calcification-related tissue degeneration remains a major contributed to failure of third-generation heart valve prostheses.

1.5.3.3 Mechanical malfunction

While cuspal tearing and structural degradation are often associated with calcification, material degeneration can occur independently of mineralization. The bioprosthetic heart valve experiences great stresses during valve function and must endure over 30 million loading cycles per year [1]. Over time, stress-induced material fatigue can lead to disruption of the extracellular matrix structure, resulting in loss of tissue integrity, tears, perforations, and ultimately

mechanical failure [93]. Additionally, enzymatic activity can mediate degradation of certain structural components [30]. Since valvular cells are devitalized by glutaraldehyde fixation, the tissue structure is entirely dependent on the integrity and preservation of the extracellular matrix components, such as collagen, elastin, and glycosaminoglycans. As the valves lack viable cells, there are no repair or regeneration mechanisms in place to reverse damage once it occurs. Material deterioration by fatigue and proteolytic enzymes is a progressive process, and damage accumulates during valve functioning. Thus, valve durability is largely determined by the quality of the preserved matrix.

Flexure stress is hypothesized to play a large role in valve durability. A loss of flexural rigidity is observed after approximately 50 million *in vitro* fatigue cycles, equivalent to 1.5 years of function [18]. Although tissue fixation with glutaraldehyde causes an undesirable increase in leaflet stiffness, loss of flexural rigidity in fatigued tissue can also be problematic. The observed increase in flexural compliance may be due to alterations in the tissue structure, such as debonding of collagen fibers or a loss of glycosaminoglycans [32]. Indeed, there is evidence for glycosaminoglycan loss in fixed tissue, as delamination between the fibrosa and ventricularis has been observed in fatigued cusps, likely due to the deterioration of the binding GAG layer [18]. Additionally, the decrease in stiffness may be due to tissue buckling, a local collapse of the tissue in highly flexed regions [24]. Thus the loss of flexural rigidity is indicative of detrimental changes in tissue composition and structural integrity.

Valve function and tissue fatigue also affect the biaxial mechanical properties of the tissue. In contrast to the loss of flexural rigidity, a decrease in material compliance in the radial direction is observed following fatigue [18]. A significant decrease in radial stretch occurs after

approximately 200 million cycles, but no corresponding change in circumferential compliance has been noted. This response may be explained by a stiffening of the collagen fibers and an overall change in fiber alignment with stress [18]. Again these results indicate that valve function greatly alters the structural and mechanical properties of the preserved tissue.

The observed changes in tissue mechanics after fixation and fatigue indicate that a purely mechanical failure mode exists in bioprosthetic valves. The cusps experience high tensile stresses during closure and flexural stresses during opening. The cyclic nature of valve function leads to tissue bending and flexural fatigue that causes progressive structural damage, which can eventually result in cuspal tearing [70]. Explanted valves showing mechanical degeneration with little to no calcification are frequently collected [94]. However, mechanical fatigue can also act synergistically with calcification to produce tissue damage. Disruption of the collagen architecture during flexing may expose new calcium binding sites on the collagen, promoting further calcification of the matrix [95]. Thus the two main modes of valve degeneration—calcification and material fatigue—can act together or independently to produce valve failure.

1.5.3.4 Pannus overgrowth

Following bioprosthetic valve implantation, the host tissue grows into the stent and/or fabric sewing cuff at the valve base. This response is a normal part of healing after surgery, and a small amount of tissue in-growth is desirable to produce a nonthrombogenic implant surface [96]. However, abnormal growth of the tissue (pannus) can be problematic if it extends to the cuspal region. Initial pannus growth is likely initiated by inflammation following surgical injury and involves fibroblast, myofibroblasts, and endothelial cell infiltration [77]. As the pannus

develops, collagen is deposited in the deep tissue layers. Eventually the collagen will retract and alter the tissue structure. Overgrowth of the pannus onto the cusp surfaces leads to cuspal thickening (Fig. 1.13), increased stiffness, and ultimately stenosis [96].

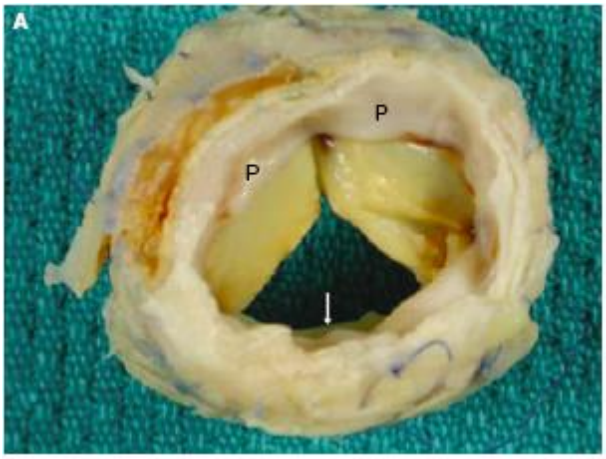

Figure 1.13: Pannus overgrowth onto the cusps is represented by P's [77]

Pannus growth onto the commissures can be especially problematic, as the tissue can produce attachments between adjacent cusps, fixing them in place and limiting opening [77]. Overgrowth at the commissures also moves the stress concentration away from the commissures and onto the cusps, possibly resulting in cuspal tears. Furthermore, when the pannus collagen contracts, valvular insufficiency can result if the cusps also retract. Pannus overgrowth has been shown to affect both mechanical and bioprosthetic valves, but may be a complication observed more frequently in stentless valves than in stented, as the stent thickness may provide somewhat of a barrier between the pannus and the cusps [97].

In summary, the major complications and failure modes associated with bioprosthetic heart valves are calcification and mechanical degeneration, and to a lesser extent, endocarditis and pannus overgrowth. Thrombosis of bioprosthetic valves is rare, but the risk of thrombosis

may be greater for bovine pericardial valves than porcine valves due to the rough surface on the inflow side of the bovine cusps [77]. The other aforementioned failure modes generally affect bovine and porcine prostheses with approximately equal frequency, and the average lifespans of these two valve models are similar. Stentless valves, on the other hand, may be more susceptible to certain complications than stented valves. Because a greater portion of the aortic wall is exposed in the stentless model, wall calcification and pannus overgrowth may be more severe [96]. While design modifications and chemical pretreatments have somewhat mitigated thrombosis, calcification, and tissue degradation, bioprosthetic valves still lag behind mechanical valves in terms of durability.

1.6 Percutaneous Heart Valves

Although current replacement heart valves are life-saving devices that have been widely implanted since their introduction in the 1950s, they still have limitations that constrain their use to certain patient populations. For example, bioprosthetic heart valves lack the durability required for use in young, growing patients, while mechanical heart valves necessitate lifelong anti-coagulation therapy, which may be dangerous in the elderly or patients with bleeding risks. Additionally, over 50% of bioprosthetic heart valves fail 10-15 years post-implantation [73]; thus, aged patients with failing prostheses may need a second surgery to replace the original implant. However, the traditional implantation procedure is very invasive, requiring opening of the chest cavity, induced cardiac arrest, and the use of a heart-lung machine. Patients who are at high operative risk, such as the elderly or those with serious comorbidities, may be denied valve replacement, a possibly life-saving surgery. Studies reveal that over 50% of elderly patients with

aortic stenosis (AS), a disease that is generally treated by valve replacement, are not offered surgery because the risk of mortality is too great [6, 7]. The proportion of patients with asymptomatic AS who are denied surgery is even greater; however, asymptomatic AS is not a benign condition. The EuroHeart survey found that the five year survival rate in patients with untreated asymptomatic AS is only 38%, compared to 90% in patients that receive aortic valve replacement [8]. These findings indicate that a need exists for a less invasive valve replacement option for patients who are not favorable candidates for traditional open heart surgery. Percutaneous surgery, a minimally invasive technique employed during angioplasty, aortic aneurysm repair, coronary stenting, and vascular graft placement, is one such option that has been gaining attention in recent years.

1.6.1 History

Percutaneous intervention for the aortic valve is not a new idea. Balloon aortic valvuloplasty (BAV) was developed in the 1980s to enlarge the orifice area of stenosed valves [98, 99]. Similarly to balloon angioplasty, BAV involved threading a balloon through a catheter to the aortic annulus and expanding the balloon to widen the constricted space. However, BAV only marginally reduces symptoms and improves orifice area and hemodynamics. In initial studies, complications were observed in 5-10% of patients, with many suffering from restenosis within 6-12 months postoperatively [100, 101]. No additional survival benefits were imparted with BAV, and it was not clinically adopted as a stand-alone therapy. However, much like stenting after coronary balloon angioplasty, the idea of valve replacement after BAV began to develop.

Percutaneous aortic valve replacement (PAVR) was first performed experimentally in pigs by Andersen et al in 1992 [102]. A porcine bioprosthesis was mounted in a wire stent and delivered to various aortic sites. Initial results showed good hemodynamic performance of the percutaneous heart valves (PHVs), but years of design optimization and implantation technique refinement were necessary before the feasibility of PAVR in humans could be assessed. Ten years after the first study by Andersen, Cribier et al performed the first successful PAVR in humans [103]. Following Cribier's success, a number of studies of balloon-expandable and self-expanding PHVs ensued [104-107]. Currently, at least 17 PAVR studies are underway; among these, two are in clinical trials and at least seven have reached the first-in-man phase [9].

1.6.2 Implantation techniques

The main benefit of PAVR is that it does not require open heart surgery. Thus it reduces operative risk and patient recovery time. Because PAVR is minimally invasive, it can be performed on patients that are considered poor candidates for traditional surgery. The basic surgical technique for PAVR involves threading a catheter to the aortic annulus, performing BAV to widen the orifice, and then expanding a stent-mounted valve in the annulus [9]. Unlike traditional bioprostheses, which are sewn in place, PHVs are fixed in place by the radial force exerted by the stent [108]. The device is visualized and positioned with fluoroscopy, aortography, and transesophagael echocardiography [9]. Although the heart is not stopped during PAVR, blood flow must be arrested to prevent the balloon and prosthesis from being propelled forward during ventricular systole. Flow arrest is achieved by pacing the right ventricle at 200 beats per minute with a temporary pacemaker [9]. While the steps outlined are

common to all PAVR methods, variations in the annulus access route are possible. Three different approaches to PAVR have been considered: antegrade transseptal, retrograde, and transapical.

The first PHVs were implanted via the antegrade transseptal technique. This procedure entails catheter access via the femoral vein. The catheter is then threaded up into the right ventricle, and the septum is punctured to gain access to the left ventricle. The catheter is steered through the mitral position and up to the aortic annulus, where it is placed antegrade across the aortic valve [108]. This method is technically difficult and presents a high risk of mitral valve injury, which could lead to mitral regurgitation, hemodynamic malfunction, and death [104, 107]. Due to the risks of the antegrade transseptal approach, a retrograde technique was adopted.

The retrograde method requires arterial access via the femoral artery. The catheter is then steered to the aortic annulus retrograde through the aortic arch [106]. The REVIVAL II clinical study found that the retrograde PAVR technique had an 86% success rate, with a steep learning curve, as the second 25 patients operated on fared better than the first 25 [109]. While this approach avoids mitral valve injury and is generally considered safer than the antegrade method, the retrograde route is not without limitations. First, a highly flexible, deflectable, and steerable catheter must be used to navigate the tortuous arterial system. Furthermore, patients with aortic stenosis or failed bioprostheses often suffer from arterial diseases such as atherosclerosis and vascular and valvular calcification that can narrow the vessels and prevent delivery of the large-profile prosthesis and catheter [9, 106, 108]. The risk of arterial injury is high, especially in patients with unusually narrow or tortuous vasculature. These complications

can preclude a patient from retrograde PAVR. The transapical approach was developed to overcome the limitations of the antegrade and retrograde methods.

The transapical approach is the method of choice in patients with small or tortuous femoral and iliac arteries or those with severe peripheral vascular disease [108]. Rather than accessing the vascular system via the femoral vein or artery, the heart is accessed via a thoracotomy in the sixth intercostal space. The pericardium is opened and a small puncture is made in the left ventricle. The catheter is threaded through the left ventricle and to the aortic annulus, where BAV and device placement are performed as described above. After the valve has been successfully positioned, the pacemaker is removed, the pericardium and thoracic cavity are closed, and a chest tube is left in overnight to ensure drainage [108]. In a clinical trial of 59 patients, the transapical route showed a 90% success rate, with a mortality rate similar to the transarterial approach [9]. This method produces less arterial injury, more direct access to the aortic annulus, and easier manipulation of the valve as compared to the retrograde method. Currently choice of surgical technique depends on patient factors and surgeon preference, but a standardized method may soon be decided upon, as studies to compare patient outcomes between the two procedures are ongoing [9].

1.6.3 Current designs

1.6.3.1 Clinically tested

Two PHVs, Edwards SAPIEN and CoreValve, have reached clinical trials. The two models differ in material and also expansion technique. Edwards SAPIEN (previously known as Cribier-Edwards) made by Edwards Lifesciences Inc. is a balloon-expandable PHV that is

comprised of three pericardial leaflets. Originally, the leaflets were made of equine pericardium, but the material was switched to bovine pericardium in second generation models [9]. The leaflets are mounted on a slotted, stainless steel tubular stent (Fig. 1.14) [103-106, 109]. A fabric cuff encircles the portion of prosthesis that is implanted proximal to the left ventricle [106]. The valves are stored in glutaraldehyde and are supplied to the surgeon in the expanded state. Preparation of the implant is required prior to surgery. A specially-designed crimping device is used to mount the valve onto the balloon catheter. Orientation of the valve depends on the approach used—retrograde transarterial or antegrade transvenous [106].

Figure 1.14: Edwards SAPIEN PHV [106]

The Edwards-SAPIEN PHV is available in two expanded diameters: 23 mm or 26 mm. The heights of these prostheses range from 14.5 mm to 16 mm. Femoral access sheaths between 22F and 24F are needed to accommodate the device. Because of the relatively large profile of the device, patients with iliac arteries less than 8 mm in diameter are not candidates for implantation via the transarterial approach [106]. Transapical implantation of the Edwards-SAPIEN has proven to be a successful alternative [9].

The second PHV in clinical testing is CoreValve (Fig. 1.15) (Medtronic CoreValve, LLC). CoreValve is also a pericardial, trileaflet valve, but differs from Edwards-SAPIEN in a number of key ways. The most prominent difference is that CoreValve is self-expandable and does not require a balloon catheter for implantation. This property is conferred by the stent, which is made from Nitinol, a shape-memory nickel-titanium alloy that expands at body temperature. The device can be described by three sections: the lower inlet portion produces a high radial force upon expansion to push aside the native leaflets; the middle portion of the stent carries the valve; the upper outlet portion is flared to securely fix the device in the ascending aorta [9]. In first generation valves, the leaflets were made from bovine pericardium and required a 25F sheath for transarterial implantation. Second generation valves utilized porcine pericardium instead, allowing for a 21 F catheter to be used [9]. An alteration in how the tissue is fixed to the stent in third generation valves has allowed for a device profile of 18F [10, 105]. The small profile enables PAVR to be performed without hemodynamic support, rapid pacing, or vascular repair of the access site [9]. Second and third generation valves have shown improved success rates, likely due to the smaller profile and operator technique improvement [10]. However, even with the thinner device, some patients are still not candidates for transarterial surgery, so transapical studies with CoreValve are in first-in-man trials [110].

CoreValve has not only been used to replace stenotic native valves or degenerated bioprostheses, but has also been deployed into another CoreValve implant. The duel implant maintained proper function and hemodynamics at three years follow-up [111], proving the feasibility of "valve-in-valve" replacement. This is an important feature of CoreValve, as this

type of secondary replacement is safer than reoperation and may be a treatment option for degenerative original implants [9].

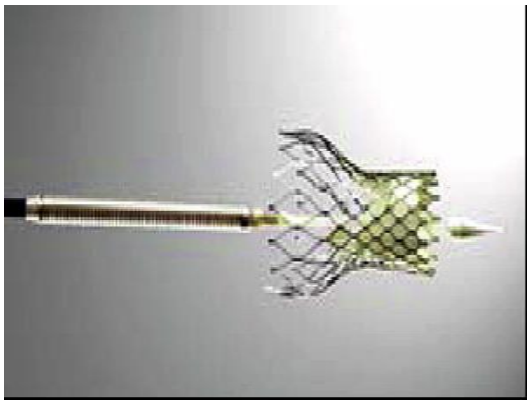

Figure 1.15: CoreValve PHV [9]

1.6.3.2 First-in-man studies

A number of PHVs have proven successful enough in preclinical studies to progress to the first-in-man testing phase. The Paniagua valve from Endoluminal Technology Research has leaflets made from pericardium and is available with a balloon-expandable stainless steel stent or a self-expanding nitinol stent [112]. The Enable self-expanding valve from ATS is similarly a pericardial valve in a simple Nitinol tube. Hansen Medical also makes a nitinol valve, the AorTX. However, this PHV has an additional feature of being repositionable by recapturing the expanded valve and deploying it a second time. The feasibility of the device and its hemodynamic properties were proven in eight patients, who temporarily received the AorTX before undergoing traditional valve replacement surgery [9]. The Direct Flow Valve by Direct Flow Medical has been tested on both temporary and permanent bases. This unique valve is neither balloon- nor self-expandable. Rather, bovine pericardial tissue is sutured in a flat

cylinder between two hydrophilic, coated rings. The device is repositionable and retrievable before it is permanently fixed in place by inflating the rings with a polymer [113].

Sadra Medical has developed the self-expanding Sadra-Lotus valve. This valve is repositionable by means of a two expansion phases. The valve first passively expands and shortens to facilitate positioning, and then actively shortens to increase the outward radial force and lock it in its final position [114]. Another unique self-expanding PHV is Perceval by the Sorin Group. This valve has two portions that function independently of each other. The self-expanding portion of the stent approximates the anatomy of the aortic root and sinuses to securely hold the device in place, while the non-expandable posts support the pericardial leaflets. A double layer of pericardial sheets is included to seal the space between the stent and wall and prevent perivalvular leaks [9].

All of the aforementioned valves have been tested in humans, albeit on a short-term basis and in a limited number of patients. These first-in-man trials are used as proof-of-concept tests to show the feasibility of implantation and the generally safety and efficacy of the device. While initial findings may be promising, large-scale and long-term clinical trials are necessary.

1.6.3.3 Experimental technologies

In addition to the PHVs that have reached clinical and first-in-man testing phases, many more experimental PHV technologies are being investigated. Some of these have been examined in animal models, while others are only in the *in vitro* developmental stage. Heart Leaflet Technologies is developing a repositionable nitinol valve with an inverted mesh design and anti-regurgitation collar (Fig. 1.16a). Zegdi et al constructed a new delivery system for nitinol valves

that allows the valve to be repositioned and also oriented with the particular angles of the native valve [115].

Tissue engineering approaches are also being considered for PHVs. However, tissue-engineered heart valves made from decellularized tissue often fail due to matrix damage by the decellularizing process and difficultly in encouraging cells to repopulate the scaffold *in vivo* [116, 117]. A new method being studied is *in vitro* seeding of bioadsorbable scaffolds with fibroblasts and endothelial cells; this technique has shown initial success in animal models [118].

Finally, nanotechnology is being used to develop new materials with specific properties tailored to optimal PHV function. The PercValve (Advanced Bioprosthetic Surfaces) utilizes a nano-synthesized elastic nitinol to construct the frame and leaflets (Fig. 1.16b). Animal studies showed that this special nitinol undergoes rapid re-endothelialization as early as two weeks after implantation. Despite the presence of metallic leaflets, thrombosis was not a problem. This data suggests that the PercValve could potentially offer the durability of a mechanical valve without the complications of anti-coagulation therapy [9].

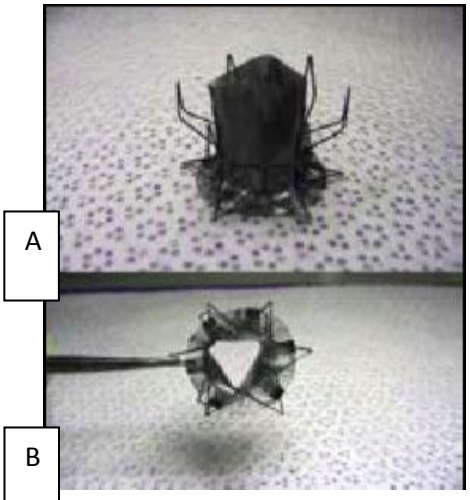

Figure 1.16: Experimental PHV Models: a) Heart Leaflet Technologies; b) PercValve

1.6.4 Pericardium as a bioprosthetic material

Pericardial tissue has been used almost exclusively in percutaneous heart valves because it offers the benefit of adaptable designs, rather than being constrained to the natural trileaflet structure like the porcine aortic valve. The pericardial leaflets can be attached to flexible stents in a wide array of configurations to produce a valve that can be crimped down and delivered percutaneously. However, the tissue architecture of bovine pericardium is not identical to that of the native valve.

Pericardium lacks the three-layered tissue structure—its thickness is almost entirely collagen-containing fibrosa. The collagen bundles are interspersed with elastin fibers and blood vessels [Fig. 1.17]. The inner surface of the pericardial sac is composed of a thin layer of loose tissue called serosa, which lubricates the surface [119]. Pericardial tissue also contains only small amounts of glycosaminoglycans, indicating that these molecules may play a less critical role in pericardial mechanics than in heart valve mechanics [120]. Additionally, the tissue surface of pericardium is different than the cusp surface. One surface of the pericardium is smooth, while the other is rough since blood and fat have been trimmed away from it. The rough surface could potentiate thrombosis, so it is generally oriented toward the valve inflow to increase surface washing [2]. These differences in tissue architecture may affect the durability of pericardial valves in the long run.

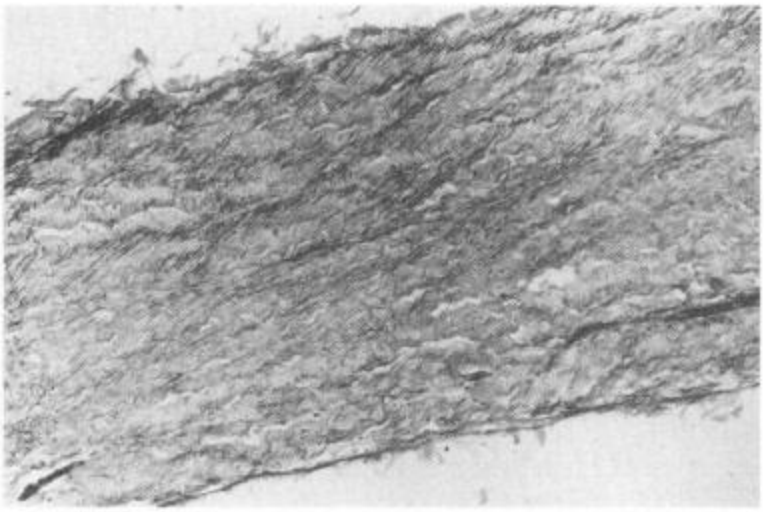

Figure 1.17: Cross-section of bovine pericardium [119]

The mechanical properties of bioprosthetic tissue are mainly determined by the extracellular matrix, especially collagen. Pericardial collagen is less compact than collagen in the cuspal fibrosa and is almost entirely type I collagen, whereas heart valve cusps contain both type I and type III collagen [121, 122]. Furthermore, the pericardial collagen is not well oriented, so the pericardial cusps are not well-adapted for enduring the pressures of cardiac functioning. A model of pericardial mechanics by Zioupos and Barbenel showed that the collagen and elastin fibers in each individual layer of the pericardium are directional, but taken as a whole, there is no dominant direction of fiber alignment in the tissue [123]. Figure 1.18 shows the various orientations of collagen fibers under polarized light. Sacks et al. demonstrated that different sections of the pericardium have preferential collagen orientations. For example, in the left frontal region, the circumferential direction predominates, while in the right frontal region, the apex-to-base direction predominates [124]. The wide variation in collagen direction makes it difficult to select pericardial tissue that is homogeneous enough to guarantee the desired

mechanical properties [125]. Highly-aligned collagen in aortic valves helps to transfer stresses from the cusp to the aortic wall, but pericardium lacks this feature, so stresses accumulate at the cuspal commissures [5]. Since collagen is less aligned in the pulmonary valve than in the aortic valve, pericardial prostheses may be better suited for the pulmonary position [9].

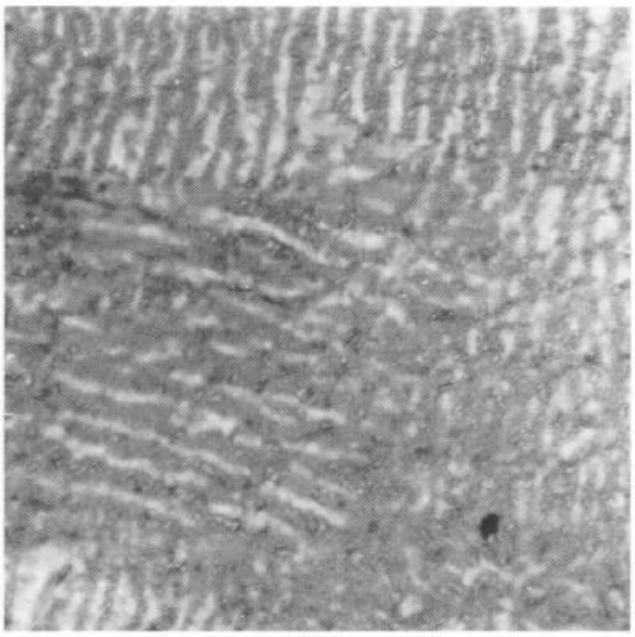

Figure 1.18: Planar section of bovine pericardium under polarized light [119]

Although the collagen fibers of pericardium are not as aligned as those of the native heart valve, pericardial tissue still displays anisotropic mechanical behavior. The circumferential direction is generally stronger and stiffer but also more extensible than the weaker axial direction [123]. Sacks et al. demonstrated that the variable mechanical behavior of the pericardium is consistent with the particular collagen arrangement in various regions of the pericardial sac [124]. The fiber direction also affects flexural rigidity, as pericardial strips are stiffer when flexed perpendicular to the local collagen orientation [126]. These results prove that the

inconsistent, complex nature of the pericardial tissue structure causes regional variations in the tissue biomechanics, which must be carefully considered when selecting materials for bioprostheses.

Apart from tissue directionality, the general mechanical properties, such as stiffness, also vary between heart valves and pericardium. The stress-strain curves for porcine pericardium, bovine pericardium, and aortic leaflets (circumferential) are shown in Figure 1.19. The slope of the stress-strain curve represents the modulus, which is a measure of stiffness. For soft tissues, a three region curve is generally obtained, where the low stress region is dominated by the response of the elastin fibers and the high stress region is dominated by load-bearing collagen fibers [127]. The highly extensible region in between the upper and lower moduli represents a transition in load-bearing capacity [119]. While all of the soft tissues display the same basic trend, the pericardial tissues have much steeper slopes in the high modulus region, suggesting they are stiffer than the native heart valve leaflets [119].

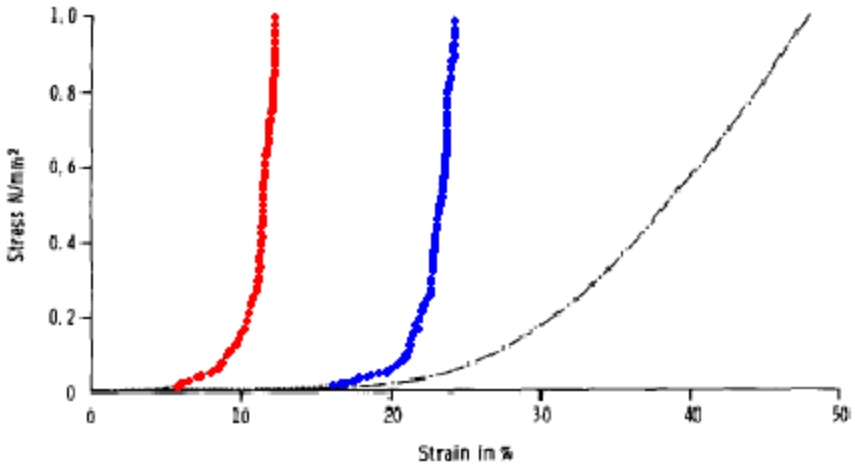

Figure 1.19: Stress strain curve of soft tissues; Porcine pericardium (red) and bovine pericardium (blue) exhibit similar stiffness, while native aortic leaflets (black) are less stiff. [adapted from 119]

Both bovine and porcine pericardium have been used to construct percutaneous heart valves [9]. The two tissue types are structurally similar and differ in only a few areas. Porcine pericardium is slightly thinner than bovine, and its fibrous layer has a more uniform thickness [120]. These differences led CoreValve to switch from bovine pericardium to porcine pericardium for its second generation percutaneous valves. The thinner porcine pericardium allows for a lower profile device that can be delivered through a smaller catheter [9]. However, the affect of crimping on tissue mechanics and durability have not yet been fully investigated [108]. Large scale clinical trials are needed to prove if pericardial tissue is sufficient for constructing successful percutaneous heart valves.

1.6.5 Complications and failure modes

As with most cardiac bioprostheses, failure modes associated with PHVs include endocarditis, calcification, tissue degeneration, and pannus overgrowth [108]. Additional complications are possible due to the method of implantation and specific design features of PHVs. During percutaneous surgery, serious vascular injury, such as perforation or occlusion, is a major risk. Incidence of vascular injury has decreased, however, due to lower profile devices and increased operator experience [105, 106]. Improper positioning of the valve in the left ventricular outflow tract can lead to mitral valve damage or valve embolization [10, 109]. This complication can also be mitigated with operator experience, as well as improved visualization and over-sizing of the stent relative to the annulus [9]. Over-sizing the PHV can also help to prevent perivalvular leaks, most of which are mild to moderate and do not cause significant consequences [10, 109, 128].

During PAVR, the native valve is typically not removed, but rather pushed aside by the stent. The native leaflets can cause coronary obstruction, especially in the left coronary artery. Recent studies show incidence rates of less than 1% for this complication [129]. However, if coronary obstruction does occur, percutaneous coronary interventions can be done following PAVR to correct the problem [130]. New studies are exploring the use of lasers to remove and ablate the native valve. The development of this technology has been slow because the ablation products must be filtered and removed to prevent embolism and stroke [131]. Similarly, atherosclerotic material can also be embolized while threading the catheter through the arteries, which could also lead to stroke or heart attack [108]. Care must be taken to avoid injuring the vessels or rupturing plaques and calcific deposits.

In addition to surgical risks, complications due to the new valve design are also possible. The expandable stents used in PHVs are similar to coronary stents, and differ greatly from the non-expandable stents and sewing rings used in traditional bioprosthetic valves. Due to the outward forces exerted on PHVs to deploy the stents, stent strut fracture can occur [132]. Also, the PHV stents are held in place by the radial force, and are not sewn into the annulus like traditional prostheses. Valve mobilization may therefore be possible, although this complication has not been clinically documented. Furthermore, most PHVs have not been tested beyond a few years in humans, so it is unclear how crimping and expanding the tissue impacts the long-term durability of the device [133]. While preliminary clinical data shows promising results for these new devices, studies are needed to prove their long-term safety and efficacy.

1.7 Bioprosthetic Tissue Fixation Strategies

The major limitation of bioprosthetic valves is durability. One strategy aimed at improving tissue integrity is crosslinking. Chemical fixation of the bioprosthetic tissue helps to preserve the structure of the tissue and mask its immunogenicity [36]. While a plethora of fixation methods have been studied in the past [1, 5, 71, 72], glutaraldehyde remains the commercial standard.

1.7.1 Glutaraldehyde

1.7.1.1 Glutaraldehyde crosslinking chemistry

Since 1969, glutaraldehyde has been used as a fixative in a number of biomedical areas, including vascular grafts, ligament replacements, pericardial patches, menisci, and bioprosthetic

heart valves [134]. Although it has been clinically employed for over 40 years, its mechanisms of action and effects on the tissue are still not completely understood. Aqueous solutions of glutaraldehyde contain free aldehydes, monomeric glutaraldehyde, and αβ-unsaturated polymers of glutaraldehyde [134]. It is generally accepted that glutaraldehyde crosslinks collagen by a reaction between the aldehyde groups on glutaraldehyde with ε-amine groups on lysine and hydroxylysine present in collagen [135]. This preliminary reaction results in formation of a non-conjugated Schiff base intermediate. Stable crosslinks form by one of two mechanisms: combination of two Schiff base intermediates or the addition of a second ε-amine to the double bond of the aldehyde group of polymeric glutaraldehyde [136]. The conjugated aldehydes in polymeric glutaraldehyde give rise to stable products, whereas monomeric reaction products are unstable and hydrolysable [134]. Thus fixation is generally carried out under alkaline conditions, as polymerization occurs quickly at alkaline pH [134, 136].

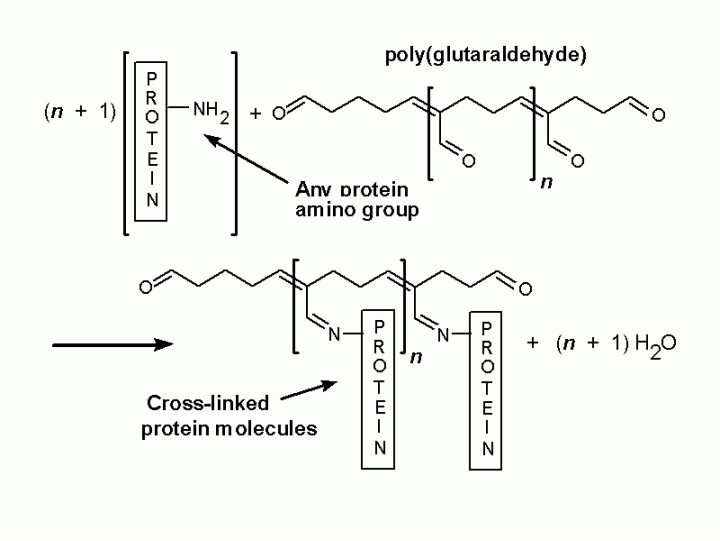

Figure 1.20: Schematic of glutaraldehyde crosslink formation [137]

Glutaraldehyde can reportedly react not only with amines, but also with carboxyl, amide, hydroxyl, and other protein groups [134, 138, 139]. However, it is most reactive with primary amines, such as those present in collagen. Therefore, glutaraldehyde is most effective at crosslinking tissue collagen, but does not preserve other structural components such as glycosaminoglycans and elastin.

Of the aldehydes, glutaraldehyde is the most effective at crosslinking tissue because it reacts quickly, can span various distances between proteins, and reacts with a larger number of amine groups [134]. For instance, formaldehyde has previously been investigated as a fixative for bioprosthetic heart valves. However, it was found that the crosslinks formed by formaldehyde are not stable and degrade during storage in saline at 37°C for ten months, whereas glutaraldehyde-based crosslinks do not degrade under the same conditions [140].

1.7.1.2 Benefits and drawbacks of glutaraldehyde crosslinking

Commercially, tissue is fixed in glutaraldehyde concentrations ranging from 0.2%-0.6%. Below this range, the tissue is not sufficiently sterilized, and above this range the tissue becomes too stiff [141]. Glutaraldehyde has several advantageous effects on preserved tissue, such as reducing biodegradation, increasing biocompatibility, rendering the tissue non-thrombogenic, and preserving anatomic integrity [134]. However, glutaraldehyde fixation has several drawbacks as well. Residual glutaraldehyde and unreacted aldehyde groups in implanted tissue can lead to inflammation, cytotoxicity, calcification, and lack of re-endothelialization. These negative effects become more pronounced with increasing glutaraldehyde concentration [142,

143]. Thorough rinsing of the prostheses prior to implantation can reduce cytotoxicity. Additionally, treatment in L-glutamic acid, glycerol, bisulphate, glycine, or other amino acid solutions can neutralize unreacted aldehyde groups to improve the biological response to the implant [134].

The main limitation of glutaraldehyde-fixed tissue is durability. Glutaraldehyde alters the mechanical properties of the tissue, making it stiffer and less extensible. As previously mentioned, glutaraldehyde devitalizes the bioprosthetic tissue, eliminating any cellular mechanisms of matrix remodeling [21]. Thus, the structural integrity of the implant depends on the quality of the preserved collagen matrix. Glutaraldehyde fixation locks collagen into one specific confirmation (generally a closed cusp with uncrimped collagen fibers). Because collagen cannot crimp and align during valve function, tissue buckling often occurs [26, 144]. Furthermore, glutaraldehyde does not stabilize glycosaminoglycans. Loss of GAGs also leads to increased tissue buckling as well as reduced shearing between tissue layers [27]. Previous work by our lab has shown that the number of tissue buckles and also the extent of tissue buckling increase when GAGs are removed from the tissue (Fig. 1.21). This study also confirmed that GAGs are lost from glutaraldehyde-fixed tissue during tissue preparation, fixation, storage, fatigue cycling, and *in vivo* [145].

Not only does glutaraldehyde fail to preserve GAGs, but it does not have the functional capability to crosslinking elastin either. Elastin is vital to proper valve function. Radially-aligned elastin in the ventricularis contributes to tissue recoil, minimizing the surface area during valve opening and stretching radially during closure to provide a large coaptation area [146, 147]. Damage to elastin distends the cusp and causes an increase in stiffness [146]. With no

regenerative processes possible in glutaraldehyde-crosslinked valves, tissue damage accumulates, eventually resulting in structural failure, for example cuspal tearing [21].

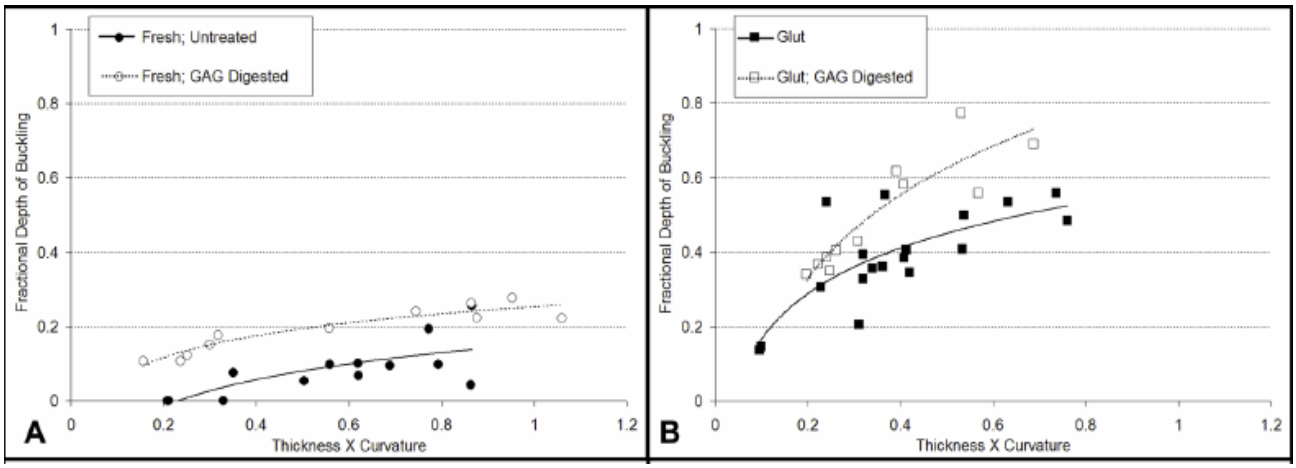

Figure 1.21: GAG loss increases tissue buckling in glutaraldehyde-fixed tissue; Glutaraldehyde-fixed cusps (B) exhibit a greater extent of tissue buckling than fresh cusps (A). Removal of GAGs increases tissue buckling in both fresh and fixed cusps. [27]

Several methods to improve mechanics of fixed tissue have been attempted, including zero-pressure fixation of bioprosthetic heart valves. This fixation method produces valves that are initially more flexible, but the valves undergo more collagen remodeling after implantation, ultimately becoming as stiff as cusps fixed under low pressures [18]. Thus, the benefits of zero-pressure fixation may not be maintained post-implantation. Dynamic fixation is a promising method of improving tissue properties. The valves are subjected to cycling while immersed in the glutaraldehyde solution. The constant movement prevents collagen layers from being crosslinked together, improving the shearing ability of the cusp tissue [28]. However, the

adverse mechanical alterations imposed by glutaraldehyde fixation cannot be completely abolished, leading researchers to consider alternative fixation strategies.

1.7.2 GAG preservation with neomycin

Studies show that glutaraldehyde fixation causes a loss of glycosaminoglycans during heart valve harvest, fixation, and storage, and also after fatigue cycling and *in vivo* implantation [27, 30, 145, 149, 150]. In the native heart valve, GAGs are mainly present in the spongiosa and serve several important functions, such as providing hydration, absorbing stresses, filling the space between the fibrosa and ventricularis, and facilitating smooth sliding between these two layers [5, 36, 146]. Previous work by our lab has shown that GAG loss has serious biomechanical consequences, such as increasing tissue buckling, a form of local tissue failure [27, 148]. Our group has hypothesized that GAG preservation will help to prevent tissue degradation, thus increasing the durability of the bioprosthesis [148]. Thus, prior studies have focused on strategies for preserving GAGs in bioprosthetic tissue.

GAG-targeted crosslinking methods, such as periodate and carbodiimide chemistry, were considered. However, these strategies only partially stabilize GAGs and cannot prevent enzyme-mediated GAG degradation [145]. Thus, an enzyme inhibitor has been incorporated into the fixation procedure to help prevent this mode of GAG loss. Neomycin trisulfate, a known hyaluronidase inhibitor, widely inhibits all hyaluronidases and has amine functionalities that can be used to chemically attach it to the cusps, thus incorporating it into the tissue [145, 151] (Fig. 1.22). Furthermore, neomycin has a hydrophilic moiety and lipophilic residues that confer affinity for hyaluronidases to the molecule [151]. Thus, enzymes are attracted to the neomycin

rather than the carboxyl groups of GAGs, which are the active sites of enzymatic degradation [145, 152, 153].

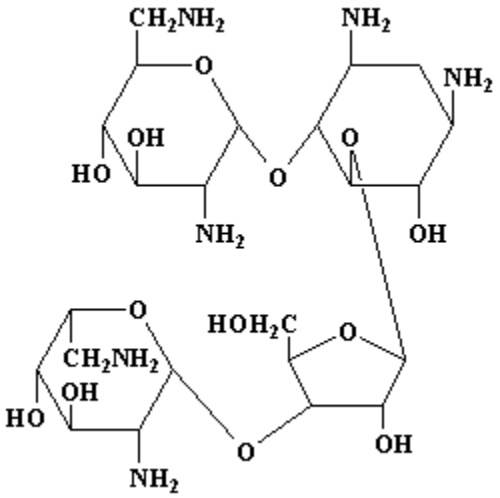

Figure 1.22: Neomycin sulfate structure [154]

Previous studies incorporated neomycin into the cusps via carbodiimide chemistry. Results showed that neomycin inhibited GAG degradation by hyaluronidase, chondroitinase, and papain [145]. This GAG preservation effect was also observed after one year of storage and after 10 million and 50 million fatigue cycles [146]. Furthermore, tissue mechanics were also improved by neomycin, as less tissue buckling was observed in cusps that had received the neomycin pretreatment [27, 146]. Interestingly, neomycin also seems to prevent elastin degradation, as neomycin-treated cusps digested with elastase lose less weight than control cusps [146]. The mechanism behind this nonspecific inhibitory effect has not been elucidated.

While the aforementioned studies were performed using neomycin with carbodiimide crosslinking, similar results were observed when neomycin was incorporated into the tissue via simple glutaraldehyde crosslinking (unpublished data). The amine groups on neomycin can react

with the aldehyde groups of glutaraldehyde to form intermediate crosslinks, thus chemically binding neomycin to the tissue. Unpublished data from our lab shows that after 400 days in storage, valves fixed with glutaraldehyde alone lose twice as many GAGs as those pretreated with neomycin and then fixed with glutaraldehyde. Furthermore, after 50 million fatigue cycles, neomycin-treated valves show negligible GAG loss while glutaraldehyde controls lose approximately 15% of GAGs. Thus, pretreating bioprosthetic tissue with neomycin prevents GAG loss, thereby reducing enzymatic tissue degradation that can lead to mechanical failure.

1.8 Vena Cava as a Bioprosthetic Material

To the best of the author's knowledge, vena cava tissue has never before been used in the construction of a bioprosthetic device. Only one account of the vena cava being used in an implant was found in the literature. The unique structural properties of the vena cava led one research group to propose using vena cava has an autologous tissue source for pulmonary valve replacement. Scharfschwerdt et al [155] hypothesized that vena cava could be fashioned into a successful pulmonary valve substitute, since its tissue structure is somewhat similar to the native pulmonary valve, and its endothelial surface may help to prevent thrombosis [156]. In their preliminary studies, the researchers obtained short cylindrical segments of fresh porcine vena cava, sutured them into PTFE vascular prostheses, and inverted and sutured the distal portion into bicuspid or tricuspid-shaped valves (Fig. 1.23). The valves were mounted in a pulsatile flow chamber, and pressure gradients and valve movements were monitored. Results showed that bicuspid valves had lower transvalvular pressure gradients but the leaflets did not open completely. Valve prolapse was also seen in several of the models. The best results were seen in

small diameter tricuspid valves, and the research group plans to perform *in vivo* experiments with this model. However the authors conclude that the durability and strength of the valves may be limited by their autologous nature, and homologous or xenograft tissue may be better suited for valve construction [155].

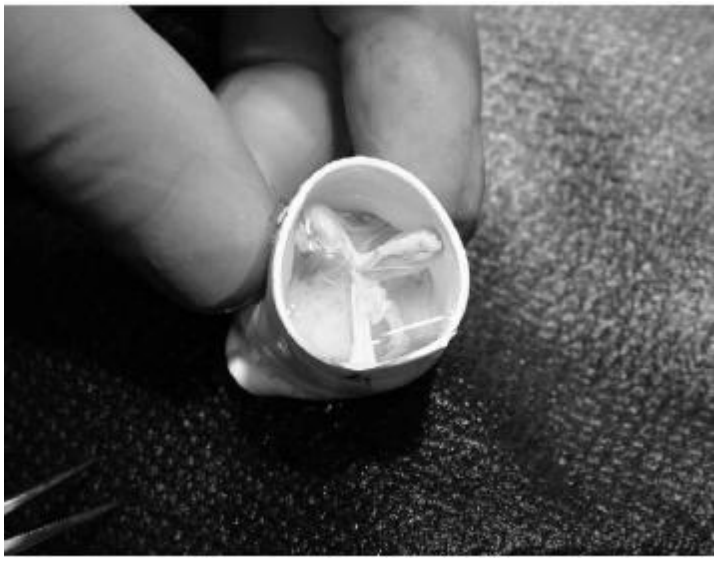

Figure 1.23: Tricuspid valve fashioned from fresh porcine vena cava [155]

The use of autologous tissue of any sort for valve replacement has many limitations [157-161], which is why bioprosthetic valves are currently the standard tissue valves used in aortic valve replacement. As vena cava has never been utilized in bioprosthetic implants, the information in the literature about the vena cava structure-function relationship and tissue mechanical properties is also sparse. The morphology of vena cava tissue is similar to that of all vascular tissue and is comprised of three layers: intima, media, and adventitia [162]. The intima lines the vessel lumen and is composed of a single layer of endothelial cells on top of a basement membrane. The media contains alternating layers of smooth muscle cells and matrix composed

of collagen and elastin fibers. The outermost tissue layer, the adventitia, is mainly extracellular matrix components such as collagen and proteoglycans (PGs) with few fibroblasts [162]. A schematic of the vascular structure is shown in Figure 1.24:

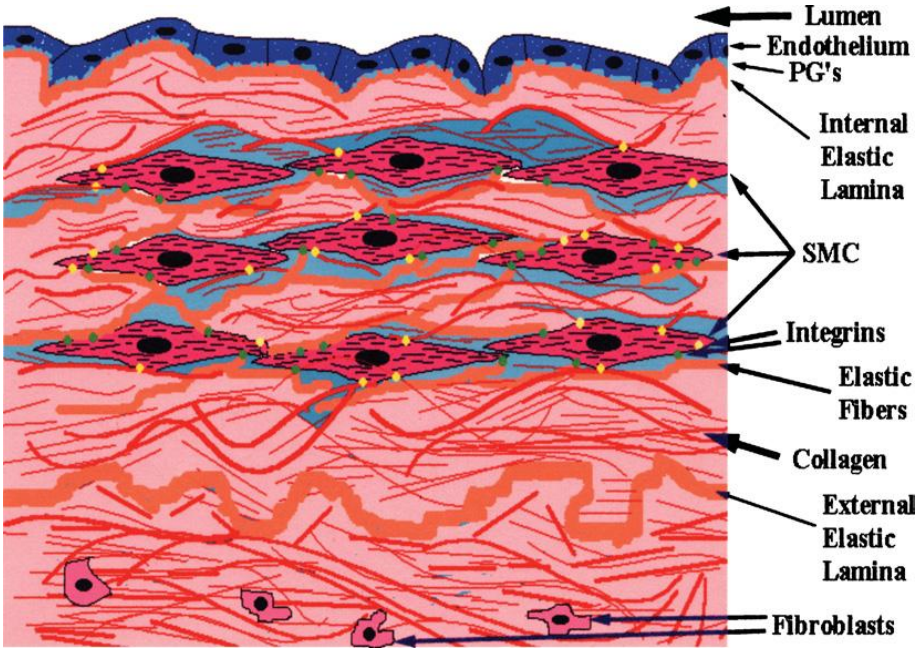

Figure 1.24: Vascular morphologic model [162]

The various tissue layers of the vena cava are exposed to differential stresses, analogous to how the fibrosa and ventricularis of the heart valve experience differing forces and flexures. The intima is exposed to shear stresses from flowing blood, as well as compressive and tensile forces due to blood pressure. The media is mainly in compression and tension due to hemodynamic loading and the contractile behavior of the smooth muscle cells [162]. The ability of the vena cava tissue to respond to these forces is likely mediated by the alignment of the extracellular matrix fibers. In the zero stress state, the fibers in the media are at a 40° to the longitudinal axis, while the fibers in the adventitia are at a 40° angle to the circumferential axis.

In the transverse plane of the tissue, the medial fibers are oriented circumferentially. In the longitudinal plane, the adventitial fibers are directed along the longitudinal axis (Fig. 1.25) [162].

The angular orientation of the ECM fibers reveals spiral wrapping, which is consistent with other studies [163-165]. The wrapping of the fibers suggests that the mechanical behavior of the vena cava is dependent on the fibers' ability to align in the direction of the applied load [162].

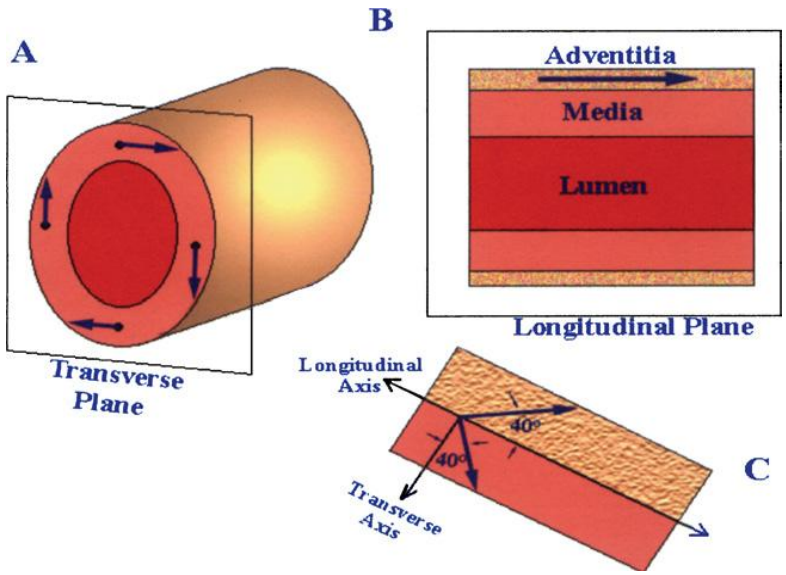

Figure 1.25: Alignment of vena cava ECM fibers; (A) The medial fibers are oriented circumferentially in the transverse plane. (B) The adventitial fibers are oriented longitudinally in the longitudinal plane. (C) Medial and adventitial fibers are at 40° angles to the longitudinal axis and transverse axis, respectively. [162]

Two studies by Snowhill [162], compared the structure and mechanics of the porcine vena cava to those of the aorta, iliac arteries, and carotid artery. The proportion of collagen and smooth muscle cells were similar among the various vascular tissues. However, vena cava was

found to contain a greater mass density of elastin than the arteries. Furthermore, the vena cava ECM was determined to be more interconnected than the arteries, as measured by water adsorption. The amount of water in the ECM is inversely related to the degree of collagen crosslinking. Since the vena cava had the lowest hydration capacity among the vessels, it was assumed to contain the greatest amount of crosslinks [162].

Alcian blue staining revealed a very small amount of GAGs in the vena cava as compared to the other vascular tissues. In general, GAGs and PGs in the vascular tissue are associated with smooth muscles cells, which may suggest that GAGs are involved in cell-to-ECM binding. Also, GAGs in heart valves are implicated in shock adsorption and energy dissipation [27]. It is possible that the vena cava contains fewer GAGs than the arteries because the vena cava is not exposed to the significant pulsatile pressures that the arterial system experiences [167]. This hypothesis is consistent with the finding that the vena cava is less viscous than the arteries, which suggests that it does not require a significant viscous response to dissipate energy and prevent stress overloads, as it does not experience great pressure variations [166]. Although GAGs may not play a large mechanical role in the vena cava, it has been suggested that GAGs in the vena cava hydrate the intimal EC layer and help to prevent thrombogenesis [168].

Further studies by Snowhill considered the elastic and viscous moduli and ultimate tensile strengths of the various vessels [166]. Since blood vessels generally operate around 10-20% strain [169], both the low strain (elastic) region and the high strain (collagen-dominated) region of the stress strain curve are relevant [171]. In general, the vena cava has a higher modulus (stiffer behavior) in the low strain region in the transverse direction than in the longitudinal, which may suggest that the elastin fibers are aligned longitudinally (perpendicular

to the transverse plane). In the high strain region, the vena cava's elastic, viscous, and total moduli are greater than those of the aorta, carotid, and iliac arteries. The vena cava also has the greatest ultimate tensile strength among the vessels. The reason for the high strength and stiffness is not well understood, as the vena cava experiences lower pressures than the aorta, and thus need not be as resistant to pressure fluctuations [166].

An interesting finding in the Snowhill et al study was that vena cava was the only vessel examined which exhibited significant strain-rate stiffening, a phenomenon which is also seen in cartilage, ligaments, and aortic valve leaflets. In the heart valve, stiffening of the leaflets is due to the close packing of collagen fibers. Shear stiffening has also been observed in crosslinked pericardium, as crosslinking effectively increases collagen fiber density per unit volume and reduces fluid motion [170]. Shear stiffening in the vena cava may be explained by the fact that it exhibits greater interconnectivity, and thus tighter collagen packing, than the other vascular tissues [171].

Although these results elucidate some of the structural and mechanical differences among the vasculature, more studies are needed to fully understand the structure and function of the vena cava. The body of literature surrounding the vena cava is rather small, and most studies have considered the inferior rather than the superior vena cava. Since the vessel properties vary so widely among the vascular tree [162] it is possible that these two segments have different properties. In general, it may be said that the native inferior vena cava has a higher elastin density, lower GAG content, and greater stiffness and strength than other vascular tissues [162]. However, vena cava has never been used as a bioprosthetic tissue, so its ability to adapt to different applications and the effects of crosslinking on tissue properties are not yet known.

CHAPTER TWO

PROJECT RATIONALE

One of the major limitations of aortic heart valve replacement surgery is the invasiveness of the procedure. Traditional heart valve replacement is performed via open heart surgery, which is traumatic to the patient and necessitates a long recovery period [6]. Elderly patients and patients with serious comorbidities are often considered "high operative risk," and may be denied a potentially life-saving valve replacement because the risk of mortality is too great [7]. This limitation of traditional valve surgery must be addressed, as more elderly patients will become candidates for surgery as the incidence of aortic stenosis and other valvular diseases increases with the aging United States population [9]. Percutaneous aortic valve replacement (PAVR) is one technology that has emerged to address the problems with traditional valve replacement.

Percutaneous surgery is a minimally-invasive technique that has proven successful in a wide array of cardiovascular areas, such as angioplasty, stent placement, and ablation therapy. Two percutaneous heart valves (PHVs) are currently in clinical trials and many more are in developmental phases. The two models in the clinical stage and almost all of the models currently described in the literature utilize pericardial tissue (bovine, porcine, or equine) to construct leaflets which are mounted onto a stainless steel or nitinol stent [9]. While initial results are promising, there are still a number of questions which must be answered before the valves can reach the market. One major factor in the success of the PHV is the quality of the leaflet material; this aspect of the device will dictate short-term performance and long-term durability of the implant. The leaflet tissue must be elastic enough to be crimped into a small diameter stent and expanded *in situ*. Furthermore, the tissue must be resilient and must not

permanently deform or incur damage upon crimping. Although pericardial tissue is used in current PHV models and is also featured in several traditional bioprosthetic valves [9, 77], the suitability of this tissue for heart valves has been questioned. The structure of pericardium is dissimilar from that of the native valve leaflet, as pericardium lacks the clearly defined layers and directionality of valve tissue [123]. Moreover, the structure and mechanical behavior of pericardial tissue varies regionally over the pericardial sac, which may make it difficult to construct leaflets with uniform properties [5, 123, 124]. Since load-bearing capability and tissue extensibility are highly dependent on tissue fiber orientation, the random structure of the pericardium limits one's ability to predict tissue behavior. Thus, pericardial tissue may not be the ideal choice for PHVs and may limit their success in the long run. However, percutaneous valve technology is a major breakthrough in valve replacement and has the potential to revolutionize the entire field, so alternative PHV designs should be considered to optimize results.

To overcome the limitations of pericardial tissue, our lab proposes utilizing an alternative tissue source, namely porcine vena cava. Vena cava tissue has a higher elastin density than most other tissues [162], suggesting that it may be more elastic and flexible, which may enable it to be more easily crimped and to regain its original configuration upon expansion. Furthermore, venous tissue is uniformly directional, with elastic fibers aligned longitudinally to allow for vasomotion and collagen fibers oriented circumferentially to prevent rupture [162]. Thus, it may be possible to construct uniform leaflets with definite fiber orientations and consistent mechanical properties similar to those of the heart valve leaflet. The overall goal of this research project is to assess the feasibility of using vena cava as an alternative to bovine pericardium for

PHVs. Fresh vena cava and pericardium, as well as glutaraldehyde-fixed samples, will be examined, as glutaraldehyde is the crosslinker used in all commercial heart valves. Additionally, neomycin-pretreated tissues will also be investigated, since neomycin has been used commercially to improve GAG retention and stabilize the mechanical properties of bioprosthetic valves [27]. To determine if vena cava tissue is a viable option for PHVs, it will be compared to bovine pericardium in the following areas: structural properties, mechanical behavior, tissue resilience, and *in vivo* stability.

2.1 Research Aims

In order to answer the overall project inquiry—is vena cava a better option for PHVs than pericardium—the following research questions were defined.

2.1.1 Structural properties

Specific aims: How do bovine pericardium and porcine vena cava differ structurally? How do glutaraldehyde and neomycin affect the structure?

Hypothesis: Vena cava may have more regularly-oriented extracellular matrix fibers than pericardium, as venous physical properties are directional and differ in the longitudinal and circumferential planes of the tissue. Because pericardial physical properties can vary locally over the pericardial sac, it is likely that the pericardial tissue is less organized than the vena cava. Vena cava may contain a greater proportion of elastin than pericardium since the tissue is highly flexible to allow for vasomotion. Furthermore, glutaraldehyde crosslinking will stabilize the

tissue components, and neomycin pretreatment will facilitate GAG preservation in both tissue types.

Experimental plan: Three groups of porcine vena cava and bovine pericardium will be investigated: a fresh control, glutaraldehyde crosslinked (GLUT), and neomycin-pretreated followed by glutaraldehyde crosslinking (NG). Samples will be cut from both the circumferential and longitudinal directions of the tissue for histological analysis to determine general morphologic differences. Relative proportions of collagen and elastin will be indirectly determined by enzymatic digestion of the fresh tissues with collagenage and elastase. The extent of tissue preservation with the fixation treatments will also be investigated using the aforementioned enzymes. Collagen and elastin stability will be measured by percent weight loss, while GAG content will be measured using the hexosamine assay. Finally, differential scanning calorimetry (DSC) will be used to assess the degree of collagen crosslinking, by measuring the collagen denaturation temperature of hydrated samples.

2.1.2 Mechanics

Specific aims: Does vena cava tissue offer enhanced mechanical properties as compared to bovine pericardium? Which extracellular matrix components are important to pericardial and vena cava mechanical properties? How do glutaraldehyde and neomycin affect the mechanics of the two tissue types?

Hypothesis: Fresh vena cava tissue may be more compliant than bovine pericardium due to the high elastin content of the tissue. The stiffness of the vena cava likely differs in the circumferential and longitudinal directions, and we expect the tissue to be more compliant in the

direction parallel to elastin fiber alignment. The directional differences in tissue mechanics may be greater in vena cava than in pericardium due to the more random orientation of pericardial ECM fibers. Furthermore, elastin likely contributes more significantly to vena cava mechanics than pericardial because it may be more abundant in the vena cava.

Tissues fixed with glutaraldehyde will be stiffer than fresh samples, as crosslinking inhibits movement in the tissue. Neomycin-treated samples may be stiffer than glutaraldehyde samples, as neomycin potentiates additional crosslinks.

Experimental plan: Fresh, glutaraldehyde-fixed, and neomycin plus glutaraldehyde-fixed samples of pericardium and vena cava will be subjected to uniaxial tension, and the elastic modulus will be calculated. Fresh samples will also be subjected to GAGase or elastase and then mechanical tests will be repeated to determine how the ECM components contribute to directional mechanical properties.

2.1.3 Tissue resilience

Specific aims: Is vena cava tissue better able to withstand compression, such as that exerted by a stent, as compared to pericardium?

Hypothesis: Vena cava may suffer less tissue damage upon crimping into a stent due to enhanced flexibility as compared to pericardium.

Experimental plan: Fixed vena cava and pericardium samples will be subjected to compressive forces similar to those supplied by a stent. The tissue will then be removed and examined for tears and deformations using general histology and scanning electron microscopy (SEM).

Additionally, the crimped tissues will be subjected to uniaxial tensile tests in order to determine if the tissues suffer fiber damage during crimping that affects the mechanical properties.

2.1.4 In vivo stability

Specific aims: Does fixed vena cava calcify to the same extent as fixed pericardium?

Hypothesis: While elastin may render vena cava more flexible and mechanically-suitable for PHVs than pericardium, the high elastin content may also cause additional calcification of vena cava.

Experimental plan: Glutaraldehyde and neomycin-plus-glutaraldehyde samples will be implanted subdermally into male, juvenile, Sprague-Dawley rats. Additionally, some samples will be treated with ethanol as an anti-calcification measure. After three weeks, the implants will be removed and examined for calcium content and histological features.

CHAPTER THREE

MATERIALS AND METHODS

3.1 Materials

Acetyl acetone, p-dimethylaminobenzaldehyde, 4-(2-hydroxyethyl)-1-piperazineethanesulfonic acid (HEPES), sodium chloride, Tris, ammonium molybdate, L-ascorbic acid, and sodium azide were purchase from Fisher Scientific (Fair Lawn, NJ). Ammonium acetate, chondroitinase ABC from Proteus *vulgaris*, collagenase type VII from Clostridium *histolyticum*, (D+) glucosamine HCl, hyaluronidase type IV-S from bovine testes, calcium carbonate, Fast Green FCF, and neomycin trisulfate hydrate were all purchased from Sigma-Aldrich Corp (St. Louis, MO). Elastase from porcine pancreas (135 U/mg) was purchased from Elastin Products Company (Owensville, MO). EM Grade Glutaraldehyde- 8% wt. in H_20 was purchased from Polysciences Inc. (Warrington, PA). Sodium carbonate, alizarin red, and 2-(N-morpholino) ethanesulfonic acid (MES) were purchased from Acros Organics, (Morris Plains, NJ). Ultra II ultra pure hydrochloric acid was purchased from J.T Baker (Phillipsburg, NJ). Sulfuric acid was purchased from EMD Chemicals, Inc. (Darmstadt, Germany). Absolute ethanol was obtained from Pharmco-AAPER (Shelbyville, KY). Alcian blue was purchased from Anatech, LTD (Battle Creek, MI). Nuclear fast red and a Verhoeff Van Gieson stain kit were purchased from Poly Scientific (Bay Shore, NY).

3.2 Methods

3.2.1 Obtaining and crosslinking xenograft tissue

Fresh bovine pericardium and porcine vena cava were obtained from Animal Technologies, Inc (Tyler, TX). The tissue was packed in saline and kept on ice and shipped overnight. All tissues were rinsed in ice cold saline prior to treatment. The pericardial sacs were cut open along the midline, laid out in a rectangular sheet, and cut into rectangular strips, with the length of the strip corresponding to the long axis of the rectangular sheet. The vena cavae were cut along the longitudinal axis and opened up into flat sheets. Rectangular pieces were cut, with the length of the rectangle corresponding to the longitudinal direction and the width corresponding to the circumferential direction of the vessel. Within three hours of obtaining the tissue, several fresh tissue pieces were directly frozen at -4°C or taken immediately for assays, while the rest were fixed using the following procedures:

GLUT: Tissues assigned to the treatment group designated GLUT were crosslinked using glutaraldehyde. Pericardial or vena cava strips were placed in 0.6% glutaraldehyde in 50 mM HEPES-buffered saline solution at pH 7.4. The tissue was kept at room temperature. After a 24 hour incubation in 0.6% glutaraldehyde, the solution was replaced by 0.2% glutaraldehyde. Tissues were stored in 0.2% GLUT for at least 6 days before assays were performed.

NG: Pericardial and vena cava tissues assigned to the treatment group designated NG were incubated in 1 mM neomycin trisulfate in 50 mM MES-buffered solution, pH 5.5, for one

hour at room temperature under constant orbital agitation. Following this incubation, the neomycin solution was drained and followed by standard GLUT crosslinking, as described above.

All tissues were fixed in approximately 30 mL of chemical solution per tissue strip.

3.2.2 Structural properties

3.2.2.1 Tissue thickness

The thicknesses of the bovine pericardium and porcine vena cava were assessed, as thickness of the tissue component of a PHV plays a large role in determining device profile. Five rectangular strips of fresh, GLUT, and NG pericardium and vena cava were randomly selected, and four thickness measurements per strip were taken with the Accura Comparator Stand (Accura Industries, Bombay) for a total of 20 measurements per group. The average thickness of each tissue type was calculated.

3.2.2.2 Collagen and elastin stability

The tissues' ability to resist enzymatic degradation of collagen and elastin was assessed for fresh, GLUT, and NG pericardium and vena cava. All tissues were rinsed in deionized (DI) water, lyophilized, and weighed (initial dry weight). Then, the tissues were treated with porcine pancreatic elastase or Type VII collagenase. Approximately 2 cm^2 pieces of tissue were immersed in 1.2 mL of 5.0 U/mL elastase (100mM Tris buffer, 1mM $CaCl_2$, .02% NaN_3) or 1.2 mL of 150 U/mL collagenase (50 mM $CaCl_2$, .02% NaN_3, pH 8.0). The elastase-treated groups were incubated at 37°C for 24 hours with constant agitation, while the collagenase-treated groups

were incubated under identical conditions for 48 hours. The samples were then rinsed in DI water, lyophilized, and weighed again (final dry weight). The degree of enzymatic degradation of the tissue was quantified as the percent weight loss, which was calculated by dividing the difference in final and initial dry weights by the initial dry weight.

3.2.2.3 Differential scanning calorimetry

Differential scanning calorimetry (DSC) was performed on fresh and crosslinked tissues to assess the collagen denaturation temperature (T_d), which is represented by an endothermic peak in the heating curve [173]. Tissue samples of approximately 7-10 mg were excised, blotted dry with Kim Wipes, and placed in hermetically-sealed aluminum pans. Samples were heated from 30°C to 60°C at 5°C per minute, held at 60°C for one minute, and then heated from 60°C to 90°C at 2°C per minute. The resulting heating curves were analyzed using Thermal Analysis software. The collagen denaturation temperature was recorded at the height of the endothermic peak, as shown in Figure 3.1.

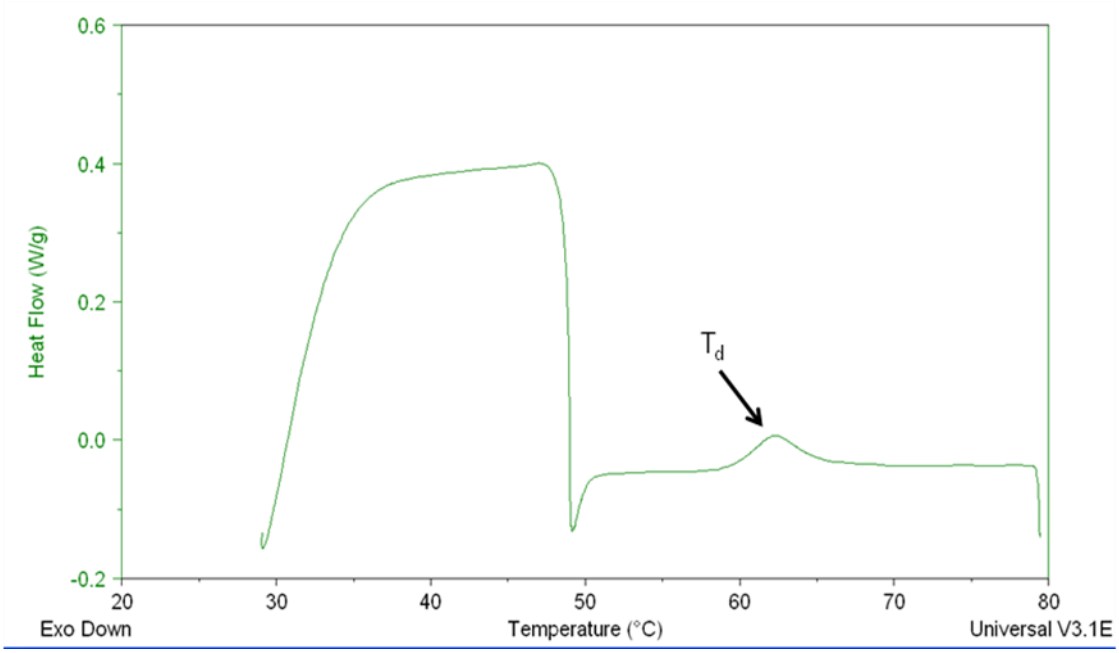

Figure 3.1: Example DSC curve; T_d is represented by the arrow

3.2.2.4 GAG quantification by hexosamine analysis

Total hexosamine content in the tissue was used as an estimate of total GAG content, as previously described [27, 146]. The sample tissues were weighed, lyophilized, and hydrolyzed in 2 mL of 6 M HCl for 20 hours at 95 °C. The samples were then dried under nitrogen gas and resuspended in 2 mL of 1 M NaCl. The samples were then reacted with 1 mL of 3% acetylacetone in 1.25 M sodium carbonate solution and incubated at 95 °C for 1 hour. The samples were then cooled to room temperature and further reacted with 4 mL of absolute ethanol and 2 mL of Ehrlich's reagent (0.18 M p-diemethyl-aminobenzaldehyde, 50% ethanol in 3.0 N HCl). The samples were incubated at room temperature for 45 minutes to allow for color

changes, which are indicative of hexosamine quantities, to develop. Then, 300 mL of each sample was pipetted into a 96-well plate, using D (+) glucosamine solutions (1-200μg) as controls. Spectrophotometric analysis was performed at 540 nm. All calculated hexosamine values were normalized to their respective dry tissue weights.

3.2.2.5 Histology

Histological assessment was performed on fresh and fixed tissue, as well as tissues that were treated with elastase as described above. Representative sections were cut from pericardial and vena cava tissue strips, along both the longitudinal (length) and circumferential (width) directions. The tissue samples were fixed overnight in 10% formalin, embedded in paraffin wax, and sectioned (5 μm sections) for light microscopy analysis. Verhoeff Van Gieson (VVG) staining was performed to assess the quantity and orientation of elastin fibers. Elastin fibers were stained black, while collagen was stained red, and all other tissue elements were stained yellow. Representative images of the sections were taken digitally using a Zeiss Axioskop 2 Plus (Carl Zeiss MicroImaging, Inc., Thornwood, NY) and SPOT Advanced imaging software (Spot Imaging Solutions; Sterling Heights, MI).

3.2.3 Mechanics

3.2.3.1 Uniaxial tests

Fresh, GLUT, and NG groups were all subjected to uniaxial testing. Additionally, the behavior of fresh tissue before and after elastase and GAGase treatments were also investigated. Briefly, the GAGase treatment consisted of incubating 4 cm^2 tissue strips in 1.2 mL of GAG-degrading enzyme solution (GAGase; 5.0 U/mL hyaluronidase and 0.1 U/mL chondroitinase

ABC in 100 mM ammonium acetate buffer, pH 7.0). The samples were incubated at 37 °C for 24 hours under constant agitation. Following the incubation, the samples were thoroughly rinsed in DI water.

For mechanical testing, small tissue strips (approximately 10 mm in length and 3 mm in width) were excised, the tissue thickness was measured with a caliper, and each sample was placed between the grips of an MTS Synergie 100 (MTS Systems Corporation; Eden Prairie, MN). A 10 N load cell was used to apply a tensile force to the tissue samples, and a stress-strain curve was obtained. TestWorks 4 software (MTS Systems Corporation; Eden Prairie, MN) was used to calculate the elastic modulus of the sample at both the low modulus and upper modulus regions of the curve.

3.2.4 Tissue resilience

3.2.4.1 Crimp test

Tissue resilience was assessed by observing the tissue response after being compressed. The crimp test was performed in collaboration with Paul Ashworth of St. Jude Medical. Rectangular samples of GLUT and NG pericardium and vena cava were folded back on themselves twice and compressed under a 35N static load for 30 minutes each. The tissue was then removed and returned to our lab for further analysis.

3.2.4.2 Stereomicroscopy

Samples were blotted dry and placed on the stage of the stereomicroscope (Meiji Techno; Santa Clara, CA). Images were captured with a Spot Insight camera and processed with Spot Advanced software (Spot Imaging Solutions; Sterling Heights, MI) on both the intimal and adventitial surfaces of the vena cava and the serosal and fibrous surfaces of the pericardium.

3.2.4.3 Scanning electron microscopy

Scanning electron microscopy (SEM) was used to assess the degree of tissue damage following the crimp test. Samples were prepared for SEM by rinsing in DI water, dehydrating through increasing concentrations of ethanol, and critical point dried. The samples were mounted on the specimen stub with double-sided carbon tape and viewed with the TM3000 (Hitachi; Tokyo, Japan).

3.2.4.4 Uniaxial testing

The crimped tissue was subjected to tensile testing in order to evaluate how crimping affects tissue mechanics. Uniaxial tensile tests, as described above, were performed on crimped GLUT and NG vena cava and pericardium. The results were compared to control tissue that had not previously been subjected to any forces.

3.2.5 In vivo stability

3.2.5.1 Subdermal implantation

Subdermal implantation of bioprosthetic tissue in small animals is frequently used to assess the *in vivo* responses, such as calcification and inflammation [5]. Small samples (approximately 2 cm^2) of GLUT and NG porcine vena cava and bovine pericardium (n=10) were excised and rinsed in sterile saline 3 x 30 minutes prior to surgery. Additionally, a second set of NG porcine vena cava and bovine pericardium samples were pretreated with ethanol (group NGE), which has been shown to prevent cell-related calcification [5, 33]. The pretreatment consisted of a 24 hour incubation in 80% ethanol in HEPEs buffer at room temperature with mild agitation. The samples were then rinsed in sterile saline 3 x 30 minutes prior to surgery. All animals received humane care in compliance with protocols that have been approved by the Clemson University Animal Research Committee and NIH. Male juvenile Sprague Dawley rats (35-40 g; Harlan Laboratories; Indianapolis, IN) were anesthetized by inhalation of isoflurane gas. Two small incisions (one on each side lateral to the spine) were made on the dorsal side of the rat. A subdermal pocket was made in conjunction with each incision, and one tissue sample was placed in each pocket. The incision was closed via surgical staples. Animals were sacrificed at three weeks using carbon dioxide asphyxiation. The implant and tissue capsule were explanted and prepared for further analysis. Additionally, small tissue slivers were excised from four samples per group for histological assessment.

3.2.5.2 Calcium and phosphorus analysis of explants

Tissue samples were immediately frozen on dry ice following the explant surgery. The samples were lyophilized, weighed, and hydrolyzed in 1 mL of 6N Ultrex II HCl for 20 hours at

95°C. The samples were then dried under nitrogen gas and resuspended in 1 mL of 0.01 N Ultrex HCl. The samples were vortexed, and the solution was diluted by 1:50 in Atomic Absorption Matrix (0.3N Ultrex HCl + 0.5% lanthanum oxide). The calcium content of each sample was determined by atomic absorption spectroscopy (Perkin-Elmer 3030 Atomic Absorption Spectrophotometer; Norwalk, CT). The results were normalized by the dry tissue weight.

For phosphorus quantification, the vortexed solution was diluted by 1:100 in DI water for a final volume of 1 mL. To this solution, 1 mL of reagent C (2.5% ammonium molybdate with 6N sulfuric acid and 10% L-ascorbic acid) was added, and the mixture was reacted at 37°C for two hours. The samples were cooled to room temperature, and 250 µl of each was pipetted into a 96-well plate. Spectrophotometric analysis was performed at 820 nm, and the results were normalized to the dry tissue weight.

Additionally, samples were diluted 1:50 in 10 mL of DI water and brought to Clemson University's Environmental Sciences Laboratory for standard elemental analysis. This set of results was used to confirm the results obtained in our lab.

3.2.5.3 Histological analysis of explants

Thin slices of tissue were excised from the center of the explants. The specimens were immediately fixed in 10% formalin for at least 24 hours. The samples were then embedded in paraffin wax and sectioned (5 µm). Calcium content was analyzed qualitatively by staining the samples with Alizarin Red and counterstaining with Fast Light Green. Digital images were obtained and analyzed as described above.

3.2.6 Statistical analysis

Results are represented as a mean ± the standard error of the mean (SEM). Statistical analysis was performed by a two-tailed student's t-test of unequal variance. Significance was defined as $p < 0.05$.

CHAPTER FOUR

RESULTS

4.1 Structural Properties

4.1.1 Tissue thickness

The thickness of fresh and fixed porcine vena cava was compared to that of bovine pericardium. Fresh vena cava and pericardium had similar thicknesses, 0.184 ± 0.016 mm and

0.195 ± 0.008 mm, respectively. Results showed that fixation caused an approximately three-fold increase in tissue thickness as compared to fresh tissue (Table 4.1). The increase between fresh and GLUT groups was approximately the same for the vena cava and pericardium (2.91-fold and 2.94-fold, respectively). Neomycin treatment did not cause a significant change in thickness as compared to GLUT tissues. In general, the differences in tissue thickness between vena cava and pericardium from each treatment group were statistically insignificant ($p>0.05$). The only exception was the NG group, in which the vena cava had a thickness of 0.492 ± 0.044 mm, while the pericardium had a statistically greater thickness of 0.616 ± 0.030 mm ($p= 0.013$).

	Fresh	GLUT	NG
Porcine Vena Cava	0.184 ± 0.016	0.536 ± 0.030	0.492 ± 0.044
Bovine Pericardium	0.195 ± 0.008	0.577 ± 0.050	0.616 ± 0.030

Table 4.1: Tissue thickness; Comparison of fresh and fixed vena cava and pericardium; results given in mm; (n=20)

4.1.2 Collagen stability

Fresh tissue lost a high amount of dry weight after incubation in collagenase (Fig. 4.1). Fresh pericardium lost significantly more weight than fresh vena cava (74.59% ± 1.008% versus 56.865% ± 3.989%). Glutaraldehyde crosslinking drastically decreased the amount of weight lost from both tissue types to less than 10% of dry weight. NG-treated vena cava lost less weight

than GLUT vena cava (1.131% ± 0.449% and 7.072% ± 3.447%, respectively), but the result was not statistically significant (p= 0.09). NG-crosslinking did not show a similar collagen-preserving effect in pericardium.

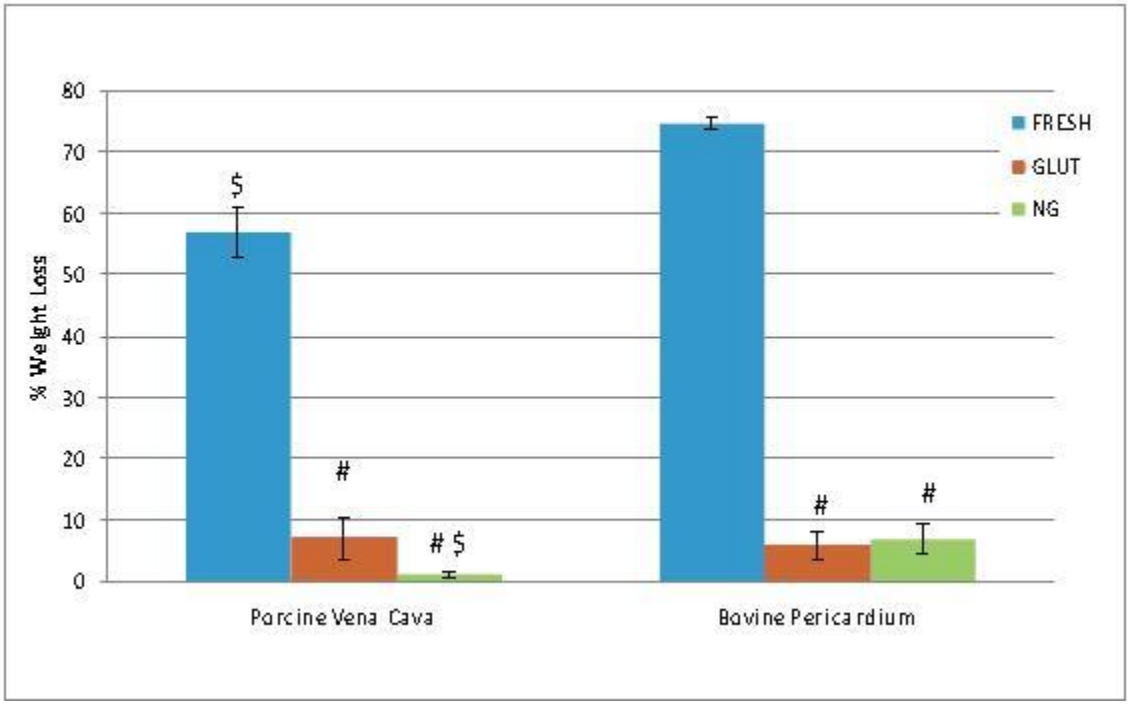

Figure 4.1: Collagen stability against collagenase, represented as a percentage of dry tissue weight loss (n= 6, # indicates difference with FRESH of same species, $ indicates difference with corresponding pericardium)

Collagen stability was also indirectly assessed by differential scanning calorimetry. The collagen denaturation temperature of hydrated tissues (T_d) was determined by analyzing the endothermic peak in the heating curve. Fresh tissues exhibited the lowest denaturation temperatures (62.783 ± 0.183 °C for vena cava and 63.630 ± 0.192 °C for pericardium) (Table 4.2). Crosslinking of the collagen by glutaraldehyde caused a significant increase in T_d to 86.383

± 0.495 °C and 85.487 ± 0.168 °C respectively. NG-crosslinking further increased T_d by approximately 2°C for both tissue types. However, there was no significant difference between T_d for vena cava and pericardium in each treatment group.

	Fresh	GLUT	NG
Porcine Vena Cava	62.783 ± 0.183	86.383 ± 0.495	88.393 ± 0.336
Bovine Pericardium	63.630 ± 0.192	85.487 ± 0.168	87.290 ± 0.705

Table 4.2: Collagen stability as represented by thermal denaturation temperature; results given in degrees Celsius (n= 4)

4.1.3 Elastin stability

Fresh vena cava incubated in elastase lost 35.656% ± 5.470% of dry weight, revealing that elastin is a major structural component in the vena cava extracellular matrix (Fig. 4.2). Fresh pericardium, in contrast, lost only 10.513% ± 0.710% of dry weight after elastase digestion. GLUT-crosslinking did not protect elastin from degradation. NG-fixation, however, caused a significant decrease in weight loss from both vena cava and pericardium (17.840% ± 4.100% and 4.176% ± 1.948% respectively). The amount of weight lost from the vena cava was significantly greater than that of the corresponding pericardium for each treatment group.

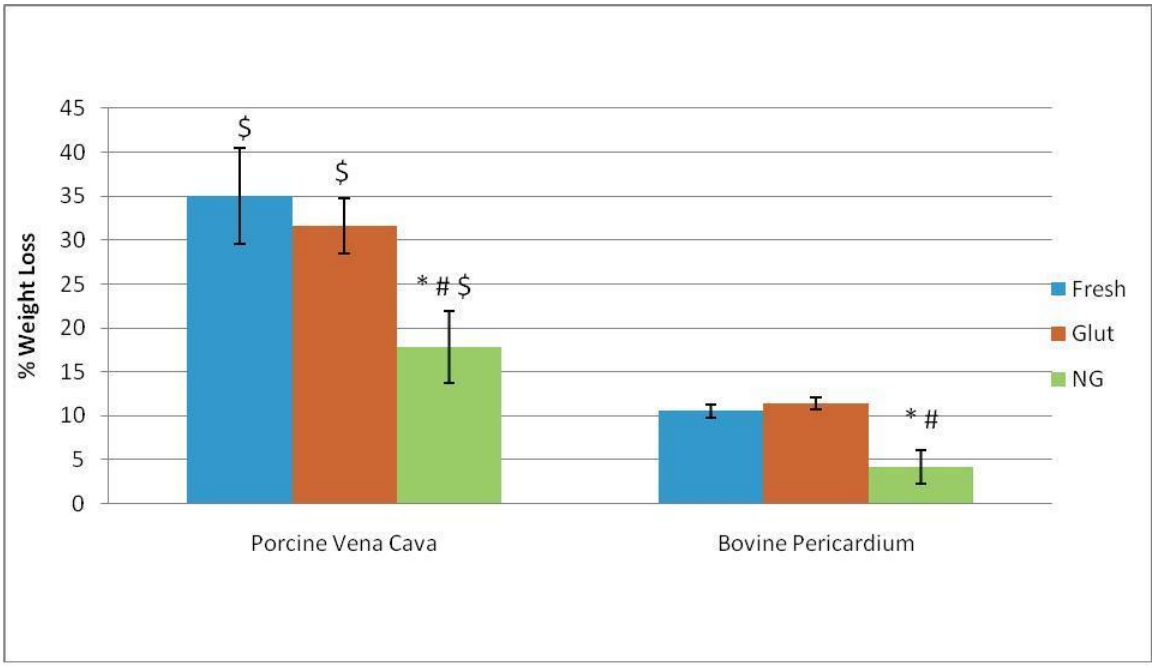

Figure 4.2: Elastin stability, as represented by the percentage of dry tissue weight lost following incubation in elastase (n= 6; $ indicates difference with corresponding pericardium, * indicates difference with FRESH of same species, and # indicates difference with GLUT of same species)

Histology was used to visualize elastin fibers and confirm elastin preservation by NG. Fresh tissue sections were taken in both the longitudinal and circumferential directions, which allowed for the determination of fiber orientation. Figure 4.3A shows that elastin fibers (black) are oriented along the longitudinal direction. In the circumferential view (Fig. 4.3B) cross-sections of elastin fiber bundles are seen, revealing that elastin is oriented perpendicularly to the circumferential plane. Figure 4.3C-D show corresponding images of bovine pericardium. In pericardium, the elastin fibers and not aligned in any one direction; thus the tissue appears intensely black because elastin is oriented in all directions and in all planes.

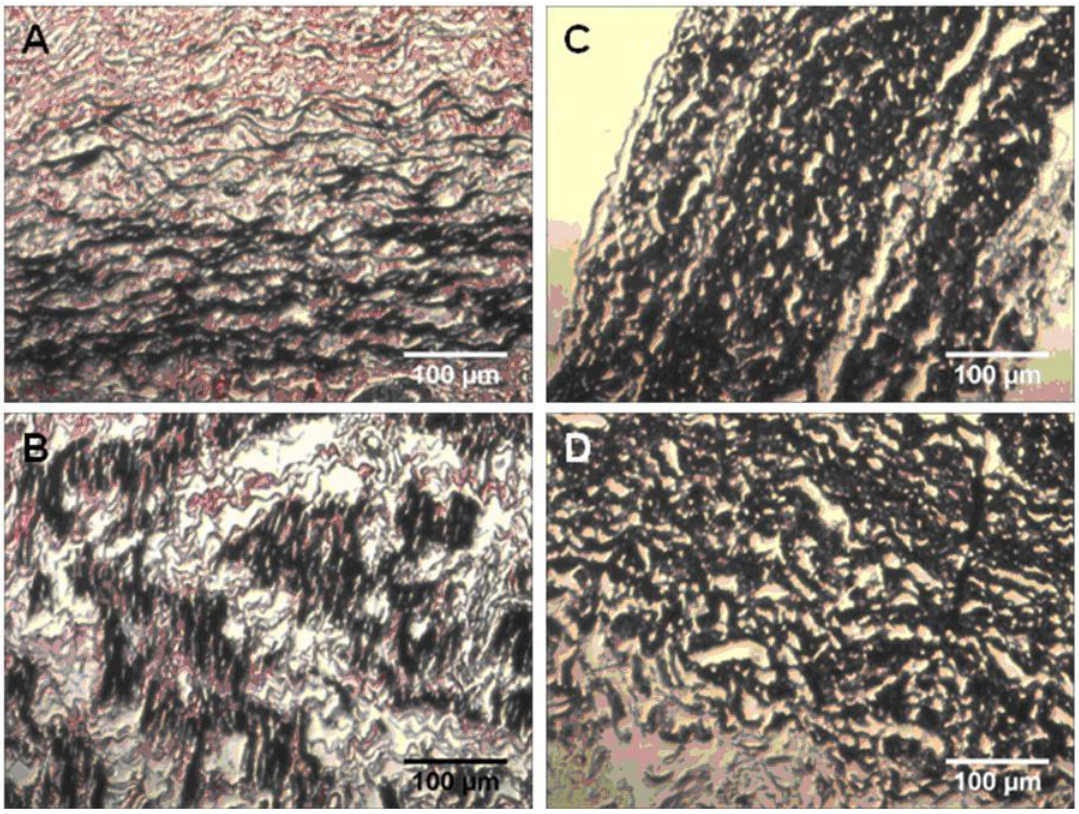

Figure 4.3: VVG stain of FRESH tissues for elastin: (A) Porcine vena cava, longitudinal; (B) Porcine vena cava, circumferential; (C) Bovine pericardium, longitudinal; (D) Bovine pericardium, circumferential. 100X magnification

Tissue sections were also stained prior to and following elastase treatment (Fig. 4.4). Histology confirms that all of the elastin was lost from the fresh vena cava after elastase treatment (Fig. 4.4D). GLUT-crosslinked tissue also shows a significant loss of structure after elastase, although few elastin fibers are still visible (E). The entire tissue structure is better preserved with NG treatment and more elastin fibers are obvious (F). Similar trends are seen in the pericardial tissue (Fig. 4.5).

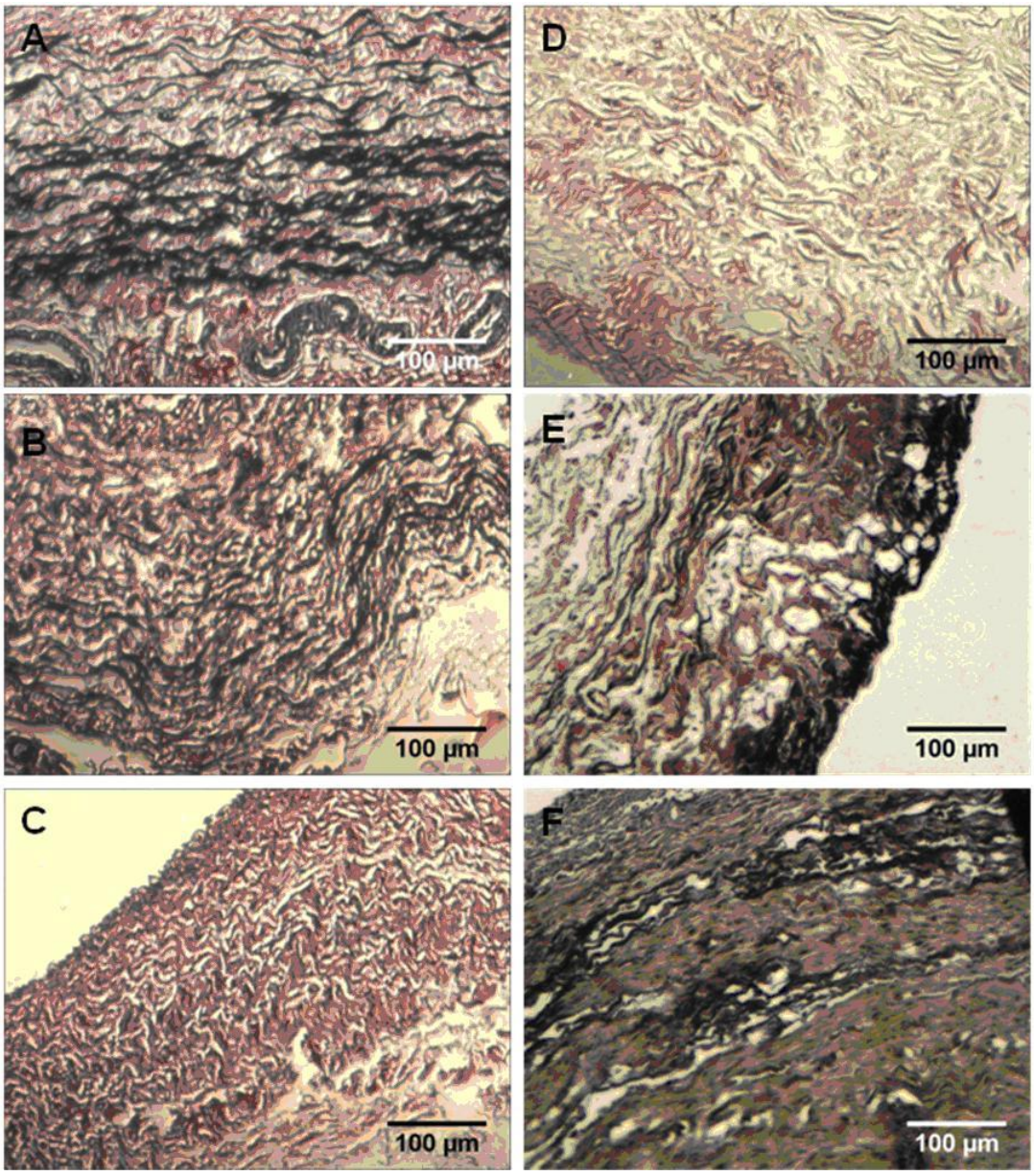

Figure 4.4: Effect of elastase on fresh and fixed porcine vena cava: (A) Fresh, untreated; (B) GLUT, untreated; (C) NG, untreated; (D-F) corresponding fixation group after elastase digestion; Longitudinal plane at 100x magnification.

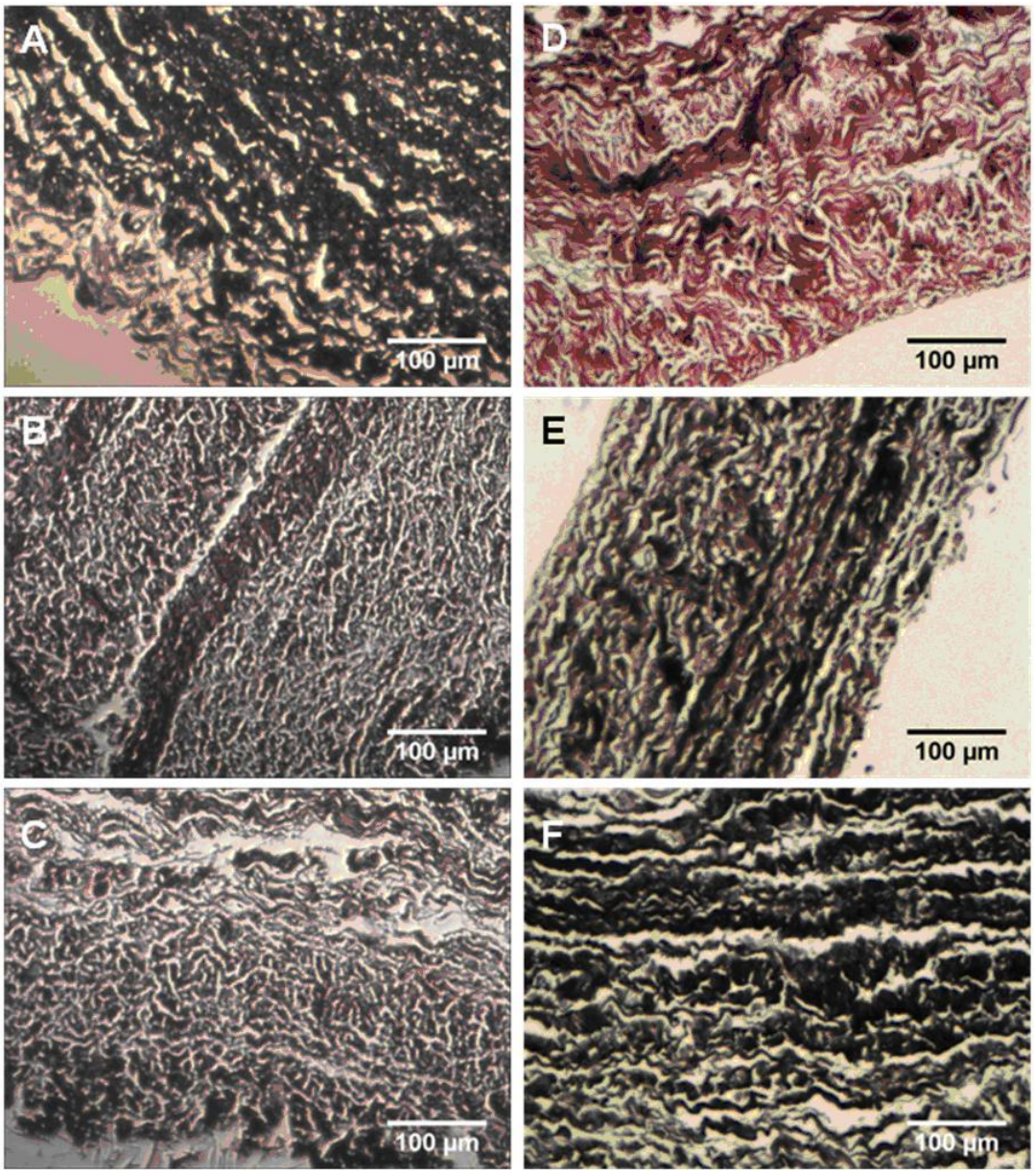

Figure 4.5: Effect of elastase on fresh and fixed bovine pericardium: (A) Fresh, untreated; (B) GLUT, untreated; (C) NG, untreated; (D-F) corresponding fixation group after elastase digestion; Longitudinal plane at 100x magnification.

4.1.4 GAG content

To measure the GAG content of heart valves, the hexosamine assay is commonly used, as GAGs contain two components—a hexosamine sugar and an uronic acid molecule. In the porcine vena cava tissue, there was no significant difference in hexosamine content among fresh, GLUT, and NG samples (Fig 4.6). In contrast, bovine pericardium showed trends similar to those of heart valves, with GLUT tissue containing fewer GAGs than fresh, and NG conferring a GAG-preserving effect [146]. However, the results express absolute amount of hexosamines. Biologic tissue contains non-GAG-related hexosamines; the quantity of these hexosamines is known for heart valve cusps and generally subtracted from hexosamine results to obtain pure GAG content. As the amount of non-GAG-related hexosamines is not known for vena cava and pericardium, only the relative quantity of GAGs in the tissue can be represented.

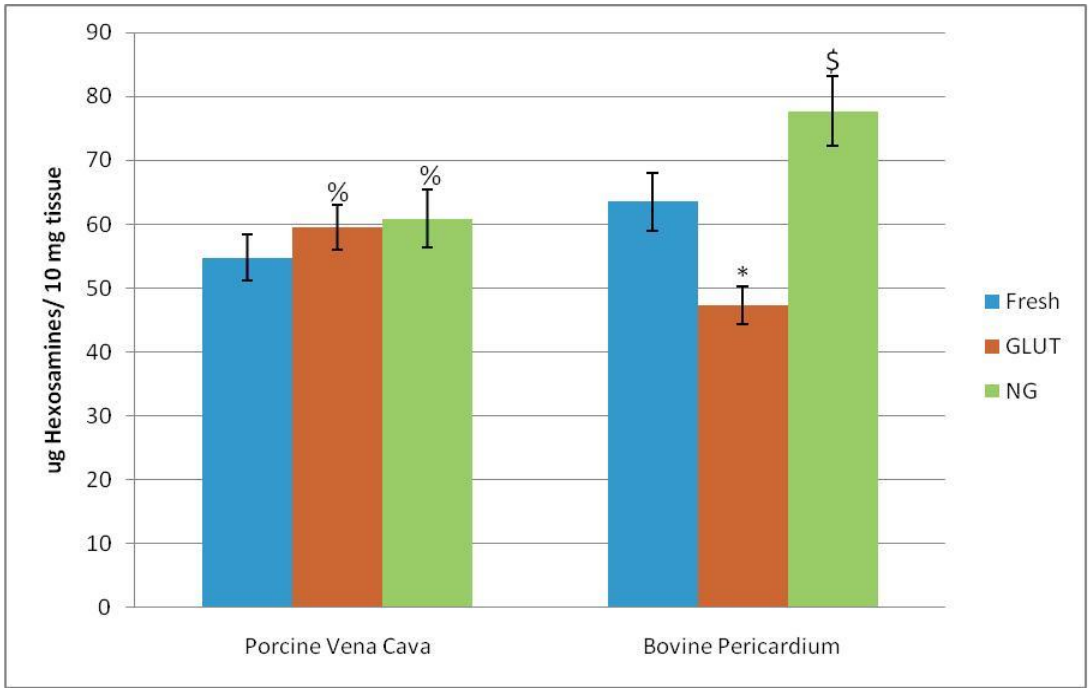

Figure 4.6: GAG content as represented by hexosamine content of tissue; (n=6; * indicates difference with Fresh of same species; $ indicates difference with GLUT of same species; % indicates difference with corresponding pericardium)

4.2 Mechanical Properties

4.2.1 Uniaxial tension

In order to determine how extracellular matrix components contribute to tissue mechanics, uniaxial tensile tests were performed on fresh vena cava and pericardium in both the longitudinal and circumferential directions prior to and following elastase and GAGase incubations. Since heart valves operate in both the elastin (lower modulus) and collagen (upper modulus) regions of the stress-strain curve, elastic moduli for both slopes were calculated.

Porcine vena cava was significantly less stiff in the longitudinal direction than the circumferential (Fig. 4.7). Removing the elastin from the tissue via elastase incubation caused a significant increase in the elastic modulus, especially in the longitudinal direction. Additionally, GAG removal caused a larger increase in stiffness in the circumferential direction than the longitudinal, suggesting that GAGs play a larger role in the circumferential mechanics.

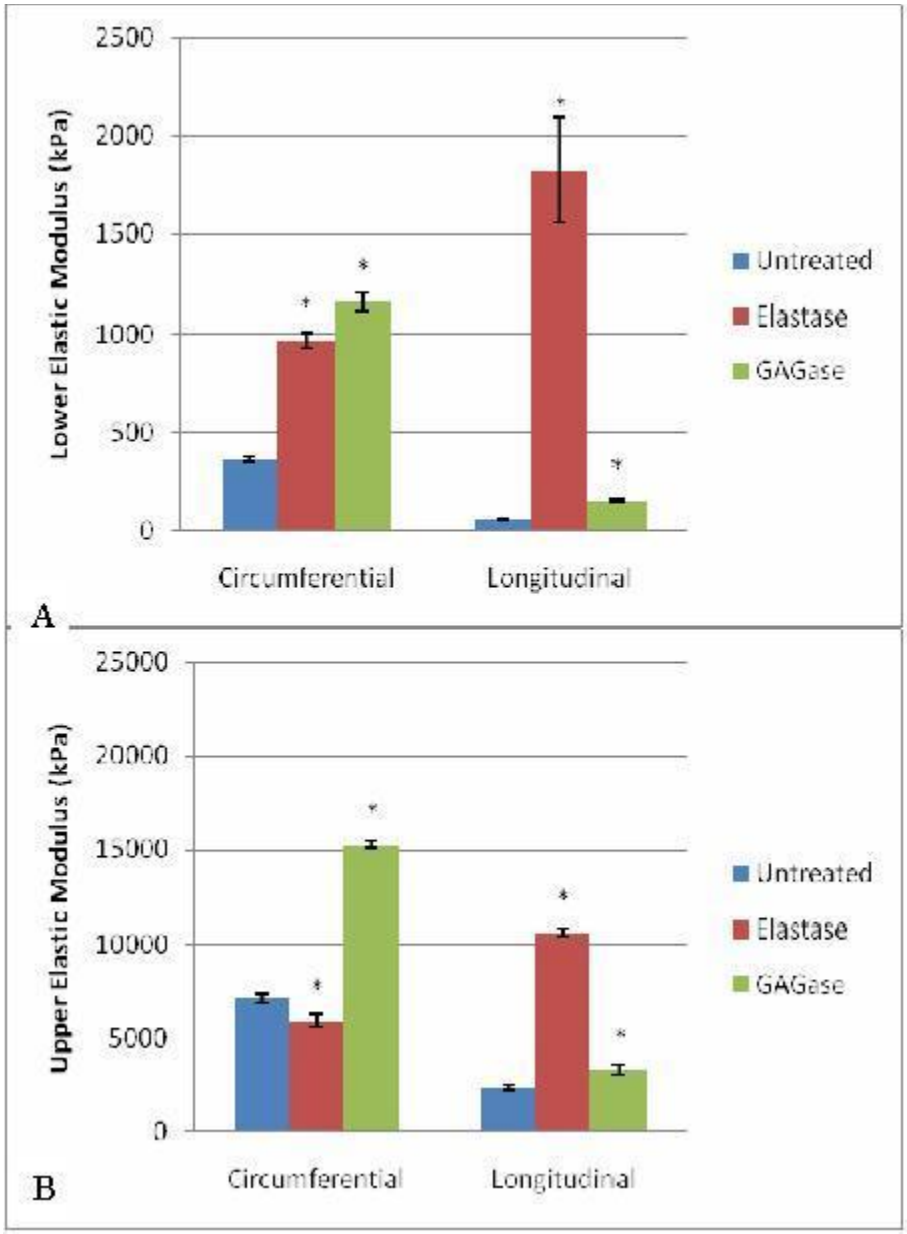

Figure 4.7: Elastic moduli of fresh porcine vena cava: (A) Lower modulus; (B) Upper modulus; (n=6; * indicates difference with corresponding untreated tissue)

Fresh bovine pericardium was significantly stiffer than fresh vena cava, with moduli at least twice those of vena cava in all orientations. Elastase treatment caused a large increase in the lower modulus in both tissue directions (Fig. 4.8). GAG removal did not affect the lower modulus in the circumferential direction, but caused a decrease in stiffness in the longitudinal direction. Conversely, GAGase treatment resulted in an increase in the upper moduli in both directions. These results are also summarized in Table 4.3.

B

	Lower Modulus (kPa)			Upper Modulus (kPa)		
	Untreated	Elastase	GAGase	Untreated	Elastase	GAGase
PVC-Circ.	362.68± 16.90	968.05± 36.91	1156.76± 41.50	7173.09± 243.21	5945.68 ± 330.80	15246.96± 182.76
PVC-Long.	54.72± 2.80	1825.88 ± 267.60	149.91± 6.85	2390.62± 132.66	10626.90± 189.71	3323.12 ± 269.50
BP-Circ.	477.13± 23.77	5518± 162.13	475.45± 16.39	18256.98± 401.92	26238.88± 247.07	43328.07± 380.84
BP-Long.	2132.54 ± 160.79	7485.33 ± 379.44	1133.56± 12.64	23601.28± 375.02	41923.69± 374.25	25935.52± 397.3419

Table 4.3: Elastic moduli of fresh porcine vena cava (PVC) and bovine pericardium (BP) in the circumferential (Circ.) and longitudinal (Long.) directions

A

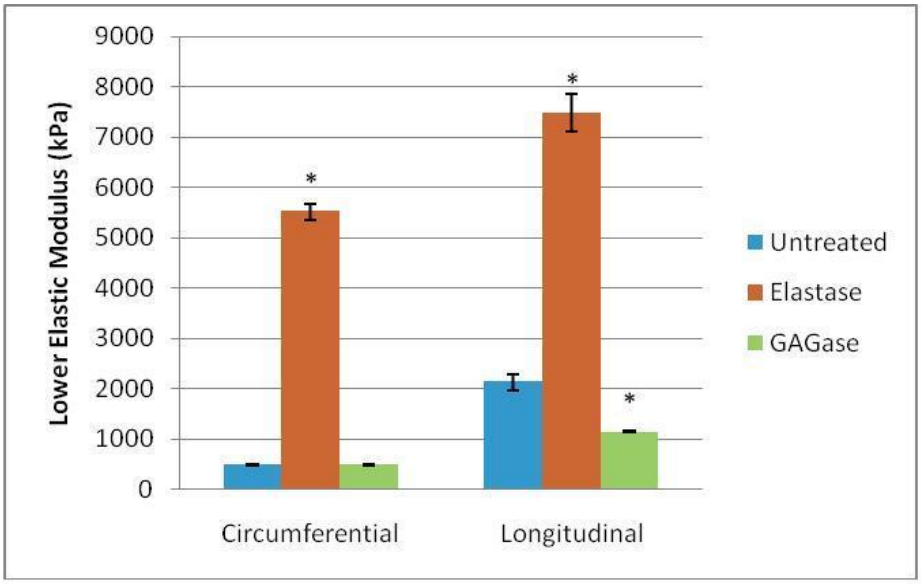

B

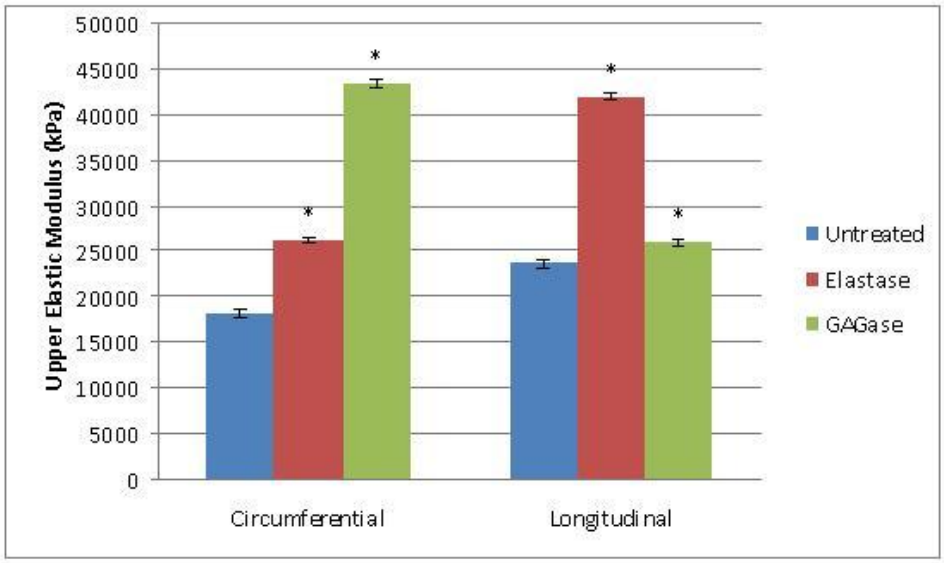

Figure 4.8: Elastic moduli of fresh bovine pericardium: (A) Lower modulus; (B) Upper modulus; (n=6; * indicates difference with corresponding untreated tissue)

In clinical practice, bioprosthetic tissue is treated with a fixative, so the mechanical effects of GLUT and NG crosslinking were also investigated (Fig. 4.9). Bovine pericardium was significantly stiffer than porcine vena cava in all treatment groups, except GLUT in the

circumferential direction. The pericardium was especially stiff in the longitudinal direction as compared to the vena cava, indicating that the longitudinal alignment of elastin fibers in vena cava greatly lends itself to the tissue compliance.

Fixation causes a significant increase in tissue stiffness. GLUT tissues were stiffer than fresh samples. NG further increases the stiffness over GLUT, likely because of additional crosslinks formed within the tissue.

A

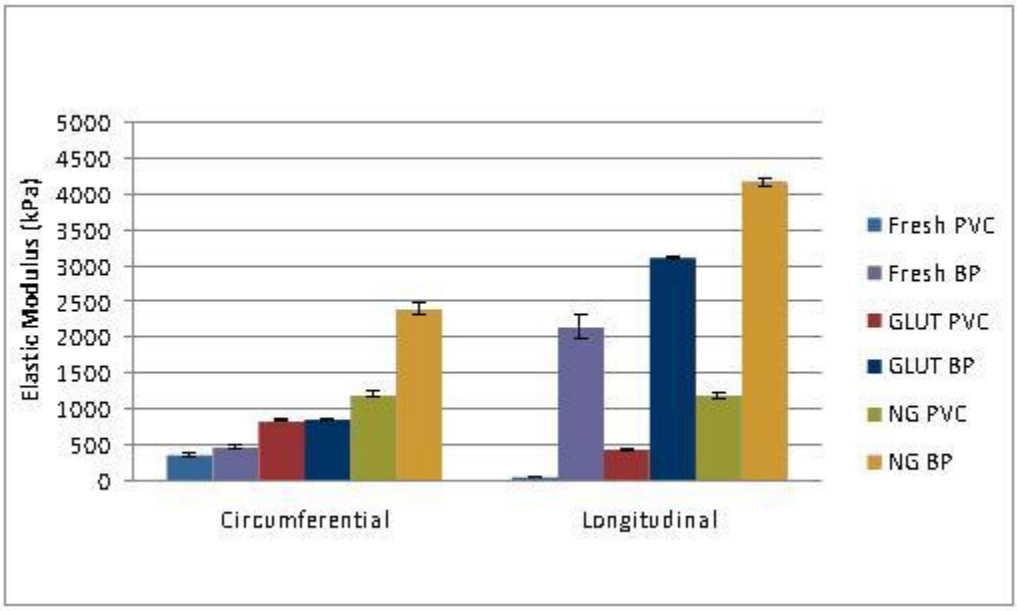

B

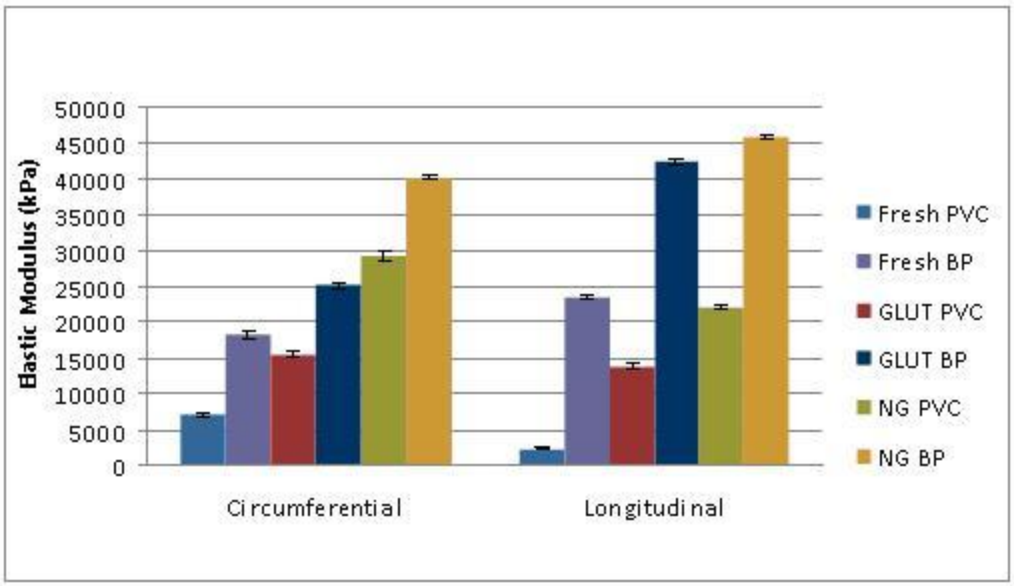

Figure 4.9: Effects of fixation on elastic moduli of porcine vena cava (PVC) and bovine pericardium (BP); (A) Lower modulus; (B) Upper modulus; (n=6; All differences between PVC and BP are significant ($p < 0.05$) except GLUT in the circumferential direction)

4.3 Tissue Resilience

4.3.1 Stereomicroscopy

Fixed vena cava and pericardium were subjected to compressive forces similar to those applied by a stent. Figure 4.10 shows the results of crimping porcine vena cava. The control tissues in the left column are highly textured, with the adventitia (C and D) being rougher than the intima (A and B). After crimping, directional striations are visible on the intima of GLUT and NG vena cava. New tissue markings are not readily apparent on the adventitial surface of the crimped tissue, as the surface of the controls was rather rough.

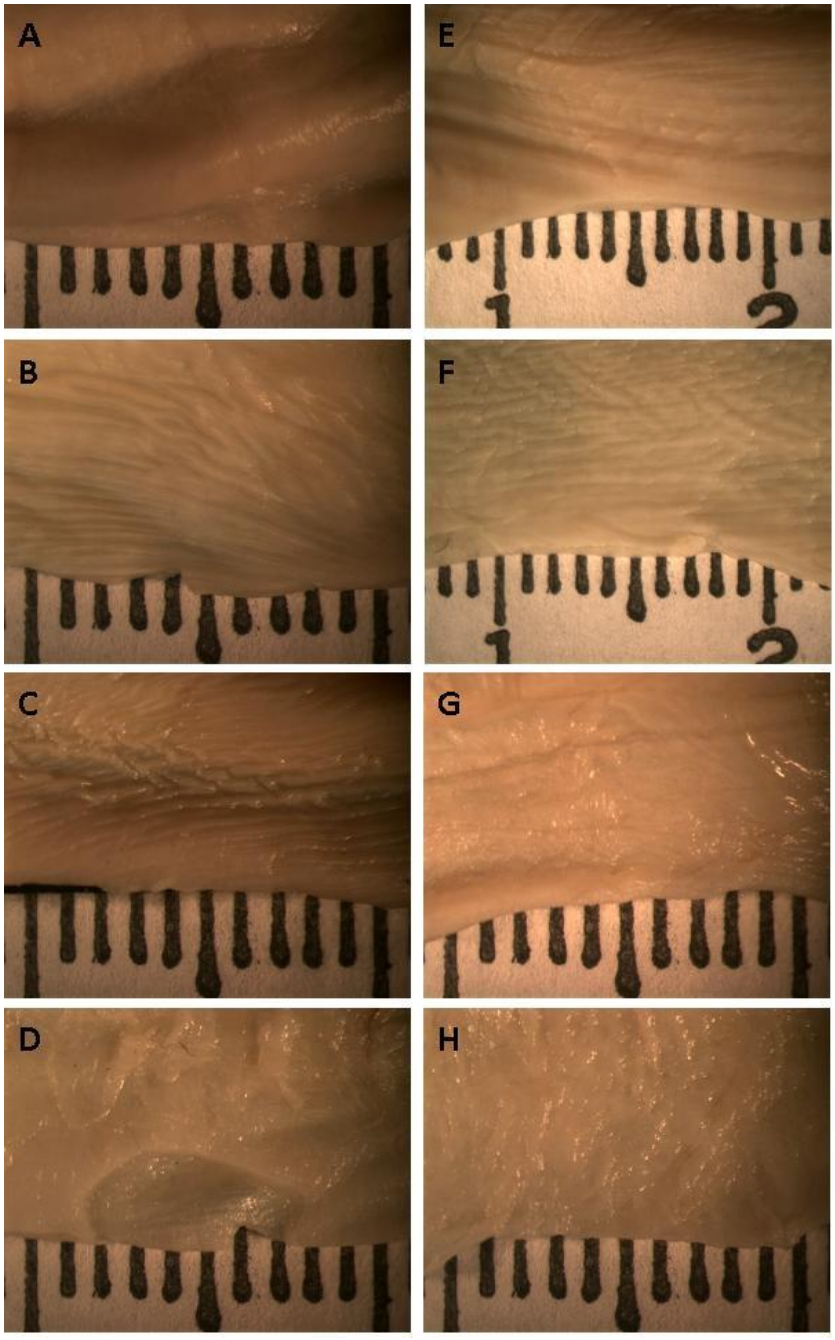

Figure 4.10: Stereomicroscopy images of control and crimped vena cava; A) Intima, GLUT control; B) Intima, NG control; C) Adventitia, GLUT control; D) Adventitia, NG control; E) Intima, GLUT crimped; F) Intima, NG crimped; G) Adventitia; GLUT crimped; H) Adventitia; NG crimped; Each scale line represents 1 mm

Similar images were captured of control and crimped bovine pericardium. The serosa surface of the pericardium is perfectly smooth (Fig. 4.11 A and B). After crimping, very faint, thin markings can be seen on the surface (E and F). The outer layer of the pericardium (C and D) is rougher; thus it is difficult to spot tissue damage caused by crimping (G and H).

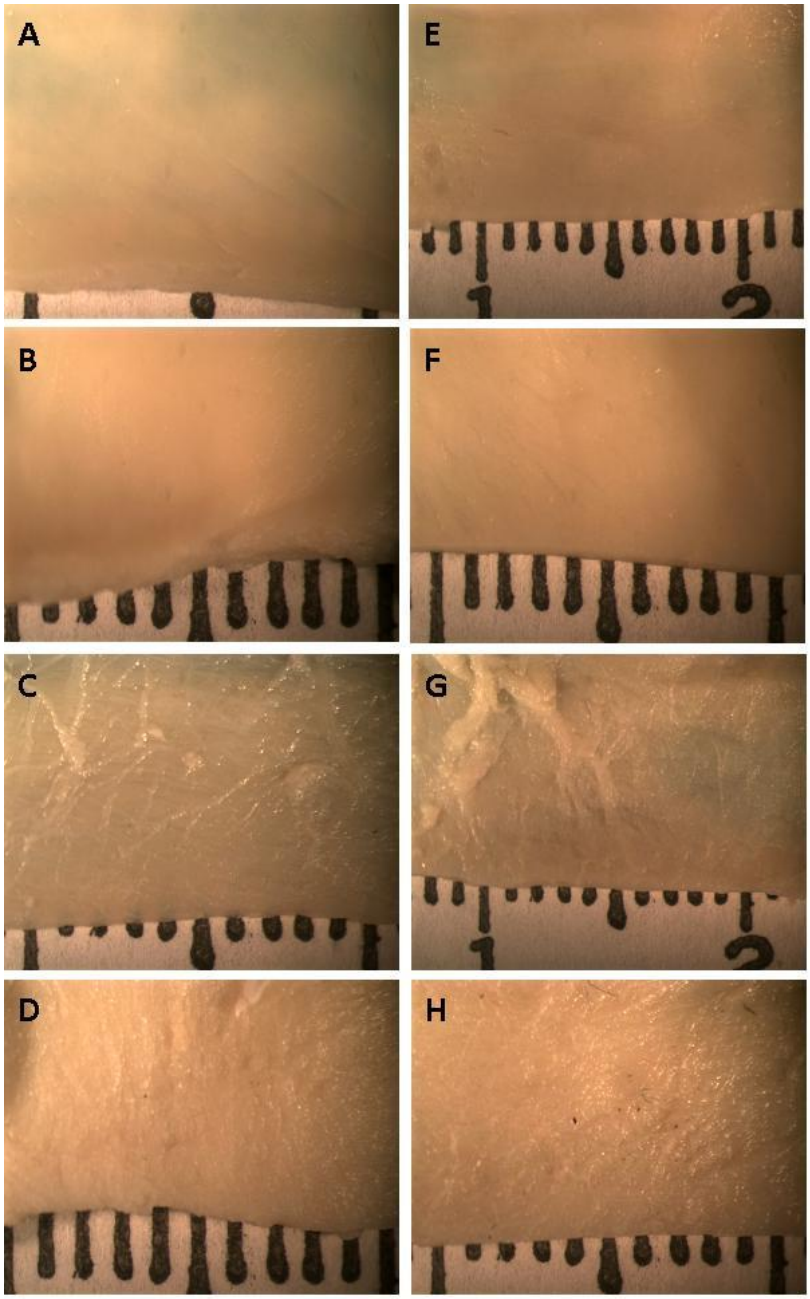

Figure 4.11: Stereomicroscopy images of control and crimped bovine pericardium; A) Serosa, GLUT control; B) Serosa, NG control; C) Outer, GLUT control; D) Outer, NG control; E) Serosa, GLUT crimped; F) Serosa, NG crimped; G) Outer; GLUT crimped; H) Outer; NG crimped; Each scale line represents 1 mm

4.3.2 SEM

The surfaces of the crimped tissues were observed with scanning electron microscopy to further detect any defects. The adventitial surface of the control vena cava and the outer surface of the control pericardium were again very rough, and additional indentations and striations were impossible to detect. However, the smooth intima and serosa exhibited some surface modifications after crimping. The intimal surface of the control vena cava samples (Fig 4.12) are generally smooth with small grooves spanning uniformly across the surface. After crimping, the GLUT sample had many new indentations and deep ridges. The NG samples also exhibited new grooves on the surface; however the NG tissue was significantly less damaged than the GLUT tissue. Similar results are seen in the bovine pericardial tissue (Fig 4.13). The serosa surfaces of the GLUT and NG control pericardium samples are smooth with uniform surface ridges. The GLUT tissue exhibited cracks and fiber damage after crimping, while the NG tissue remained relatively smooth.

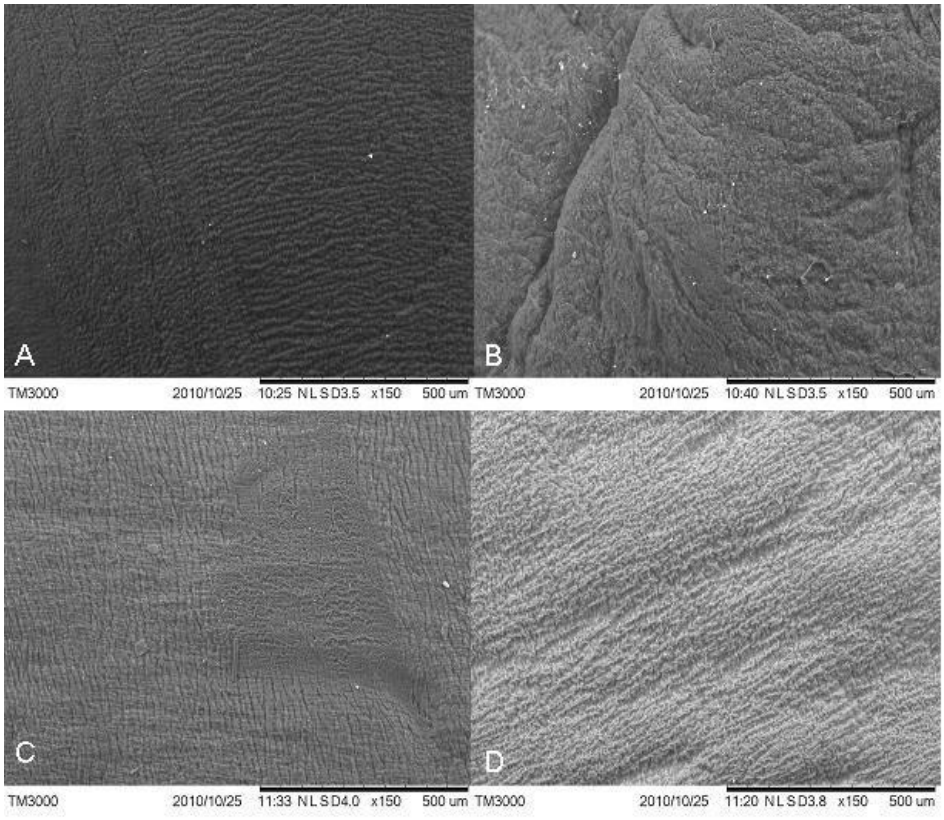

Figure 4.12: SEM images of intimal surface of control and crimped vena cava; A) GLUT control; B) GLUT crimped; C) NG control; D) NG crimped; 150x magnification

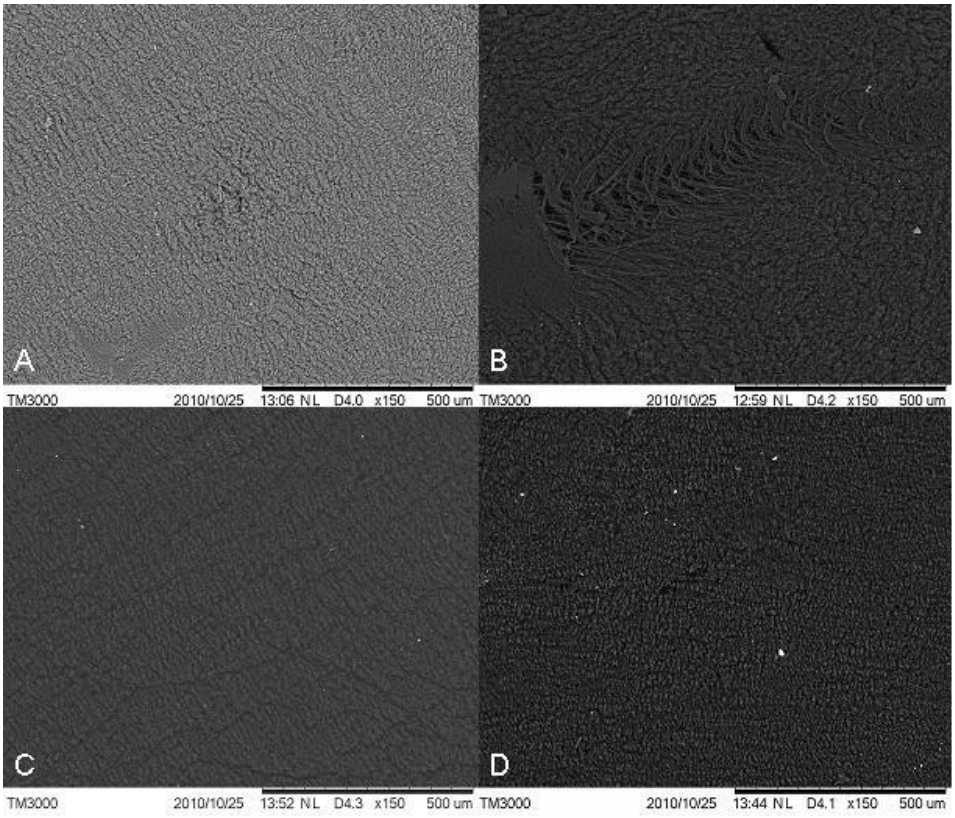

Figure 4.13: SEM images of the serosa of control and crimped bovine pericardium; A) GLUT control; B) GLUT crimped; C) NG control; D) NG crimped; 150x magnification

4.3.3 Mechanical properties of crimped tissue

Following crimping, the vena cava and pericardium were subjected to uniaxial tensile tests. The results were compared to uncrimped controls in order to determine how the compressive forces experience during crimping affect tissue fibers and mechanical properties (Fig. 4.14).

In the circumferential direction, crimping caused a significant increase in the lower elastic modulus of all tissue groups. Additionally, the GLUT-fixed bovine pericardium became

stiffer than the corresponding vena cava after crimping. The effects of crimping were not obvious in the upper modulus in the circumferential direction, as only GLUT-fixed PVC was significantly stiffer than the control in this group.

The trends in mechanical behavior in the longitudinal direction differed slightly from the circumferential behavior. After crimping, a significant increase in the lower elastic modulus was again seen among all tissue groups. However, the pericardium became much stiffer than the vena cava, reaching a lower elastic modulus of 13,212.03 ± 846.23 kPa for NG tissue, while NG vena cava had a modulus of only 3,036.43 ± 808.33 kPa after crimping. Considering the upper modulus, the crimped pericardium again increased in stiffness as compared to the controls, but the difference was not as great as for the lower modulus. The upper elastic modulus of the vena cava decreased in the longitudinal direction, resulting in vena cava tissue that was significantly less stiff than pericardial tissue for both tissue groups.

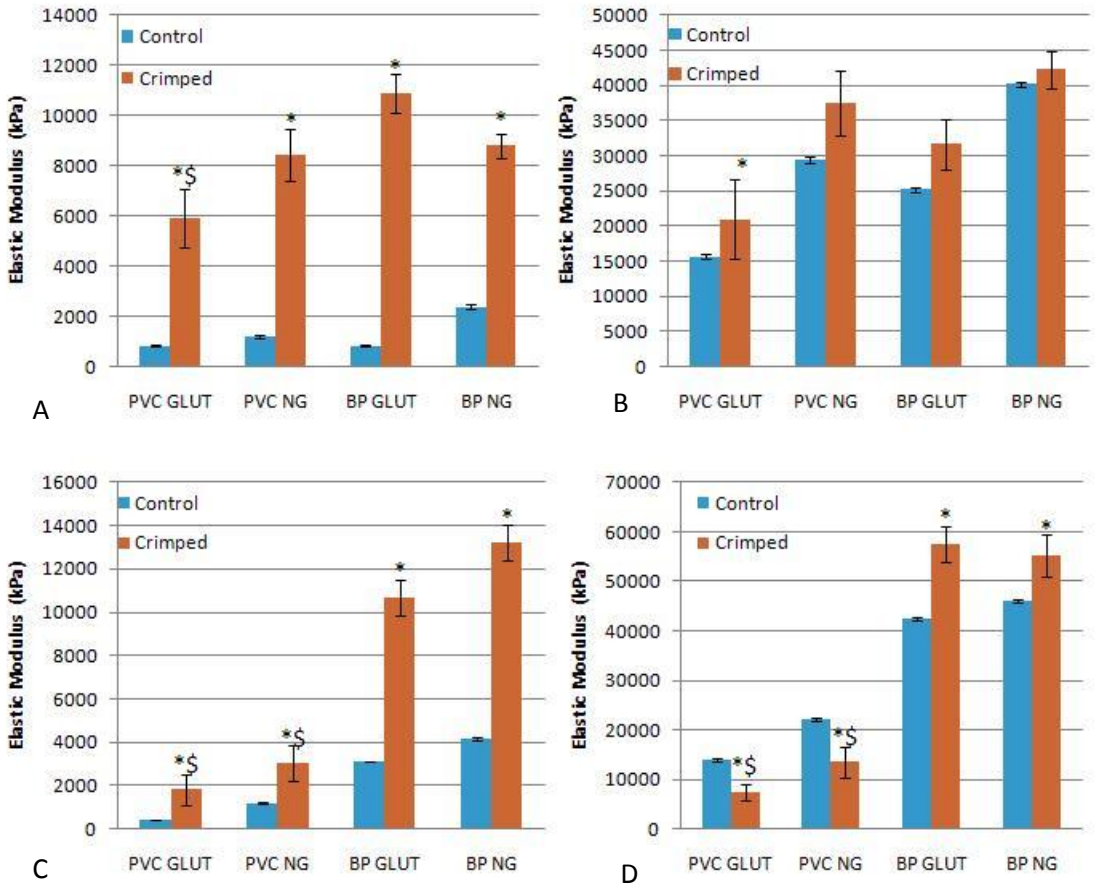

Figure 4.14: Elastic modulus of tissue after crimping; A) Lower modulus, circumferential; B) Upper modulus, circumferential; C) Lower modulus, longitudinal; D) Upper modulus, longitudinal; (n=6; * indicates difference with control tissue; $ indicates difference with crimped BP tissue)

4.4 *In vivo* stability

4.4.1 Calcium and phosphorus content

Subdermal implants were used to study the mineralization tendency of the tissues. The juvenile rat model was selected, as juvenile rats exhibit accelerated calcification [5]. GLUT and

NG pericardium and vena cava were studied. Additionally, another group of NG tissue was treated with ethanol (NGE) as an anti-calcification therapy.

After 3 weeks of implantation, GLUT-fixed vena cava calcified significantly less than pericardium (Fig. 4.15). However, neomycin treatment led to an increase in mineralization of the vena cava, and the difference in calcium content between NG vena cava and pericardium is not significant (p= 0.246). Ethanol treatment resulted in an 82.69% decrease in the calcium content of the bovine pericardium, but only a 50.90% decrease in calcification of vena cava. The difference between calcium content of the NGE vena cava and pericardium was not statistically significant (p = 0.106) due to large variability among the various rats.

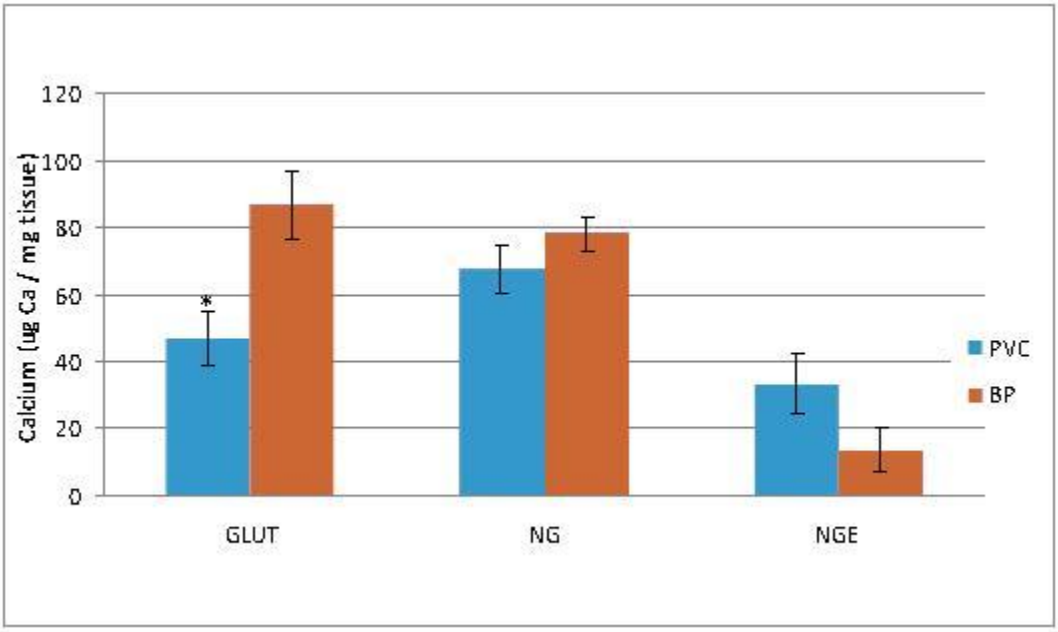

Figure 4.15: Calcium content of subdermally implanted tissue; (n = 10 (GLUT and NG); n = 6 (NGE);* indicates significant difference with corresponding bovine pericardium (BP) group)

Phosphorus content is often used as a complement to calcium data, as mineral deposits in heart valves are generally composed of calcium phosphate. Trends similar to those in the calcium data are observed in the phosphorus results for the various tissue groups (Fig 4.16).

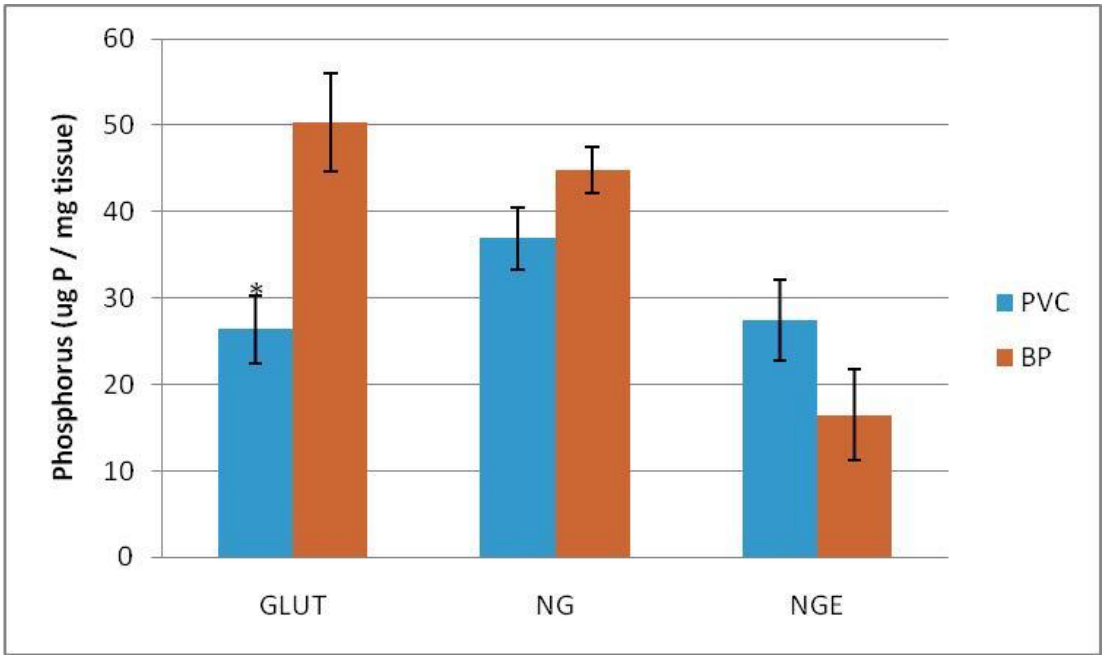

Figure 4.16: Phosphorus content of subdermally implanted tissue; (n = 10 (GLUT and NG); n = 6 (NGE)* indicates significant difference with corresponding bovine pericardium (BP) group)

Additionally, the Ca:P molar ratio for each sample group was calculated (Table 4.4), as this statistic provides information about the organization of the calcium phosphate in the tissue.

	Vena Cava	Pericardium
GLUT	1.37± 0.039	1.33± 0.007
NG	1.42± 0.012	1.35± 0.003
NGE	0.93± 0.094	0.64± 0.102

Table 4.4 Ca:P molar ratio of rat subdermal implants

4.4.2 Histology

Calcium content was also viewed histologically via the Alizarin red stain, which stains calcium red. Light green was used as a counter stain. The histological results complement the aforementioned quantitative data. Denser clusters of calcification are observed in the pericardial tissue than in the vena cava (Fig. 4.17). However, after ethanol treatment, almost no calcium is apparent in the bovine pericardium, while the vena cava still exhibits bands of calcium deposits throughout the tissue.

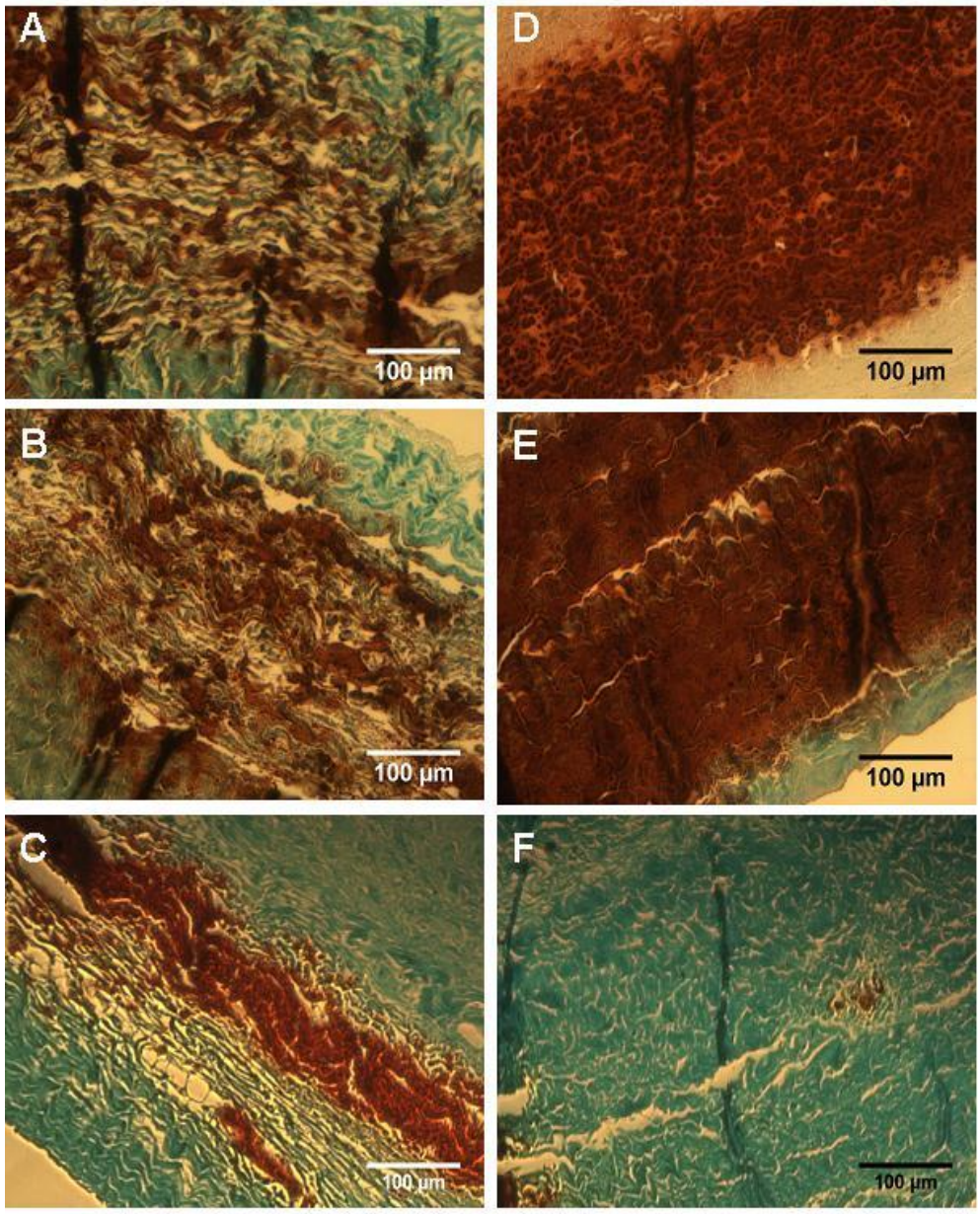

Figure 4.17: Alizarin red histology; Calcium content of subdermally implanted porcine vena cava (PVC) and bovine pericardium (BP) is represented by red staining, while background tissue is stained green; A) GLUT PVC; B) NG PVC; C) NGE PVC; D) GLUT BP; E) NG BP; F) NGE BP; Images taken at 100x

CHAPTER 5

DISCUSSION

While percutaneous technology is revolutionizing the field of replacement heart valves, these new devices are not without limitations, the most important of which is device profile. The ability to access the aorta via a catheter is largely determined by the diameter of the catheter that is required. Tortuous vasculature or narrow atherosclerotic arteries can only be accessed with small diameter catheters [9, 106, 108]. First generation PHVs were too wide for transcatheter delivery in many patients and necessitated transapical delivery instead. However, the transapical approach requires a thoracotomy and puncture of the left ventricular, so it is inherently more invasive than the transcatheter route [108]. In order to produce a smaller diameter valve, Medtronic CoreValve switched from bovine pericardium to porcine pericardium, which is reportedly thinner than bovine [9]. Additionally, they altered their tissue fixation method in such a way as to manufacture a smaller PHV.

Another possible method to decrease device profile is to use a highly elastic alternative tissue source. Vena cava is denser in elastin fibers than other blood vessels and may be a good option for PHVs. However, vena cava has not previously been used as a bioprosthetic tissue, and its structural properties are not fully characterized in the literature. The aim of this project is to understand the tissue structure and matrix properties of porcine vena cava in order to predict how such tissue might behave in this application.

All of the current bioprosthetic percutaneous heart valves are composed of either porcine or bovine pericardial tissue [9], and bovine pericardium is also used to construct traditional bioprosthetic heart valve implants. Any alternative tissue source will have to perform at least as

well as bovine pericardium in order to be a desirable option for PHVs. Therefore, porcine vena cava was compared directly to bovine pericardium in all of our studies. The structure, mechanics, tissue resilience, and *in vivo* behavior of vena cava were investigated in order to assess the feasibility of using the tissue in bioprosthetic PHVs.

5.1 Tissue Structure

The profile of a PHV is highly related to tissue thickness, as the bioprosthetic tissue must be folded into the supporting stent [9]. The tissue thickness of fresh and fixed vena cava was compared to that of bovine pericardium. Fresh vena cava and pericardium were similar in thickness, both measuring about 0.20 mm. The glutaraldehyde fixation process causes an increase in thickness, as crosslinks cause the tissue to contract in the longitudinal and circumferential directions. While GLUT vena cava and pericardium were also similar in thickness (0.54 ± 0.03 mm and 0.58 ± 0.05 mm respectively), NG vena cava was significantly thinner (0.49 ± 0.03 mm) than NG pericardium (0.62 ± 0.03 mm). A possible explanation of this phenomenon may be that pericardial tissue contains a greater proportion of collagen fibers than vena cava. The addition of neomycin may enhance GLUT crosslinking of those fibers to cause additional contraction and a greater increase in thickness. The native heart valve has a thickness of approximately 0.605 ± 0.196 mm [172], so the thicknesses of fixed vena cava and bovine pericardium are anatomically compatible with the application. Although vena cava and pericardium were generally similar in thickness, we have also hypothesized that the vena cava may be more flexible, a factor which could also help reduce device diameter.

The mechanical properties of bioprosthetic heart valves are largely dictated by the extracellular matrix. In native heart valve leaflets, circumferentially-aligned collagen fibers in the fibrosa support loads during cyclic functioning, while radially-aligned elastin fibers in the ventricularis allow for extensibility and coaptation [172]. Additionally, glycosaminoglycans in the spongiosa help to hydrate the tissue and adsorb shock. Thus, the composition and orientation of tissue extracellular matrix components are crucial to proper valve function. It is known that bovine pericardium contains planar fibers, specfically collagen type I and a small amount of elastin [176]. Vena cava, in contrast, has a high elastin density, helically-oriented elastin fibers in the media, and circumferentially-aligned collagen fibers in the adventitia [162]. We further examined the extracellular matrix components in the tissue quantitatively using enzyme digestion studies. Fresh and fixed tissues were digested in elastase and collagenase, and the percent weight loss was calculated. It was assumed that fresh tissue offered no enzymatic resistance, so the percent weight loss represented the weight fraction of each tissue component. Fresh bovine pericardium lost significantly more weight after collagenase than did porcine vena cava (74.59± 1.01% and 56.86± 3.99% respectively). This result suggests that the pericardial extracellular matrix is more collagen-dense than vena cava ECM. Fixation with glutaraldehyde greatly enhances collagen stability, decreasing the percent weight loss to less than 10% in both tissue types. GLUT forms stable crosslinks with collagen through a Schiff base reaction between the aldehyde group and the amine group on the lysine and hydroxylysine residues of collagen [27]. The crosslinks help prevent enzymatic degradation of the collagen fibers. NG did not improve collagenase resistance in pericardium, but reduced percent weight loss to 1.13± 0.45% in vena cava tissue. While neomycin is a hyaluronidase inhibitor, it has been shown to affect

collagen and elastin preservation as well [146]. Neomycin likely increases the crosslinking density of the GLUT-fixed tissue, providing steric hinderance for enzyme diffusion into the tissue. Differences in collagen structure between vena cava and pericardium may affect how the neomycin is incorporated into the GLUT crosslinks in each tissue, which would subsequently affect how the crosslinked fibers are affected by the enzyme.

The main component of the heart valve extracellular matrix is collagen, a structural protein which provides the strength needed to withstand cyclic loading [5]. The collagen molecule is a triple helix of glycine, proline, and hydroxyproline. Upon heating, the collagen helices transition to random coils. This process of collagen denaturation is endothermic and irreversible [173]. Differential scanning calorimetry (DSC) measures the collagen denaturation temperature (T_d) by monitoring the heat flow in the tissue sample while heating at a set rate. Collagen denaturation is represented as an endothermic peak on the heating curve, as heat is taken in to break bonds and unwind the collagen helix. The T_d's for fresh vena cava and pericardium were 62.78 ± 0.18 ºC and 63.63 ± 0.19 ºC, respectively. GLUT fixation significantly increased T_d, as GLUT-based crosslinks between collagen increase the stability of the fibers. The thermal denaturation temperature of the GLUT vena cava and pericardium is in agreement with previously reported values of 88.3 ± 0.56 ºC in GLUT porcine aortic valves [92]. The denaturation temperature of NG tissue was slightly, but significantly, greater than that of GLUT. Neomycin induces additional crosslinks in the tissue. Crosslinking pulls the fibers closer together, reducing the number of possible molecular configurations. Thus, the entropy is reduced and the Gibb's Free Energy increased. More energy is needed to induce a change of state, resulting in a higher T_d [174]. While DSC confirmed that collagen is indeed protected by

GLUT and NG fixation, the method was not sensitive enough to detect subtle differences in collagen content between pericardium and vena cava.

Elastin is the second major component of the tissue extracellular matrix. In the native heart valve, radially-aligned elastin fibers provide tissue extensibility that allows for coaptation during valve closure. Furthermore, elastin provides the recoil to return the tissue to its compressed state between loading cycles [175]. Studies have shown that elastin fibers are vital to proper valve mechanics, and elastin damage in the native heart valve results in tissue elongation, reduced radial extensibility, and increased stiffness [175]. Therefore, preservation of elastin is vital to bioprosthetic tissue mechanics. Previous literature reports that the vena cava is more elastin-dense than other vascular tissues. Elastase digestion was used to quantify the proportion of elastin in fresh tissue. Fresh vena cava lost significantly more weight (35.10± 5.47%) after elastase treatment than did bovine pericardium (10.51± 0.76%), which suggests that elastin constitutes a larger proportion of vena cava ECM. GLUT fixation did not render the tissue more enzyme resistant, as GLUT does not crosslink elastin fibers [175]. However, NG treatment led to a significant decrease in percent weight loss in both tissue types. This result was also confirmed histologically, as more elastin fibers were visible in NG tissue after elastase digestion than in fresh and GLUT tissue. Neomycin has previously been shown to inhibit elastase-mediated elastin degradation of bioprosthetic heart valve cusps [146]. This result again supports that increased crosslinking density in NG tissue impedes enzymatic access to the tissue fibers, thus decreasing enzymatic degradation of the tissue. Over time, elastin damage by elastase increases the shock loading on collagen fibers, rendering the bioprosthesis less durable

[177]. Thus the addition of neomycin to the GLUT crosslinking procedure may help to preserve the tissue structure and mechanical properties *in vivo*.

In addition to elastin content, the orientation of the elastin fibers was also studied. Verhoeff van Gieson staining was performed to visualize the elastin in the tissue. It has been suggested that the elastin fibers are wrapped around the vena cava helically in the longitudinal direction [162]. Our results show that in fresh vena cava, the elastin fibers were clearly oriented in the longitudinal direction, while cross-sections of the fibers were seen in the circumferential plane. The longitudinally-oriented elastin imparts elasticity to the vena cava along the length of the vessel. Conversely, no clear fiber orientation was apparent in the bovine pericardium. The fiber directionality varies regionally in pericardium, and also may vary between planes [123]. The non-uniformity and unpredictability of the fiber orientation causes great variability in mechanical properties across the pericardial tissue, making it difficult to construct a consistent heart valve [124, 125]. In the native heart valve, the elastin fibers are aligned to impart radial extensibility to the cusps. Because the vena cava consists of highly aligned fibers, a more consistent valve may be constructed which better mimics the fiber structure of a native valve.

Glycosaminoglycans play a large role in heart valve mechanics by hydrating the tissue, dissipating energy, and facilitating shearing between tissue layers [146]. While the role of GAGs in heart valve mechanics is well understood, their function in other vascular tissues, such as the vena cava, has not been elucidated. The literature suggests that GAGs may help to lubricate the vena cava's intimal layer [168]. Similarly, GAGs provide hydration and lubrication to the serosa layer of the pericardium [120]. GAGs are composed of a hexosamine sugar and a uronic acid molecule. The hexosamine assay [145] was performed on vena cava and pericardial tissue. The

vena cava had no significant difference in hexosamine content among fresh, GLUT, and NG tissue. However, the pericardium had more hexosamines in fresh and NG tissue than in GLUT, a result that has also been found in heart valves [145, 146]. It is known that the porcine heart valve contains tissue hexosamines that are not related to GAGs. Previous research has determined that 90 ug of non-GAG-related hexosamines are present in the heart valve [149, 150]. However, the quantity of non-GAG-related hexosamines in vena cava and pericardium is not known. Thus the amount of hexosamines cannot be taken as an absolute measure of GAG content. However, when viewed as a relative measure of GAGs, certain conclusions may be drawn. GAGs are lost during tissue preparation and GLUT fixation, and GLUT-fixed cusps typically contain fewer GAGs than fresh tissue [27, 146]. Moreover, since neomycin has been shown to be effective at preserving GAGs [145, 146], it is expected that the NG group will contain more GAGs than the GLUT tissue. However, the amounts of hexosamines in fresh, GLUT, and NG vena cava were equal; thus most of these hexosamines are likely non-GAG-related. Indeed, it has been reported that the quantity of GAGs in the vena cava is quantitatively undetectable [167]. However, as expected, the hexosamine content of NG bovine pericardium is greater than that of GLUT tissue. Thus, GAGs are detectable in pericardium, and NG treatment effectively preserved GAGs in pericardial tissue. Although GAGs are vital to native heart valve mechanics, it is unclear if the lack of GAGs in vena cava will be detrimental to valve performance. Fatigue cycling and *in vivo* studies are needed to determine if the vena cava can withstand constant flexure and shearing without a significant amount of GAGs to adsorb shock and dissipate energy in the tissue.

5.2 Mechanical properties

Extracellular matrix fiber orientation plays a large role in biologic tissue mechanics [172, 176]. Elastin fibers provide flexibility and extensibility in the tissue direction parallel to their alignment, whereas load-bearing collagen fibers impart strength and stiffness along their length [2, 5, 21]. Blood vessels, such as the vena cava, are composed of circumferentially-aligned collagen fibers to allow the vessel to withstand the forces from pulsatile blood flow [162]. Previous studies also suggest that the elastin fibers helically wrap along the longitudinal axis of the vena cava [162]. Thus, there is a great contrast in extracellular matrix orientation between the circumferential and longitudinal axes of the vena cava, which should correspond to substantial mechanical differences between the two directions. In contrast, the collagen and elastin fibers in the pericardium are not well-aligned and vary regionally, making the pericardium less uniform and predictable mechanically [5, 9, 123-125].

For many biological tissues subjected to tensile testing, the stress-strain curve contains two regions: a lower modulus region that is dominated by elastin fibers and an upper modulus region that is dominated by the collagen response [119, 127]. Indeed the stress-strain curves for the vena cava and pericardium displayed the expected two-region behavior. Tensile testing of fresh tissue samples confirmed histological findings regarding fiber orientation. The lower elastic modulus of fresh vena cava was significantly lesser in the longitudinal direction than the circumferential, indicating longitudinal alignment of the elastin fibers. The upper modulus was greater in the circumferential direction due to the circumferentially-aligned collagen fibers. Following elastase treatment, the longitudinal lower modulus increased more than 30-fold, while the circumferential lower modulus increased only about 2.5-fold. Therefore, disruption of the elastin fibers causes a massive increase in the stiffness along the fiber direction, while only a

small increase is seen in the perpendicular direction. In the circumferential direction, the upper modulus decreased with elastase treatment, as fewer perpendicular fibers were present to impede motion in this direction [176]. Thus, the alignment of the elastin fibers plays a critical role in the vena cava tissue mechanics in the longitudinal direction.

Conversely, the longitudinal moduli of the fresh bovine pericardium were greater than the circumferential moduli. Following elastase treatment, the lower modulus increased by 11.5 times in the circumferential direction and 3.5 times in the longitudinal. This result suggests that the elastin fibers of the pericardium tend to be aligned more toward the circumferential direction, which would allow outward extensibility of the pericardial sac as the heart beats. However, the pericardial elastin fiber alignment is not as profound as that of the vena cava. The upper moduli of the fresh pericardium also did not differ as starkly in the circumferential and longitudinal directions as those of the vena cava, confirming a more random orientation of collagen fibers in the pericardium. The varied collagen alignment serves to provide strength to the pericardium in multiple directions, as the sac must withstand a number of different forces, including outward tension and torsion during the cardiac cycle [123]. However, this diverse alignment causes variations in mechanical properties that are not ideal for constructing a mechanically stable heart valve.

The role of GAGs in pericardium and vena cava tissue mechanics are not well understood. Thus, fresh tissues were treated with GAG-degrading enzymes, and the tensile response was examined. GAGase treatment caused a significantly larger increase in the upper and lower moduli in the circumferential direction than the longitudinal in the vena cava. This result indicates that GAGs may be associated with the circumferentially-aligned collagen fibers

and may help to facilitate movement and shearing between the fibers, which is major function of GAGs in heart valve mechanics [5]. Similary, GAGase had a significant effect on the upper modulus of the pericardium in the circumferential direction, also suggesting an association between GAGs and collagen in the pericardium. GAGs in the pericardium may therefore provide lubrication and facilitate shearing between collagen fiber layers during torsion.

Direct comparison of the corresponding moduli between the fresh vena cava and pericardium revealed that the pericardium is stiffer than the vena cava in all tissue orientations. The difference is especially significant in the upper modulus, likely due to the greater collagen content of the pericardium. A denser collagen network in the pericardial tissue impedes fiber movements and causes the tissue to be less compliant.

The tissue fixation process has also been shown to have a significant effect on tissue mechanics [27]. Chemical crosslinking of the collagen matrix improves tissue stability, but also hinders fiber movement, leading to increased tissue stiffness [21, 26, 144]. GLUT fixation increased the moduli of both the vena cava and pericardium, due to crosslink formation. Addition of neomycin to the crosslinking procedure (NG) led to a further increase in stiffness, as neomycin is incorporated into GLUT crosslinks, thereby increasing the crosslink density. While the moduli of the two tissue types were only modestly different in the circumferential direction, the pericardium was enormously stiffer than the vena cava in the longitudinal direction, a result which was exacerbated by GLUT and NG crosslinking. The higher collagen content of the pericardium was more affected by crosslinking, resulting in very high elastic moduli for fixed pericardium. As GLUT and NG do not crosslink elastin [146], the vena cava was able to retain much of its flexibility, especially in the lower modulus region. While the vena cava did increase

in stiffness during crosslinking, it remained at least twice as compliant as the pericardium in the longitudinal direction after fixation. Increased stiffness following crosslinking is cited as a major contributor to bioprosthetic valve mechanical failure [27]. Use of vena cava in valve construction may therefore improve prosthesis durability by enhancing bioprosthetic tissue flexibility.

5.3 Tissue resilience

The main advantage of percutaneous heart valves is their ability to be implanted without open chest surgery. The unique PHV design allows the entire valve to be crimped into a small diameter and delivered via a transcatheter route to the aortic position [9]. However, this design feature also raises concerns about the integrity of the crimped tissue [108]. Stents are crimped under large compressive forces. Subjecting the tissue to excessive loads prior to implantation may alter the mechanical properties, damage the implant surface, or harm extracellular matrix fibers. Thus, the response of the vena cava and pericardium to compression was studied. The tissues were folded three times and compressed under a 35N load, similar to that applied during stent crimping. After 30 minutes of loading, the tissue was removed and the surface structure and mechanical properties were compared to uncrimped controls. Stereomicroscopy and SEM images showed that both the vena cava and pericardium controls contained a smooth and a rough surface. The smooth surface of the vena cava corresponds to the intima and the rough surface to the adventita [162], whereas the serosa of the pericardium is smooth and the outer surface is rough [5]. Stereomicroscope images of the surface revealed faint parallel striations on the intimal side of GLUT and NG vena cava, indicating that the crimping process caused dents in the

tissue surface. SEM images further showed that the intima of GLUT vena cava was greatly affected by crimping, but that NG tissue was more resistant to surface damage. Similarly, faint dents, markings, and fiber tears are apparent on the serosa of the pericardium, with more damage to GLUT than NG. However, both the adventitia and outer pericardium are already too rough and textured to distinguish any new indentations with either stereomicroscopy or SEM. The results suggest that crimping in a stent alters the surface topography of the vena cava and pericardium, and pressure from the stent struts may cause damage to the tissue surface. A rough surface on the inflow surface of the valve can potentiate thrombosis formation [5], so the smooth tissue surfaces should be oriented inward and the crimping process carried out in such a way as to minimize compressive pressure from the stent struts on the inner surface.

NG tissue exhibited less surface damage than GLUT tissue. Neomycin enhances preservation of elastin and collagen in the tissue during fixation and storage [146]. The NG group contains a denser network of crosslinked fibers, which may be better able to withstand stress during tissue crimping. As a result, the NG tissue appears to be more resilient and better suited for constructing a PHV.

Loading has been shown to cause changes in tissue mechanics [172, 176]; thus the elastic modulus of the crimped tissue was compared to that of the controls. Crimping increased the lower elastic modulus for all tissue types, suggesting that the compressive force stiffened the tissue. The lower modulus is dominated by the response of the elastin fibers [127]. The increase in lower modulus was especially evident in the circumferential direction. Applied stress causes fiber realignment in the direction of the force to help the tissue bear the load [176]. The elastin fibers may have realigned circumferentially to increase the stiffness in that direction. The

increase in lower modulus in the longitudinal direction is small for the vena cava, and is likely due to the elastin fibers uncrimping under the load, causing slight stiffening of the tissue [172]. The increase in stiffness in the longitudinal direction is greater for the pericardium, possibly because the elastin fibers are less aligned and do not all react to the load uniformly by realigning to the same degree in the same direction.

The upper elastic modulus is dominated by collagen fibers, which uncrimp and realign in response to an applied load [127, 172, 176]. The upper elastic modulus in the circumferential direction for most of the tissue groups did not show a significant increase after compression. However, the GLUT vena cava had a slight increase in modulus in this orientation. Conversely, in the longitudinal direction, the vena cava exhibited a decrease in the upper elastic modulus while the pericardium exhibited an increase. The results suggest that the collagen fibers of the vena cava realigned in the circumferential direction, causing stiffening. The tissue is less stiff in the longitudinal direction because fewer fibers are available to bear the load. For the pericardium, the increase in upper modulus in the longitudinal direction was small, suggesting that some of the randomly-oriented collagen fibers realigned longitudinally. In general, the crimped vena cava samples were less stiff than the corresponding pericardium samples, especially in the longitudinal direction. After crimping, the vena cava maintained its mechanical directionality, exhibiting greater compliance in the longitudinal direction than the circumferential. Thus, the crimping process does not negate the mechanical benefits offered by the vena cava.

5.4 *In vivo behavior*

One of the major failure modes of glutaraldehyde crosslinked bioprosthetic heart valves is calcification. Calcium deposits form hard nodules on the cusps or aortic wall that can lead to cuspal tears or stenosis [77]. Calcification is often cell-related, as glutaraldehyde devitalizes cells, eliminating active calcium regulation processes [88]. Upon exposure to body fluids, intracellular calcium levels in the bioprostheses rise dramatically, and calcium deposits form on the phospholipid-rich membranes and organelles [87]. Extracellular matrix proteins such as collagen and elastin have also been noted as secondary nucleation sites [89]. The calcium deposits eventually aggregate to form hard, sharp nodes that can stiffen or perforate the tissue [88]. A number of anti-calcification strategies have been studied [5]. Ethanol pretreatment of the valves specifically targets cellular-based calcification. Incubating the heart valve in at least 80% ethanol solution prior to implantation extracts phospholipids and cholesterol from the tissue, thus removing those nucleation sites of calcification. Ethanol also causes a change in the collagen confirmation that renders the collagen less susceptible to mineralization [148].

Calcification can be studied *in vivo* using the juvenile rat subdermal implant model, which offers accelerated mineralization kinetics and is often used as a screening method for anti-calcification techniques [5]. GLUT, NG, and NGE vena cava and pericardium samples were implanted into juvenile Sprague Dawley rats. After three weeks, the implants were removed and analyzed for calcium content. GLUT vena cava exhibited significantly less calcification than GLUT pericardium, possibly due to differences in cell density between the tissue types. Addition of neomycin caused a significant increase in mineralization of the vena cava, but did not significantly alter the pericardium calcium content. The dramatic increase in the NG vena cava is likely due to its high elastin content, as neomycin preserves elastin fibers, thus making

the tissue more susceptible to elastin-mediated calcification. Furthermore, ethanol pretreatment was more effective at reducing pericardial calcification (82.69% decrease) than vena cava calcification (50.90% decrease). The vena cava extracellular matrix contains a higher proportion of elastin than that of the pericardium. Thus, elastin-mediated calcification likely accounts for the difference in ethanol efficacy. In the native heart valve, ethanol pretreatment reduces cuspal calcification, but does not prevent mineralization of the aortic wall due to its high elastin content [92]. The aortic valve cusps are approximately 10% elastin, while the aortic wall is 50% elastin [177]. Similarly, the high elastin density of vena cava, approximately 35%, renders the tissue more prone to ECM-based calcification than pericardial tissue. Histological findings confirmed that GLUT and NG pericardium contained dense clusters of calcium deposits, while NGE pericardium exhibited almost no calcium staining. NGE vena cava, in contrast, displayed bands of calcium deposits along its length, perhaps corresponding to the longitudinally-aligned elastin fibers. Since ethanol does not sufficiently prevent calcification of the vena cava, an alternative anti-mineralization strategy will have to be implemented if the tissue is to be used clinically.

Additionally, the Ca:P molar ratio of the mineralized explants was calculated, as different types of calcium phosphate contain varying proportions of these elements [179]. Pure hydroxyapatite (HAP), which comprises bone, has a Ca:P ratio of 1.67, while precursor phases such as octocalcium phosphate (OCP) and dicalcium phosphate dehydrate (DCPD) have ratios of 1.33 and 1.00, respectively. HAP formation is thought to be a process of phase transitions from transient forms of calcium phosphate, such as DCPD, to OCP, and finally to mature, stable HAP. Furthermore, the transition phase can be determined by crystal structure, as DCPD is large and irregular, while OCP is plate-like, and HAP is composed of small crystals [179]. Based on the

calculated Ca:P ratios, the calcium phosphate deposits in GLUT and NG vena cava and pericardium are likely in an intermediate phase between OCP and HAP. Ethanol treatment causes a change in the calcification behavior, resulting in deposits that contain less calcium and are predominantly phosphorus. In NGE vena cava, the deposits are likely similar to DCPD; however, in the NGE pericardium, the ratio is only 0.64± 0.102, indicating that these deposits may be even less thermodynamically stable than DCPD.

CHAPTER 6

CONCLUSIONS AND RECOMMENDATIONS

6.1 Conclusions

In recent years, a major trend in medicine has been a drive toward minimally invasive procedures. This movement is especially important to cardiology, where open chest surgeries account for high mortality rates and limit the pool of patients who are offered certain procedures. Aortic heart valve diseases such as aortic stenosis are becoming more prevalent in the United States as the population ages. However, traditional valve replacement surgery requires open chest surgery with cardiopulmonary bypass, a procedure which is too risky to perform on the elderly or patients with comordibities. As a result, many patients are denied a possibly life-saving procedure. The advent of minimally invasive valve replacement surgery has the potential to revolutionize the field of heart valves. Two percutaneous heart valves, which are delivered transcatheter to the aortic root and held in place by a stent, are currently undergoing clinical trials and may receive FDA approval within the next year or two. However, these devices have certain limitations which must be overcome before they can reach the market. A unique aspect of PHVs is that they must be crimped into a stent to a diameter small enough for transcatheter delivery through narrow, stenotic, or tortuous vasculature. While certain design modifications to the first generation GLUT-fixed bovine pericardium PHVs have allowed for percutaneous delivery, the affects of crimping on the tissue have yet to be elucidated. We have proposed an alternative

tissue source, vena cava, which may be more compliant and resilient than pericardium, and may offer enhanced properties to PHVs.

The results of our studies clearly show that vena cava has several advantages over pericardium. While the two tissues are equal in tissue thickness and collagen stability, the vena cava has a significantly higher elastin content, a factor which imparts enhanced flexibility to the tissue. Moreover, the elastin and collagen fibers in the vena cava are highly aligned, resulting in mechanical directionality and consistency. In contrast, the pericardium contains more collagen and less elastin, and the extracellular matrix fibers are more randomly oriented, leading to a stiffer tissue with less predictable mechanical properties. While the pericardium stiffens drastically after GLUT and NG fixation, the vena cava retains much of its flexibility. After crimping, both the GLUT vena cava and pericardium exhibited surface damage, while the NG tissues were less affected. Furthermore, the vena cava experienced a less significant change in elastic modulus after crimping, suggesting that the tissue may be more resilient to the compressive forces imparted by a stent.

While the vena cava offered several structural and mechanical benefits over the pericardium, certain features of the vena cava produced ambiguous results. Both the vena cava and pericardium contain significantly fewer GAGs than the native heart valve, with the vena cava comprising the least amount. GAGs are vital to native heart valve mechanics, serving to lubricate, adsorb shock, and facilitate shearing between tissue layers. However, given the differences in tissue structure and extracellular matrix composition between the vena cava and heart valve, it is unclear whether the lack of GAGs in the vena cava will be detrimental to PHV function. Additionally, the vena cava exhibited confounding *in vivo* behavior. While GLUT

vena cava calcified less than GLUT pericardium, the addition of neomycin caused a dramatic increase in vena cava mineralization, but an insignificant increase in pericardium mineralization. Ethanol treatment helped to attenuate the calcification of the pericardium, but did not greatly reduce that of the vena cava, likely due the high elastin content of the vena cava. Under the tested treatments, the vena cava calcifies too heavily *in vivo*, and an elastin-targeting anticalcification treatment will be necessary to overcome this problem.

Thus, we have shown that vena cava improves upon current PHVs by enhancing structural orientation, mechanical properties and tissue resilience. Furthermore, NG treatment of the vena cava preserves elastin fibers and reduces tissue surface damage after crimping. While certain features such as GAG content and calcification tendency still need clarification, it appears that vena cava is a viable alternative tissue source for use in PHVs.

6.2 Recommendations

The studies described here represent initial work in assessing the feasibility of using vena cava in PHVs. The structural properties, mechanics, and calcification potential of fresh and fixed vena cava have been characterized. However, in order to draw conclusions about the behavior of the vena cava in a replacement valve, further work is needed. First, the structure-function relationship must be fully characterized. Specifically, the quantity and role of GAGs should be determined. The uronic acid assay or fluorophore-assisted carbohydrate electrophoresis can be used to quantify the amount of GAGs in the fresh vena cava. Furthermore, transmission electron microscopy (TEM) can be used to identify the position of GAGs among the extracellular matrix fibers. Additional mechanical testing, such as cyclic

loading and creep tests, should be carried out prior to and following GAGase treatment of fresh and crosslinked vena cava to evaluate the role of GAGs in the viscoelastic response of the tissue.

In order to be clinically useful, *in vivo* mineralization of the NG vena cava must be reduced. Future studies should focus on identifying an anticalcification treatment to minimize elastin-mediated mineralization. Trivalent metal ions, such as aluminum or ferric chloride, have been used in the past for this purpose. Long term rat studies should investigate several anticalcification options, including combination therapies which target both cellular and elastin-based calcification. Additionally, the types of calcium phosphate crystals in the implants should be further characterized. The size and shape of the crystals can be observed with TEM and compared to the Ca:P ratios to identify the types of deposits present.

After fully assessing the tissue properties of the vena cava, a model heart valve should be constructed from the NG tissue. Several current bioprosthetic valves and PHVs use bovine pericardium that has been cut and sewn into stents to create trileaflet valves. Vena cava should be similarly shaped and formed into a valve, and the prototype should undergo cyclic fatigue. Such testing will reveal how the tissue responds to continual loading and unloading. Following fatigue testing, the valves should be evaluated by DSC, TEM, tensile testing, and biochemical analysis in order to fully understand the effects of pulsatile valve function on the tissue structure.

Finally, a true percutaneous valve should be constructed from the vena cava. The design should be modified until the lowest profile configuration is reached. Crimping the tissue inside of the stent and deploying it will help to further characterize the tissue resilience.

All of the aforementioned studies should be undertaken using NG bovine pericardium as a control. The performance of the vena cava can then be compared to an accepted standard, and

the potential benefits and disadvantages of replacing the pericardium with vena cava clearly assessed.

REFERENCES

1. Simionescu DT. Artificial Heart Valves. Wiley Encyclopedia of Biomedical Engineering. (2006) Wiley Interscience.

2. Sacks MS, Merryman WD, Schmidt DE. On the biomechanics of heart valve function. J Biomech. (2009) 42: 1804-1824.

3. Society of Thoracic Surgeons National Cardiac Surgery Database. (2005) available at http://www.sts.org/documents/pdf/Spring2005STSExecutiveSummary.pdf.

4. Iung B, Baron G, Butchart EG, et al. A prospective survey of patients with valvular heart disease in Europe: The Euro Heart Survey on Valvular Heart Disease. Eur Heart J (2003) 24:1231-43.

5. Schoen FJ, Levy RJ. Tissue Heart Valves: Current Challenges and Future Research Perspectives. Founder's Award, presented at 25th Annual Meeting of the Society for Biomaterials, Providence, RI. April 28-May 2, 1999.

6. Culliford AT, et al. Aortic valve replacement for aortic stenosis in persons aged 80 years and over. Am J Card. (1991) 67:1256-60.

7. Kvidal P, et al. Observed and relative survival after aortic valve replacement. J Am Coll Card. (2000) 35:747-56.

8. Pai RG, et al. Malignant natural history of asymptomatic severe aortic stenosis: benefit of aortic valve replacement. Ann Thorac Surg. (2006) 82:2116-22.

9. Chaim PT, Ruiz CE. Percutaneous transcatheter aortic valve implantation: Evolution of the technology. J Am Heart Assoc. (2009) 157:229-242.

10. Grube E, et al. Percutaneous aortic valve replacement for severe aortic stenosis in high-risk patients using the second- and current third-generation self-expanding CoreValve prosthesis: device success and 30-day clinical outcome. J Am Coll Card. (2007) 50:69-76.

11. Vesely I, Noseworthy R. Micromechanics of the fibrosa and the ventricularis in aortic valve leaflets. J Biomech. (1992) 25(1): 101-113.

12. Vesely I. The role of elastin in aortic valve mechanics. J Biomech. (1998) 31(2): 115-123.

13. Lovekamp J, Vyavahare N. Periodate-mediated glycosaminoglycan stabilization in bioprosthetic heart valves. J Biomed Mater Res. (2001) 56(4): 478-486.

14. Duran CMG, Gunning AJ. The vascularization of the heart valves: a comparative study. Cardiovasc. Res. (1968) 2: 290.

15. Schoen FJ. Aortic valve structure-function correlations: role of elastic fibers no longer a stretch of the imagination. J Heart Valve Dis. (1997) 6: 1-6.

16. Sacks MS, Yoganathan AP. Heart valve function: a biomechanical perspective. Philosophical Transactions of the Royal Society B. (2007) 1369-1391.

17. Reul H, Talukder N. Heart valve mechanics. In: *The heart.* (1989) New York, NY: McGraw Hill.

18. Sacks MS. The Biomechanical Effects of Fatigue on the Porcine Bioprosthetic Heart Valve. Journal of Long-Term Effects of Medical Implants. (2001) 11 (3-4) 231-247.

19. Ferrans VJ, et al. Morphologic abnormalities in explanted bioprosthetic heart valves. In: *Cardiovascular pathology*. (1991) Philadelphia, PA: W.B Saunders. 373-398.

20. Sacks MS, Smith DB, Hiester ED. The aortic valve microstructure: Effects of transvalvular pressure. J Biomed Mater Res. (1998) 41: 131-141.

21. Schoen FJ. Evolving Concepts of Cardiac Valve Dynamics: The Continuum of Development, Functional Structure, Pathobiology, and Tissue Engineering. Circulation. (2008) 118: 1864-1880.

22. Lo D, Vesely I. Biaxial strain analysis of the porcine aortic valve. Ann Thorac Surg. (1995) 60: S374-S378.

23. Christie GW. Anatomy of the aortic heart valve leaflets: the influence of glutaralehyde fixation on function. Eur J Cardio-Thorac Surg. (1992) 6: S25-S33.

24. Mirnajafi A, et al. The flexural rigidity of the aortic valve leaflet in the commissural region. J Biomech. (2006) 39: 2966-2973.

25. Sugimoto H, Sacks MS (in press). The effects of leaflet stiffness on the dynamic geometry of the bioprosthetic aortic heart valves. Ann. Biomed. Eng. (2009)

26. Vesely I, Boughner D, Song T. Tissue buckling as a mechanism of bioprosthetic valve failure. Ann Thorac Surg. (1988) 46(3): 302-308.

27. Shah SR, Vyavahare NR. The Effect of Glycosaminoglycan Stabilization on Tissue Buckling in Bioprosthetic Heart Valves. Biomaterials. (2008) 29(11): 1645-1653.

28. Song T, Vesely I, Boughner D. Effects of dynamic fixation on shear behavior of porcine xenograft valves. Biomaterials. (1990) 11: 191-196.
29. Talman EA, Boughner DR. Internal Shear Properties of Fresh Porcine Aortic Valve Cusps: Implications for Normal Valve Function. J Heart Valve Dis. (1996) 5: 152-159.

30. Simionescu DT, Lovekamp JJ, Vyavahare NR. Extracellular matrix degrading enzymes are active in porcine stentless aortic bioprosthetic heart valves. J Biomed Mater Res. (2003) 66(4) 755-763.

31. Sacks MS, Smith DB. Effects of accelerated testing on porcine bioprosthetic heart valve fiber architecture. Biomaterials. (1998b) 19(11-12): 1027-1036.

32. Vyavahare N, et al. Mechanisms of bioprosthetic heart valve failure: fatigue causes collagen denaturation and glycosaminoglycan loss. J Biomed Mater Res. (1999) 46(1): 44-50.

33. Schoen FJ. Cardiac valves and valvular pathology: update on function, disease, repair, and replacement. Cardiovasc Path. (2005) 14(4): 189-194.

34. Clivir Learning Community. Valvular Heart Disease. Updated May 29, 2009. Accessed Sept. 1, 2010. http://t0.gstatic.com/images?q=tbn:KJFITdpG3HFn6M:http://my-simple-host.com/pics/stenosis.jpg&t=1

35. Rabkin-Akawa JE, Mayer E, Schoen FJ. Heart valve regeneration. Adv Biochem Engr Biotech . (2005) 94:141-179.

36. Zilla P; Prosthetic Heart Valves: Catering for the Few. Biomaterials (2008) 29: 365-406.

37. Butany J et al. Mechanical heart valve prostheses: Identification and evaluation (erratum). Cardiovasc Path. (2003) 12: 322-344.

38. Lefrak EA, Starr A. Cardiac valve prostheses. New York: Prentice Hall. (1979)

39. Yoganathan AP, et al. The Starr-Edwards aortic ball valve: flow characteristics, thrombus formation, and tissue overgrowth. Artif Organs. (1981) 5:6– 17.

40. Blackstone EH. Could it happen again? The Bjork-Shiley convexo-concave heart valve story. Circ. (2005) 111(21): 2717-9.

41. Wieting DW, et al. Strut fracture mechanisms of the Bjork-Shiley convexo-concave heart valve. J Heart Valve Dis. (1999) 8(2): 206-217.

42. Halkos ME, Puskas JD. Are all bileaflet mechanical valves equal? Curr Opin Card. (2009) 24: 136-141.

43. Laas J, et al. Orientation of tilting disc and bileaflet aortic valve substitutes for optimal hemodynamics. Ann Thorac Surg. (1999) 68:1096– 9.
44. Akins CW. Results with mechanical cardiac valvular prostheses. Ann Thorac Surg. (1995) 60:1836–44.

45. Sezai A, et al. Evaluation of valve sound and its effects on ATS prosthetic valves in patients' quality of life. Ann Thorac Surg. (2000) 69: 507-512.

46. Hwang NH, et al. In vitro evaluation of the long body On-X bileaflet heart valve. J Heart Valve Dis. (1998) 7: 561-568.

47. Palatianos GM, et al. Multicentered European study on safety and effectivenss of the On-X prosthetic heart valve: intermediate follow-up. Ann Thorac Surg. (2007) 83: 40-46.

48. Emery RW, et al. The St. Jude Medical cardiac valve prosthesis: a 25-year experience with single valve replacement. Ann Thorac Surg. (2006) 79: 776-782.

49. Ibrahim M, et al. The St. Jude Medical prosthesis: A thirteen-year experience. J Thorac Cardiovasc Surg. (1994) 108(2): 221-230.

50. Beaudet RL, et al. The Medtronic-Hall cardiac valve: 7 ½ years' clinical experience. Ann Thorac Surg. (1986) 42(6): 644-650.

51. Grunkemeier GL, et al. Long-term performance of heart valve prostheses. Curr Prob Card. (2000) 25(2): 73-154.

52. Arom KV, et al. Ten years' experience with the St. Jude Medical valve prosthesis. Ann Thorac Surg (1989) 47(6): 831-837.

53. Nistal JF, et al. Clinical experience with the CarboMedics valve: early results with a new bileaflet mechanical prosthesis. J Thorac Cardiovasc Surg. (1996) 112(1): 59-68.

54. Aoyagi S, et al. Long-term results of valve replacement with the St. Jude Medical valve. J Thorac Cardiovasc Surg. (1994) 108(6): 1021-9.

55. Mathiesen T, et al. Intracranial traumatic and non-traumatic hemorrhagic complications of warfarin treatment. Acta Neurol Scand. (1995) 91(3): 208-14.

56. Brown ML, et al. Aortic valve replacement in patients aged 50 to 70 years: improved outcome with mechanical versus biologic prostheses. J Thorac Cardiovasc Surg. (2008) 135: 878-884.

57. Vitale N, et al. Obstruction of mechanical mitral prostheses: analysis of pathologic findings. Ann Thorac Surg. (1997) 63(4): 1101-6.

58. Girard SE, et al. Reoperation for prosthetic aortic valve obstruction in the era of echocardiography: trends in diagnostic testing and comparison with surgical findings. J Am Coll Card. (2001) 37(2): 579-584.

59. Bonfield T, Anderson J. Functional versus quantitative comparison of IL-1 beta from monocytes/macrophages on biomedical polymers. J Biomed Mater Res. (1993) 27(9): 1195-9.

60. Bryan AJ, et al. Prospective comparison of CarboMedics and St. Jude Medical bileaflet mechanical heart valve prostheses: ten-year follow-up. J Thorac Cardiovasc Surg. (2007) 133: 614-622.

61. Research and Markets. Global Heart Valve Market: 2008-2012. Infiniti Research Limited. (2010) www.researchandmarkets.com. Accessed May 2010.

62. O'Brien M, et al. A comparison of aortic valve replacement with viable cryopreserved and fresh allograft valves with a note on chromosomal studies. J Thorac Cardiovasc Surg. (1987) 94: 812-823.

63. Matsuki O, et al. Long-term performance of 555 aortic homografts in the aortic position. Ann Thorac Surg. (1988) 46: 187-191.

64. Kirklin JK, et al. Long-term function of cryopreserved aortic homografts. J Thorac Cardiovasc Surg. (1993) 106: 154-165.

65. Hilbert SL, et al. Allograft heart valves: the role of apoptosis-mediated cell loss. J Thorac Cardiovasc Surg. (1999) 49:619-624.

66. Mitchell RN, Jonas RA, Schoen FJ. Pathology of explanted cryopreserved allograft heart valves: comparison with aortic valves from orthotopic heart transplants. J Thorac Cardiovasc Surg. (1998) 115: 118-127.

67. Chambers JC, et al. Pulmonary autograft procedure for aortic valve disease: long-term results of the pioneer series. Circ. (1997) 96: 2206-2214.

68. Kouchoukos NT, et al. Replacement of the aortic root with a pulmonary autograft in children and young adults with aortic-valve disease. New Eng J Med. (1994) 330: 1-6.

69. Love JW, et al. Experimental evaluation of an autologous tissue heart valve. J Heart Valve Dis. (1992) 1: 232-241.

70. Vesely I. The evolution of bioprosthetic heart valve design and its impact on durability. Cardiovasc Path. (2003) 12: 277-286.

71. Turina J, et al. Cardiac bioprostheses in the 1990s. Circ. (1993) 88:775-781.
72. Schoen, FJ. Interventional and surgical cardiovascular pathology: clinical correlations and basic principles. (1989) Philadelphia: WB Saunders.

73. Jamieson WR, et al. Carpentier-Edwards standard porcine bioprosthesis: clinical performance to seventeen years. Ann Thorac Surg. (1995) 60: 999-1006.

74. Grunkemeier GL, et al. Actuarial versus actual risk of porcine structural valve deterioration. J Thorac Cardiovasc Surg. (1994) 108: 709-718.

75. Shemin RJ, et al. Hemodynamic and pathological evaluation of a unileaflet pericardial bioprosthetic valve. J Thorac Cardiovasc Surg. (1988) 95: 912-919.

76. Walker DK, et al. Development and in-vitro assessment of a new two-leaflet replacement heart valve designed using computer-generated bubble surfaces. Med Biol Eng Comput. (1983) 21:31-38.

77. Siddiqui RF, et al. Bioprosthetic heart valves: modes of failure. Histopath. (2009) 55: 135-144.

78. Kallikourdis A, Jacob S. Is a stentless aortic valve superior to convential bioprosthetic valves for aortic valve replacement? Interact Cardiovasc Thorac Surg. (2007) 6: 665-672.

79. Jaffe W.M., et al. Early follow-up of patients with the Medtronic Intact porcine valve: a new cardiac bioprosthesis. J Thorac Cardiovasc Surg. (1989) 98:181-192.

80. Yoganathan AP, et al. Hydrodynamic performance of the Medtronic Freestyle aortic root bioprosthesis. Journal of Heart Valve Disease. (1994) 3(5): 571-580.

81. Mohammadi S, et al. Structural deterioration of the Freestyle aortic valve: Mode of presentation and mechanism. Journal of Thoracic and Cardiovascular Surgery. (2006) 132(2): 401-406.

82. Gleason TG, et al. St. Jude Medical Toronto biologic aortic root prosthesis: Early FDA phase II IDE study results. Ann Thorac Surg. (2004) 78: 786-793.

83. Jamieson, W.R Eric. Advanced Technologies for Cardiac Valvular Replacement, Transcatheter Innovations, and Reconstructive Surgery. (2008) Surg Tech Internatl XV-Cardiovasc Surg. 15: 1-9.

84. Edmunds L, et al. Guidelines for reporting morbidity and mortality after cardiac valvular operations. Ann Thorac Surg. (1996) 62: 932-935.

85. Butany J, et al. Prosthetic heart valves: Part II: Clincal management. Geriatric and Aging. (2007) 10: 28-35.
86. Schoen FJ and RJ Levy. Calcification of Tissue Heart Valve Substitutes: Progress Toward Understanding and Prevention. Ann Thorac Surg. (2005b) 79: 1072-80.

87. Kim KM, et al. Role of Glutaraldehyde in Calcification of Porcine Aortic Valve Fibroblasts. Am J Pathol. (1999) 154: 843-852.

88. Schoen FJ and RJ Levy. Heart valve bioprostheses: antimineralization. Eur J Cardio-Thorac Surg. (1992) 6: S91-S94.

89. Golomb G, et al. The Role of Glutaraldehyde-Induced Cross-links in the Calcification of Bovine Pericardium Used in Cardiac Valve Bioprostheses. Am J Pathol. (1987) 127: 122-130.

90. Sucu N, et al. Two-stage EDTA anti-calcification method for bioprosthetic heart valve materials. Med Sci Monit. (2006). 12(6): MT33-38.

91. Chen W, Schoen FJ, Levy RJ. Mechanism of efficacy of 2-amino oleic acid for inhibition of calcification on glutaraldehyde-pretreated porcine bioprosthetic heart valves. Circ. (1994) 90: 323-329.

92. Vyavahare NR,et al. Prevention of bioprosthetic heart valve calcification by ethanol preincubation. Efficacy and mechanism. Circ. (1997) 95: 479–488.

93. Sacks MS, Schoen FJ. Collagen fiber disruption occurs independent of calcification in clinically explanted bioprosthetic heart valves. J Biomed Mater Res. (2002) 62(3): 359-371.

94. Vesely I, et al. Tissue damage and calcification may be independent mechanisms of bioprosthetic heart valve failure. J of Heart Valve Dis. (2001) 10(4): 471-477.

95. Sabbah HN, et al. Mechanical stresses on closed cusps of porcine bioprosthetic valves: correlation with sites of calcification. Ann Thorac Surg. (1986) 42(1) 93-96.

96. Butany J, Leask R. The failure modes of biological prosthetic heart valves. J Long Term Effects of Med Imp. (2001) 11:115-136.

97. Butany J, David T. Pathology of explanted stentless porcine valves (human experiences). In Gabay S, Frater RWM eds. New horizons and the future of heart valve prosthesis. (1994) Boston, TX. Silent Partners, Inc. 183-189.

98. Cribier A, et al. Percutaneous transluminal balloon valvuloplasty of adult aortic stenosis: report of 92 cases. J Am Coll Card. (1987) 9:381-6.

99. McKay RG. The Mansfield Scientific Aortic Valvuloplasty Registry: overview of acute hemodynamic results and procedural complications. J Am Coll Card. (1991) 17:485-91.

100. Otto CM, et al. Three-year outcome after balloon aortic valvuloplasty. Insights into prognosis of valvular aortic stenosis. Circ (1994) 89:642-50.

101. Kuntz RE, et al. Predictors of event-free survival after balloon aortic valvuloplasty. New Eng J Med. (1991) 325:17-23.

102. Andersen HR, Knudsen LL, Hasenkam JM. Transluminal implantation of artificial heart valves. Description of a new expandable aortic valve and initial results with implantation by catheter technique in closed chest pigs. Euro Heart J. (1992) 13:704-8.

103. Cribier A, et al. Percutaneous transcatheter implantation of an aortic valve prosthesis for calcific aortic stenosis: first human case description. Circ. (2002) 106:3006-8.

104. Cribier A, et al. Early experience with percutaneous transcatheter implantation of heart valve prosthesis for the treatment of end-stage inoperable patients with calcific aortic stenosis. . J Am Coll Card. (2004) 43:698-703.

105. Grube E, Laborde JC, Gerckens U, et al. Percutaneous implantation of the CoreValve self-expanding valve prosthesis in high-risk patients with aortic valve disease: the Siegburg first-in-man study. Circ (2006) 114:1616-24.

106. Webb JG, et al. Percutaneous Valve Implantation Retrograde from the Femoral Artery. Circ. (2006) 113: 842-850.

107. Hanzel GS, et al. Retrograde percutaneous aortic valve implantation for critical aortic stenosis. Cath Cardiovasc Interv. (2005) 64:322-6.

108. McRae ME, Rodger M, and Bailey BA. Transcatheter and Transapical Aortic Valve Replacement. Crit Care Nurse. (2009) 29: 22-36.

109. Webb JG, et al. Percutaneous transarterial aortic valve replacement in selected high-risk patients with aortic stenosis. Circ. (2007) 116:755-63.

110. Lange R, et al. First successful transapical aortic valve implantation with the Corevalve Revalving system: a case report. Heart Surg Forum. (2007) 10:E478-9.

111. Ruiz CE, et al. First percutaneous transcatheter aortic valve-in-valve implant with three year follow up. Cath Cardiovasc Interv. (2008) 72:143-8.

112. Paniagua D, et al. First human case of retrograde transcatheter implantation of an aortic valve prosthesis. Texas Heart Inst J. (2005) 32:393-8.

113. Schofer J, et al. Retrograde transarterial implantation of a nonmetallic aortic valve prosthesis in high-surgical-risk patients with severe aortic stenosis. A first-in-man feasibility and safety study. Circ: Cardiovasc Interv. (2008) 1:126-33.

114. Buellesfeld L, Gerckens U, Grube E. Percutaneous implantation of the first repositionable aortic valve prosthesis in a patient with severe aortic stenosis. Cath Cardiovasc Interv. (2008) 71: 579-84.

115. Zegdi R, et al. A repositionable valved stent for endovascular treatment of deteriorated bioprostheses. J Am Coll Card. (2006) 48:1365-8.

116. Rieder E, et al. Tissue engineering of heart valves: decellularized porcine and human valve scaffolds differ importantly in residual potential to attract monocytic cells. Circ (2005) 111:2792-7.

117. Vesely I. Heart valve tissue engineering. Circ Res. (2005) 97:743-55.

118. Hoerstrup SP, et al. Functional living trileaflet heart valves grown in vitro. Circ (2000) 102:III44-9.

119. Van Noort R, et al. A study of the effects of glutaraldehyde and formaldehyde on the mechanical behavior of bovine pericardium. Biomaterials. (1982) 3: 21-26.

120. Braga-Vilela AS, et al. Extracellular Matrix of Porcine Pericardium: Biochemistry and Collagen Architecture. J Memb Biol. (2008) 221: 15-25.

121. Schoen FJ, Tsao JW, Levy RJ. Calcification of bovine pericardium used in cardiac valve bioprostheses: implications for the mechanisms of bioprosthetic tissue mineralization. Am J Path. (1986) 123: 134-145.

122. Mannschott P, et al. Collagen heterogeneity in pig heart valves. Biochem Biophys Acta. (1976) 434: 177-183.

123. Zioupos P, Barbenel JC. Mechanics of native bovine pericardium: II. A structure based model for the anisotropic mechanical behavior of the tissue. Biomaterials. (1994) 15(5): 374-382.

124. Sacks MS, Chuong CJC, More R. Collagen fiber architecture of bovine pericardium. ASAIO J (1994) 40:M632–M637.

125. Garcia Paez JM, et al. Porcine pericardial membrane subjected to tensile testing: preliminary study of the process of selecting tissue for use in the construction of cardiac bioprostheses. J Mater Sci: Mater in Med. (2001) 12: 425-430.

126. Mirnajafi A, et al. The effects of collagen fiber orientation on the flexural properties of pericardial heterograft biomaterials. Biomaterials. (2005) 26(7): 795-804.

127. Cohn D, et al. Mechanical behavior of isolated pericardium: species, isotropy, strain rate, and collagenase effect on pericardial tissue. Clin Mater. (1987) 2: 115-124.

128. Cribier A, et al. Treatment of calcific aortic stenosis with the percutaneous heart valve: mid-term follow-up from the initial feasibility studies: the French experience. J Am Coll Card. (2006) 47:1214-23.

129. Valhanian A, et al. Transcatheter valve implantation for patients with aortic stenosis: a position statement from the European Association of Cardio-Thoracic Surgery (EACTS) and the European Society of Cardiology (ESC), in collaboration with the European Association of Percutaneous Cardiovascular Interventions (EAPCI). (2008) Eur Heart J. 29: 1463-70.

130. Zajarias A, Eltchaninoff H, Cribier A. Successful coronary intervention after percutaneous aortic valve replacement. Cath Cardiovasc Interv. (2007) 69:522-4.

131. Lutter G, et al. Percutaneous aortic valve replacement: an experimental study, I: studies on implantation. J Thorac Cardiovasc Surg. (2002) 123(4):768-776.

132. Nordmeyer J, et al. Analysis of stent fractures after percutaneous pulmonary valve implantation. Circ. (2006) 114(suppl 18):II-385.

133. Walther T, et al. Minimally invasive transapical beating heart aortic valve implantation—proof of a concept. Eur J Cardiothorac Surg. (2007) 31(1):9-15.

134. Jayakrishnan A, Jameela SR. Glutaraldehyde as a fixative in bioprostheses and drug delivery matrices. Biomaterials. (1996) 17: 471-484.

135. Olde Damink LHH, et al. Glutaraldehyde as a crosslinking agent for collagen-based biomaterials. J Mater Sci: Mater in Med. (1995) 6: 460-472.

136. Wine Y, et al. Elucidation of the Mechanism and End Products of Glutaraldehyde Crosslinking by X-Ray Structure Analysis. Biotech and Bioeng. (2007) 98(3): 711-718.

137. Kiernan JA. Formaldehyde, formalin, paraformaldehyde and glutaraldehyde: What they are and what they do. Microscopy Today. (2000) 00-1: 8-12

138. Bowers JH, Cater CW. The reaction of glutaraldehyde with proteins and other biological materials. J Microscopy. (1966) 85: 193-200.

139. Blauer G, et al. The interaction of glutaraldehyde with poly(alpha-l-lysine), N-butyl amine and collagen. I. The primary photon release in aqueous media. Biophysics. (1975) 14: 2585-2598.

140. Woodroof EA. Tissue Heart Valves. (1979) In: Ionescu MI, ed. London: Butterworths. 347-362.

141. Ferrans VJ, Hilbert SL, Jones M. Biomaterials. In: Replacement Cardiac Valves. (1991b) Bodner E, Frater RWM, eds. Elmsford, NY: Pergamon Press. 49-76.

142. Oliver RF, et al. Histological studies of subcutaneous and intraperitoneal implants of trypsin-prepared dermal collagen allografts in the rat. Clin Ortho Rel Res. (1976) 115: 291-302.

143. Cooke A, Oliver RF, Edward M. An *in vivo* cytotoxicity study of aldehyde-treated pig dermal collagen. Brit J Path. (1983) 64: 172-176.

144. Fisher J, Davies GA. Buckling in bioprosthetic valves. Ann Thorac. (1989) 48: 147–148.

145. Raghavan D, Simionescu DT, Vyavahare NR. Neomycin prevents enzyme-mediated glycosaminoglycan degradation in bioprosthetic heart valves. Biomaterials. (2007) 28: 2861-2868.

146. Raghavan D, Starcher BC, Vyavahare NR. Neomycin binding preserves extracellular matrix in bioprosthetic heart valves during in vitro cyclic fatigue and storage. Acta Biomat. (2009) 5: 983-992.

147. Padera FSaR. Cardiac surgical pathology. New York: McGraw Hill. (2003)

148. Raghavan D, Shah SR, Vyavahare NR. Neomycin fixation followed by ethanol pretreatment leads to reduced buckling and inhibition of calcification in bioprosthetic valves. J Biomed Mater Res, Part B: App Biomater. (2010) 92(1): 168-177.

149. Lovekamp JJ, et al. Stability and function of glycosaminoglycans in porcine bioprosthetic heart valves. Biomaterials. (2006) 27(8): 1507-1508.

150. Mercuri JJ, et al. Glycosaminoglycan-targeted fixation for improved bioprosthetic heart valve stabilization. Biomaterials. (2007) 28(3): 496-503.

151. Salmen S, et al. Sulphated oligosaccharides as inhibitors of hyaluronidases from bovine testis, bee venom and Streptococcus agalactiae. Planta Medica (2005) 71(8):727–32.

152. Zhong SP, et al. Biodegradation of hyaluronic acid derivatives by hyaluronidase. Biomaterials. (1994) 15(5):359–65.

153. Menzel EJ, Farr C. Hyaluronidase and its substrate hyaluronan: biochemistry, biological activities and therapeutic uses. Cancer Letters. (1998) 11;131(1):3–11.

154. Neomycin trisulfate structure. Clinical Pharmacology. Elsevier. (2010) Accessed 30 Oct. 2010 via http://www.clinicalpharmacology.com/apps/images/structures/001/neomycin.gif

155. Scharfschwerdt M, et al. Vena cava as autologous tissue for pulmonary valve substitute. Interact Cardiovasc Thorac Surg. (2008) 7: 973-976.

156. Della Rocca F, et al. Cell composition of the human pulmonary valve: a comparative study with the aortic valve – The VESALIO Project. Ann Thorac Surg. (2000)70:1594–1600.

157. Senning A. Fascia lata replacement of aortic valves. J Thorac Cardiovasc Surg. (1967) 54:465–471.

158. Bjork VO, Hultquist G. Teflon and pericardial aortic valve prostheses. J Thorac Cardiovasc Surg (1964) 47:693–701.

159. Puig LB, et al. Homologous dura mater cardiac valve. Preliminary study of 30 cases. J Thorac Cardiovasc Surg (1972) 64:154–160.

160. Gundry SR, et al. Fate of the pericardial monocusp pulmonary valve for right ventricular outflow tract reconstruction. Early function, late failure without obstruction. J Thorac Cardiovasc Surg (1994) 107:908–912.

161. Macartney FJ, Scott O, Ionescu MI. Late results of fascia lata reconstruction of the right ventricular outlet. Am Heart J (1975) 89:195–199.

162. Snowhill, P.B. Foran, D.J. Silver, F.H. A Mechanical Model of Porcine Vascular Tissues-Part I: Determination of Macromolecular Component Arrangement and Volume Fractions. Cardiovasc Eng: An International J. (2004) 4: 281-294.

163. Reis FP, and Ferraz de Carvalho CA. The architecture of the splenic artery in the adult man. (1985) Anat Anz. 160: 323–331.

164. Reis FP, and Ferraz de Carvalho CA. Functional architecture of the splenic vein in the adult human. (1988) Acta Anat (Basel). 132: 109–113.

165. Ninomiya H, Inomata T, and Ogihara K. Collagen fiber arrangement in canine hepatic venules. (1999) J Vet Med Sci. 61: 21–25.

166. Snowhill, P.B. Silver, F.H. A Mechanical Model of Porcine Vascular Tissues-Part II: Stress–Strain and Mechanical Properties of Juvenile Porcine Blood Vessels. Cardiovasc Eng: An International J. (2005) 5:157-169.

167. Fischer GM, Swain ML, and Cherian K. Increased vascular collagen and elastin synthesis in experimental atherosclerosis in the rabbit. Variation in synthesis among major vessels. Atherosclerosis. (1980) 35: 11–20.

168. Nitschmann E, et al. Morphologic and Biochemical Features Affecting the Antithrombotic Properties of the Inferior Vena Cava of Rabbit Pups and Adult Rabbits. Ped Res. (1998) 43(1): 62-67.

169. Kalath S, Tsipouras P, and Silver FH. Non-invasive assessment of aortic mechanical properties. Ann Biomed Eng. (1986) 14: 513–524.

170. Boughner DR, et al. The pericardial bioprosthesis: Altered tissue shear properties following glutaraldehyde fixation. J Heart Valve Dis. (2000) 9: 752–760.

171. Silver FH, Snowhill PB, and Foran DJ. Mechanical behavior of vessel wall: A comparative study of aorta, vena cava, and carotid Artery. Ann Biomed Eng. (2003) 31: 793–803.

172. Joyce EM, et al. Functional Collagen Fiber Architecture of the Pulmonary Heart Valve Cusp. Ann Thorac Surg. (2009) 87: 1240-1249.

173. Samouillan V, et al. Comparison of chemical treatments on the chain dynamics and thermal stability of bovine pericardium collagen. (2003) J Biomed Mater Res. 64A: 330–338,

174. Miles CA, et al. The increase in denaturation temperature following cross-linking of collagen is caused by dehydration of the fibres. (2005) J Mol Biol. 346(2):551-556.

175. Lee TC, et al. The effect of elastin damage on the mechanics of the aortic valve. (2001) J of Biomechanics. 34: 203-210.

176. Sellaro TL, et al. Effects of collagen fiber orientation on the response of biologically derived soft tissue biomaterials to cyclic loading. (2009) J Biomed Mater Res. 80A: 194-205.

177. Simionescu A, Simionescu D, Deac R. Biochemical pathways of tissue degeneration in bioprosthetic cardiac valves. The role of matrix metalloproteinases. (1996) ASAIO J. 42(5):M561-7.

178. Vyavahare NR. Preventing bioprosthetic heart valve calcification: Are we there yet? (2005) Perspectives in Cardiac Surgery. 2(2): 5-12.
179. Mavrilas D, et al. Development of bioprosthetic heart valve calcification in vitro and in animal models: Morphology and composition. (1999) J Crystal Growth. 205: 554-562.